

See discussions, stats, and author profiles for this publication at: <https://www.researchgate.net/publication/229750460>

# Bioelectrodes

Chapter · April 2006

DOI: 10.1002/0471732877.emd013

---

CITATIONS

25

READS

3,202

1 author:



Eric McAdams

Institut National des Sciences Appliquées de Lyon

153 PUBLICATIONS 2,516 CITATIONS

SEE PROFILE

Some of the authors of this publication are also working on these related projects:



DIALYDOM [View project](#)



BIPPED [View project](#)

## BIOELECTRODES

ERIC MCADAMS  
University of Ulster at  
Jordanstown  
Newtownabbey,  
Ireland

### INTRODUCTION

Biomedical electrodes are used in various forms in a wide range of biomedical applications, including:

1. The detection of bioelectric events such as the electrocardiogram (ECG).
2. The application of therapeutic impulses to the body [e.g., cardiac pacing and defibrillation and transcutaneous electrical nerve stimulation (TENS)].
3. The application of electrical potentials in order to facilitate the transdermal delivery of ionized molecules for local and systemic therapeutic effect (iontophoresis).
4. The alternating current (ac) impedance characterization of body tissues.

Good electrode design is not as simple and straightforward a matter as is often assumed, and all electrode designs are not equal in performance (1). One must, therefore, not simply choose an electrode with as conductive a metal plate as possible, which unfortunately, was and appears to still be the case in many designs. Probably due to this mistaken view, it would appear that the associated electronic systems are often first developed and the electrode design is left to the end, almost as an afterthought. If the clinician is to properly diagnose the patient's cardiac problem, for example, it is imperative that the measured biosignal is clear, undistorted, and artifact-free. Unfortunately, monitoring bioelectrodes, if they are not chosen correctly, give rise to significant problems that make biosignal analysis difficult, if not impossible. Similarly, stimulation electrodes must be well-chosen if they are to optimally supply the therapeutic waveforms without causing trauma to the patient.

Current or charge is carried by ions inside the patient's body and by electrons in the electronic device itself and in its leads. The "charge-transfer" mechanism between current/charge carriers takes place at the electrode-patient interface and is of major importance in the design of an optimal electrode. Both the electrode-electrolyte interface and the skin under the electrode (collectively known as the contact) give rise to potentials and impedances that can distort the measured biosignal or adversely affect the electrotherapeutic procedure.

Implanted electrodes are generally made from inert or noble materials that do not react with surrounding tissues. Unfortunately, as a consequence, they tend to give rise to large interface impedances and unstable potentials. Implanted biosignal monitoring electrodes, in particular, require stable potentials and low interface impedances to minimize biosignal distortion and artifact problems. External biosignal-monitoring electrodes can generally use

high electrical performance nonnoble materials such as silver-silver chloride without fear of biocompatibility problems (2). They do, however, have to address the additional and very significant problem of the skin with its sizeable impedance and unstable potential. Along with the desired biosignal, one amplifies the difference between the two contact potentials. If the contact potentials were identical (highly improbable), they would cancel each other out due to the use of a differential amplifier. If the potential mismatch were very large (several hundred mV), the amplifier would not be able to cope and would saturate. If the mismatch in contact potentials is small and stable, this mismatch will be amplified along with the biosignal, and the biosignal will appear shifted up or down on the oscilloscope screen or printout paper, which would generally not be a major problem as the additional voltage offset can be easily removed. What is a significant problem, however, is when the contact potentials fluctuate with time. Their mismatch, therefore, varies and the baseline of the biosignal is no longer constant, which leads to the problem termed baseline wander or baseline drift, which makes analysis of some of the key features of the biosignal difficult. Filtering out of the drift is often not an option, as the filtering often also removes key components of the desired biosignal.

Large mismatched contact impedances can cause signal attenuation, filtering, distortion, and interference in biosignal monitoring. If contact impedances are significant compared with the input impedance of the amplifier, they can give rise to signal attenuation as a result of the voltage divider effect. Attenuation of the signal is not a major problem, after all, the amplifier is going to be used to amplify the signal by a factor of around 1000 (in the case of an ECG). A significant problem develops, however, because the contact impedance varies with frequency. The frequency-dependence of the contact impedance is a consequence of the presence of parallel capacitances at the electrode-electrolyte interface or at the skin under the electrode. At very high frequencies, the contact impedances are very small and, therefore, no attenuation of the high frequency parts of the biosignal exists. At low frequencies, the contact impedances can be very large and, hence, significant attenuation of low frequency components of the biosignal can exist. The overall signal is not only attenuated, it is also distorted with its low frequency components selectively reduced. The measurement system in effect acts as a high pass filter and the signal is differentiated. In the case of the ECG, the P, S, and T waves are deformed, leading in particular to a modification of the S-T segment. The S-T segment is of vital importance to the electrocardiologist, hence the importance of avoiding such biosignal distortions.

50/60 Hz interference can be amplified along with any monitored biosignal due to the mismatch of the contact impedances. Displacement currents flow from power lines through the air to the monitor cables and then through the electrodes and the patient to ground. If the contact impedances are not identical, the displacement currents flowing through the two contact impedances connected to a differential amplifier will give rise to different voltages at the amplifier's inputs. This 50 Hz offset voltage will be amplified along with the desired biosignal and its amplitude

is proportional to an electrode-skin impedance mismatch (3).

Other applications, such as electrical impedance plethysmography and electrical impedance tomography (4), do not monitor intrinsic biosignals emanating from the body, but inject small currents or voltages into the body and record the resultant voltages or currents. The electrical properties of the body or a body segment can then be calculated. In many of these applications, the magnitude and mismatch of contact impedances can give rise to significant errors or artifacts (5). As relatively high frequencies are often involved in these techniques, even the series resistance of the gel pad (which is generally ignored) may become significant.

Although interface impedance and potential are generally less critical for implanted stimulation electrodes, many such electrodes (e.g., implanted pacing electrodes) are used to monitor biosignals as well as to deliver the required stimulation impulses. Even in the case of a purely stimulating electrode, a low interface impedance is required to minimize energy waste and to prolong the life of the power source. Various techniques are therefore used to effectively decrease the otherwise large interface impedances of the noble or inert materials used for their biocompatible properties. Electrode material and high electrical performance is generally less critical for external stimulation electrodes such as TENS and external defibrillation electrodes. Current density distribution is of major importance in these applications in order to avoid electrical hotspots and resultant burns to the skin. In some applications, such as TENS and external pacing, it is even sometimes advantageous to use a relatively resistive electrode material or gel, as this has been found to optimize current density distribution under the stimulation electrode.

As in the above applications, the avoidance of current density hotspots is one of several key factors in iontophoretic, transdermal delivery (6). An additional important constraint that is generally not relevant in other electrotherapies is the maintenance of the delicate electrochemical balance at the electrode/reservoir/skin interface. The electrode potential and impedance, as well as the composition of the drug reservoir, must generally remain within certain narrow ranges in order to avoid the deterioration of the electrode, the contamination of the drug reservoir, and the irritation of the patient's skin.

The electrical properties of the electrode contacts are, therefore, of great importance in most applications. Ideally, the contact with the patient should give rise to the following:

- Zero potential. Unfortunately, zero potential is not possible and a more realistic goal is to achieve a low, stable potential at each of the contacts.
- Zero Impedance. Unfortunately, zero impedance too is not possible and a more realistic goal is to achieve impedances at the two contacts that are low and as similar as possible.

The potentials and impedances of the electrode-electrolyte interface and the skin will therefore be studied in more depth in the following sections.

## ELECTRICAL PROPERTIES OF ELECTRODE–SKIN INTERFACE

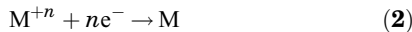
As briefly outlined above, the electrode–electrolyte interface and the skin under the electrode both give rise to potentials and impedances that can either distort any measured biosignal or give rise to problems during electrical stimulation.

### The Electrode–Electrolyte Interface

**The Electrode–Electrolyte Potential.** When a metallic electrode comes in contact with an electrolyte (in body tissues or in an electrode gel), an ion–electron exchange occurs as a result of an electrochemical reaction. A tendency exists for metal atoms M to lose  $n$  electrons and pass into the electrolyte as metal ions,  $M^{+n}$ , causing the electrode to become negatively charged with respect to the electrolyte (Fig. 1). Reaction (1) is termed oxidation.



Similarly, under equilibrium conditions, some of the ions in solution  $M^{+n}$  take  $n$  electrons from the metal and deposit onto the electrode as metal atoms M. The electrode becomes positively charged with respect to the electrolyte. Reaction (2) is termed reduction.



The overall chemical reaction taking place at the interface is therefore



Under equilibrium conditions, the rate at which metal atoms lose electrons and pass into solution is exactly balanced by the rate at which metal ions in solution deposit onto the electrode as metal atoms. The current flowing in one direction,  $i_0$ , is equal to and cancels out the current flowing in the opposite direction. The electrode is said to be

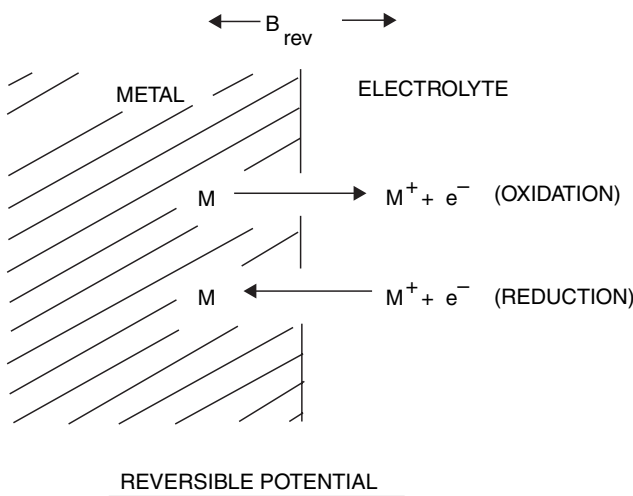


**Figure 1.** The electrode–electrolyte interface and reactions involved in generating its reversible or equilibrium potential.

behaving reversibly and the common value of currents,  $i_0$ , is termed the exchange current (density). Although the net current flowing through the electrode interface is zero, a potential difference is found to exist between the electrode and the electrolyte and depends on the position of the equilibrium between the two processes (1) and (2). Generally, the metal is negative relative to the electrolyte. The potential difference depends on the relative activities (or concentrations) of the ions present and on the electrode metal (7). This potential has been termed the equilibrium, reversible, or half-cell (i.e., one interface only) potential in the literature.

When trying to measure the potential of a half-cell (i.e., one interface only), one is immediately faced with a problem, as one requires two electrodes to make a potential measurement, thus effectively creating an electrochemical cell with two electrode–electrolyte interfaces. One, therefore, measures not only the potential of the electrode–electrolyte interface under study, but also that of the second electrode used to complete the circuit. If one uses the same metal for the second electrode to that used in the first, the potentials will be identical (in theory at least) and will cancel each other out. The measured potential will be (theoretically) equal to zero. (In practice, however, slight differences in the composition of the metal used, the electrode surfaces, and in the gel will result in differences in the two half-cell potentials.) If, on the other hand, one uses a different metal for the second electrode, the measured potential of the cell will be due to the combination of the potentials of the two half-cells. It will be impossible to separate the potential of the half-cell under investigation.

In order to resolve this problem, early electrochemists decided to measure all electrode interface potentials with respect to a standardized electrode or reference electrode. The standard hydrogen electrode (SHE) was chosen to be the universal reference electrode and its half-cell potential was specified as zero. Other metal-to-ion interface potentials were then measured with reference to SHE and the entire measured offset voltage was attributed to electrode system being tested.

Hydrogen electrode consists of a platinized plate submerged to one-half its height HCl over which hydrogen gas at atm is bubbled. The half-cell potential of SHE depends on concentration of hydrogen ions in the solution, hence it is quite stable and reproducible. At the time that this decision was reached, the necessary glass blowing and silver soldering were common skills and the SHE was thus easy and inexpensive to make. Although, however, it is no longer convenient for modern routine measurements as a reference electrode (the flowing hydrogen gas is potentially explosive), electrode potentials are standardized with respect to the SHE (7).

The reversible, equilibrium, or half-cell potential of a given electrode–electrolyte interface depends on the activity (almost synonymous with concentration) of the ions taking part in the reactions (Table 1). This potential,  $E_{rev}$ , is given by the Nernst equation,

$$E_{rev} = E_0 + [RT/nF] \ln [\text{activity of oxidized form} / \text{activity of reduced form}] \quad (1)$$

**Table 1. Reversible Potentials for Common Electrode Materials at 25 °C<sup>a</sup>**

Metal and Reaction	Potential $E^{\circ}$ , V
$\text{Al} \rightarrow \text{Al}^{3+} + 3\text{e}^-$	-1.706
$\text{Zn} \rightarrow \text{Zn}^{2+} + 2\text{e}^-$	-0.763
$\text{Cr} \rightarrow \text{Cr}^{3+} + 3\text{e}^-$	-0.744
$\text{Fe} \rightarrow \text{Fe}^{2+} + 2\text{e}^-$	-0.409
$\text{Cd} \rightarrow \text{Cd}^{2+} + 2\text{e}^-$	-0.401
$\text{Ni} \rightarrow \text{Ni}^{2+} + 2\text{e}^-$	-0.230
$\text{Pb} \rightarrow \text{Pb}^{2+} + 2\text{e}^-$	-0.126
$\text{H}_2 \rightarrow 2\text{H}^+ + 2\text{e}^-$	0.000 by definition
$\text{Ag} + \text{Cl}^- \rightarrow \text{AgCl} + \text{e}^-$	+0.223
$2\text{Hg} + 2\text{Cl}^- \rightarrow \text{Hg}_2\text{Cl}_2 + 2\text{e}^-$	+0.268
$\text{Cu} \rightarrow \text{Cu}^{2+} + 2\text{e}^-$	+0.340
$\text{Cu} \rightarrow \text{Cu}^+ + \text{e}^-$	+0.522
$\text{Ag} \rightarrow \text{Ag}^+ + \text{e}^-$	+0.799
$\text{Au} \rightarrow \text{Au}^{2+} + 3\text{e}^-$	+1.420
$\text{Au} \rightarrow \text{Au}^+ + \text{e}^-$	+1.680

<sup>a</sup>The metal undergoing the reaction shown has the magnitude and polarity of standard half-cell potential,  $E_0$ . Listed when the metal is referenced to the standard hydrogen electrode (3).

$E_{\text{rev}}$  is the reversible, equilibrium, or half-cell potential  
 $E_0$  is the standard half-cell potential (measured relative to the standard hydrogen electrode)

R the universal gas constant,

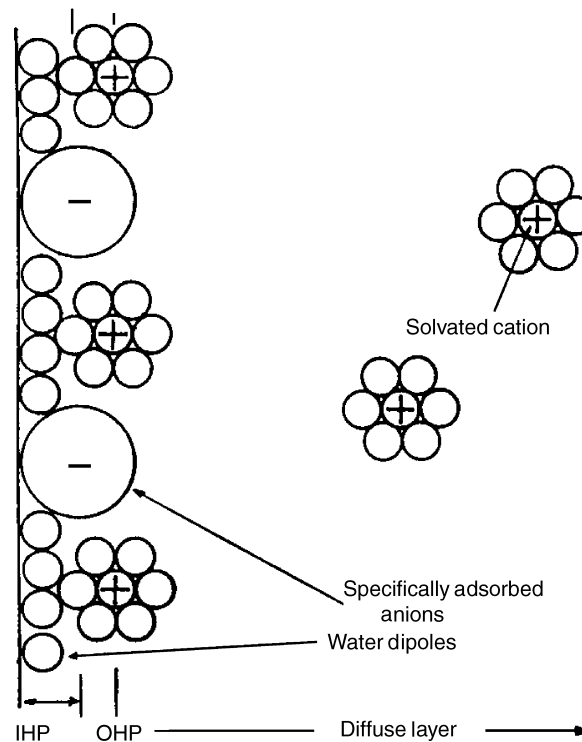
n the number of electrons involved in reaction,

T the absolute temperature (K).

Activity,  $a = \gamma C$ , where  $C$  is concentration and  $\gamma$ , the activity coefficient, is a measure of the interaction between ions. When solution is infinitely dilute,  $\gamma = 1$  and activity is equal to concentration.

Note the two components of  $E_{\text{rev}}$ . One is constant,  $E_0$ , whereas the other will vary due to slight variations in concentration, from one electrode to another. If two chemically identical electrodes make contact with the same electrolyte/body, the two interfaces should, in theory, develop identical half-cell potentials. When connected to a differential amplifier, the half-cell potentials of such electrodes would cancel each other out and the offset voltage would be zero. The electrode potentials would, therefore, make zero contribution to a biosignal they were being used to detect. Unfortunately, slight differences in electrode metal or gel result in the creation of offset voltages, which can greatly exceed the physiological variable to be measured. Generally, a more significant problem is that the electrode offset voltage can fluctuate with time, thus distorting the monitored biosignal (8).

**The Electrode-Electrolyte Impedance.** It has already been stated that in the electrode and the connecting lead, electrical charge is carried by electrons, whereas in the gel and in the human body, charge is carried by ions. A transition exists at the interface between the electrode and the electrolyte where charge is transferred from one kind of carrier to the other. In order for some of the ions in the electrode gel or in the body fluids to transfer their charge across the interface, many must first diffuse to



#### ELECTRODE-ELECTROLYTE INTERFACE

**Figure 2.** The electrode-electrolyte interface. A metal in an electrolyte forms a double layer of charge. (Redrawn from Ref. 7).

the electrode-electrolyte interface under the influence of electrostatic attraction. Here they stick (or adsorb, as it is termed in electrochemistry) to the electrode surface and form the outer Helmholtz plane (OHP) (7). If the electrode has a negative charge relative to the electrolyte, positive ions will be attracted to the interface region and adsorb onto the electrode surface. As a consequence, there is a layer of negative charge on the metal surface and a layer of equal but opposite charge on the electrolyte side of the interface, both separated by a small distance across the OHP (see Fig. 2). A double layer of charge therefore exists at the interface, and such a system behaves like a parallel-plate capacitor. Not altogether surprising, the interface's capacitance is often termed the double-layer capacitance,  $C_{\text{dl}}$ , and is connected in parallel to the charge-transfer resistance in our simple equivalent circuit model.

Just in case one believed that the electrode interface was that simple, one must point out, for example, that as well as the cations electrostatically attracted to the negatively charged electrode surface (coulombic adsorption) anions may exist that are adsorbed on the electrode surface and form the inner Helmholtz layer or plane (IHP). These anions have tended to lose their hydration sphere and, consequently, are in close contact with the electrode. As they are negative ions adsorbed onto a negative electrode surface, electrostatic forces cannot be responsible. Some force specific to the ion (rather than its electric charge) must be responsible, hence the use of the term specific

adsorption to describe this phenomenon. The van der Waals or chemical forces is thought to be responsible (7).

In order to understand some aspects of the double-layer capacitance, it is good to consider the basic equation for a parallel-plate capacitor. If two identical conductive plates, each of area  $A \text{ cm}^2$ , are separated by a distance  $d \text{ cm}$ , which is filled with a material of dielectric constant  $\epsilon_0$ , then the capacitance of this parallel-plate capacitor,  $C_{\text{pp}}$ , is given by:

$$C_{\text{pp}} = \epsilon_0 A / d \quad (2)$$

and the magnitude of the capacitive impedance,  $Z_{\text{pp}}$ , is given by

$$Z_{\text{pp}} = 1/2\pi f C_{\text{pp}} \quad (3)$$

where  $f$  is the frequency of the applied ac signal and  $\pi$  is a constant.

Some dc (or faradaic) current does, however, manage to leak across the double layer due to electrochemical reactions (1) and (2) taking place at the interface. These reactions experience a charge transfer resistance,  $R_{\text{CT}}$ , which can be thought of as shunting the nonfaradaic, double-layer capacitance and whose expression can be derived from the Butler–Volmer equation.

For small applied signal amplitudes (7),

$$R_{\text{CT}} = \frac{RT}{nF} \frac{1}{i_0} \quad (4)$$

A good electrode, from an electrical point of view, will have a very low value of  $R_{\text{CT}}$ . Charge will be transferred across the interface almost unimpeded and little voltage will be dropped across the interface. One should note that  $R_{\text{CT}}$  is inversely proportional to  $i_0$ .  $i_0$  is the exchange current [i.e., the current flowing across the interface (in both directions) under equilibrium conditions (no net current flow)]. Simplistically, if an interface can cope with large currents under equilibrium conditions, it will be able to cope well with currents under nonequilibrium conditions. A good electrode system will therefore be characterized by a large value of exchange current or a low value of  $R_{\text{CT}}$ .

The interface impedance should theoretically be well represented by an equivalent circuit model comprising the double-layer capacitance in parallel with the charge transfer resistance,  $R_{\text{CT}}$ . Both are in series with  $R_{\text{TOTAL}}$ , the relatively small resistance due to the sum of the lead and electrolyte resistances.

**Complex Impedance Plot.** If, for each frequency of ac signal used to measure the impedance, the real part of the measured impedance ( $Z'$  or  $R_S$ ) is plotted on the  $x$  axis and the imaginary part ( $Z''$  or  $X_S$ ) on the  $y$  axis of a graph, one obtains a Nyquist or complex impedance plot. The impedance locus for the above simple equivalent circuit model (Fig. 3.) of the interface impedance is plotted on a complex impedance plot in Fig. 4. Note: Electrochemists plot  $-X_S$  versus  $R_S$  and not  $X_S$  versus  $R_S$  as electrode (and tissue) impedances tend to be capacitive and thus negative. It is generally found easier to look at the plots with the  $Z''$  axis inverted. Low frequency data are on the right side of the

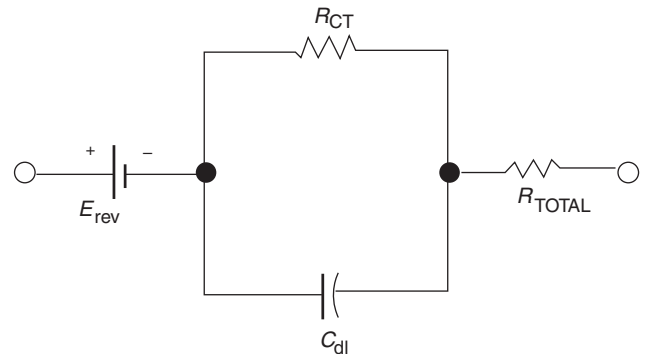


**Figure 3.** Simple equivalent circuit model of the electrode-electrolyte interface.  $C_{\text{dl}}$  represents the double-layer capacitance,  $R_{\text{CT}}$  the charge transfer resistance,  $R_{\text{TOTAL}}$  the sum of the lead and electrolyte resistances, and  $E_{\text{rev}}$  represents the reversible or equilibrium potential.

plot and higher frequencies are on the left, which is generally the case for electrode interface data.

The impedance locus has the form of a semi-circle with high and low frequency intercepts with the real axis at  $90^\circ$  (due to the presence of  $C_{\text{dl}}$  in parallel with  $R_{\text{CT}}$ ). At very low frequencies, the impedance is equal to  $R_{\text{TOTAL}} + R_{\text{CT}}$ , the diameter of the semicircle being equal to  $R_{\text{CT}}$ . At higher frequencies, the impedance is influenced by the value of the parallel capacitance  $C_{\text{dl}}$ . As the capacitive impedance decreases with increasing frequency, current therefore flows through it and the total impedance of the parallel combination decreases. The reactive component and the phase angle increases from zero, reaches a maximum value (which depends on the relative sizes of  $R_{\text{TOTAL}}$  and  $R_{\text{CT}}$ ), and then decreases again toward zero (see Figs. 4 and 5). The frequency at which the reactive component reaches its maximum value ( $\omega_0$ ) is given by  $\omega_0 = 1/R_{\text{CT}}C_{\text{dl}}$  (Fig. 4).

At high frequencies, the impedance is determined by the series resistance  $R_{\text{TOTAL}}$ .

**Bode Plot.** Another popular method of presenting impedance data is the Bode plot. The impedance is plotted

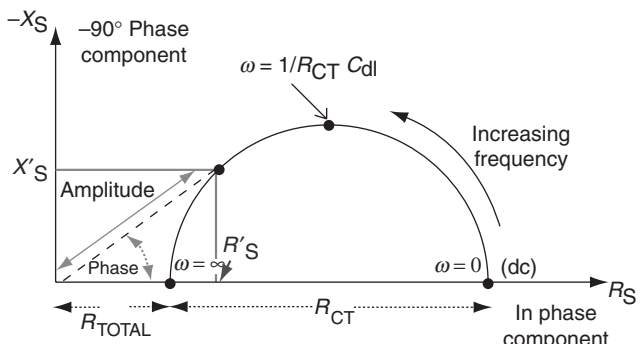


**Figure 4.** Impedance plot for simple equivalent circuit model of the electrode-electrolyte interface. The impedance locus is semi-circular as a result of the parallel combination of  $C_{\text{dl}}$  (the double layer capacitance) and  $R_{\text{CT}}$  (the charge transfer resistance), both of which are in series with  $R_{\text{TOTAL}}$ , the sum of the lead and electrolyte resistances.

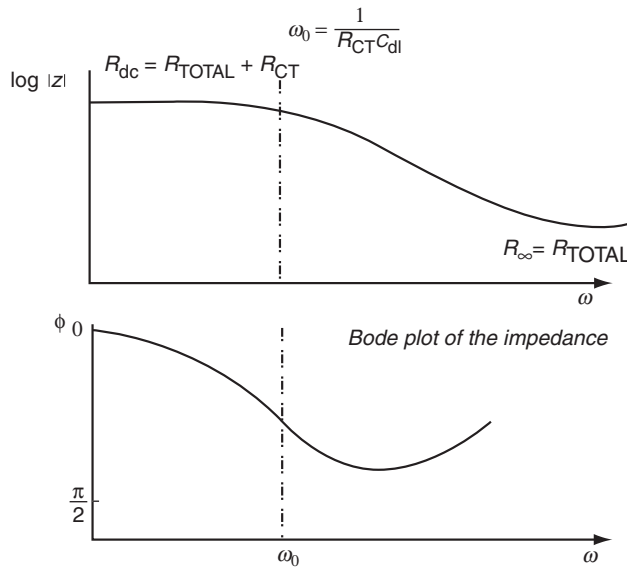


**Figure 5.** Bode plot for the simple ‘3-component’ equivalent circuit model. The magnitude of the impedance decreases from its low frequency value ( $R_{\text{TOTAL}} + R_{\text{CT}}$ ) to  $R_{\text{TOTAL}}$  at very high frequencies. The phase angle of the overall interface impedance increases from  $0^\circ$  at low frequencies, reaches a maximum, which depends on the relative sizes of  $R_{\text{TOTAL}}$  and  $R_{\text{CT}}$  and then decreases again.

with log frequency on the  $x$  axis and both the absolute value of the impedance ( $|Z| = [Z'^2 + Z''^2]^{1/2}$ ) and the phase-shift ( $\phi = \tan^{-1}[Z''/Z']$ ) on the  $y$  axis. Unlike the complex impedance plot, the Bode plot explicitly shows frequency information.

The Bode plot for the electric circuit of Fig. 3 is shown in Fig. 5.

As in the complex impedance plot, the magnitude of the impedance is equal to  $R_{\text{TOTAL}} + R_{\text{CT}}$  at very low frequencies ( $R_{\text{dc}}$ ). The phase angle is zero at this point as the impedance is purely resistive. At very high frequencies, the magnitude of the impedance ( $R_\infty$ ) is equal to that of the series resistance  $R_{\text{TOTAL}}$ . At frequencies in between these two limits, the interface impedance is influenced by the value of the parallel capacitance  $C_{\text{DL}}$ . As the capacitive impedance decreases with increasing frequency, current therefore flows through it and the total impedance of the parallel combination decreases. The phase angle increases from zero, reaches a maximum value (generally less than  $90^\circ$  or  $\pi/2$  rad), and then decreases again toward zero (see Fig. 5).

The above model can be used to explain most key aspects of the electrode–electrolyte interface. It must be pointed out, however, that the equivalent circuit is a gross approximation.

For example, diffusion of ions to the interface from the bulk of the electrolyte (gel or patient) takes place at a finite rate and thus gives rise to impedance to current flow, especially at low frequencies. The diffusion (often termed Warburg) impedance is generally located in series with the charge transfer resistance, both of these being in parallel with the double-layer capacitance. The diffusion impedance has been ignored in the above model as it tends

not to be observed for many biomedical electrode systems over the range of frequencies typically used.

A further simplification is the use of a simple capacitance in the above model. Such ideal capacitive behavior is rarely observed with solid metal electrodes. Instead, an empirical pseudo capacitance or constant phase angle impedance,  $Z_{\text{CPA}}$ , is often used that has a constant phase angle, much like a capacitor.

$$Z_{\text{CPA}} = K(i\omega)^{-\beta} \quad (5)$$

where  $K$  is a measure of the magnitude of  $Z_{\text{CPA}}$  and has units of  $\Omega s^{-\beta}$ , and  $\beta$  is constant such that  $0 < \beta < 1$ . The phase angle of this empirical circuit element ( $\phi = \beta\pi/2$  radians or  $90\beta^\circ$ ) generally lies between  $45^\circ$  and  $90^\circ$  (9). Typically,  $\beta$  has a value of 0.8 for many biomedical electrode systems.

Fricke (10) used the term polarization to describe the constant phase angle impedance and postulated that it was due to spontaneous depolarization of the electrode. Although he did not enlarge on the hypothesis, many authors have used Fricke’s terminology over the intervening years. The present author must concur with Cole and Curtis’ observation that “the use of the term polarization for describing the unexplained effects occurring at the metal–electrolyte interface is only an admission of our ignorance” (11).

The two most likely causes of the observed constant phase angle impedance are specific adsorption and surface roughness effects (12). With solid biomedical electrodes, the nonideal behavior is probably due to the surface roughness of the electrodes (13), which is supported by reports that roughing an electrode surface decreases the measured value of phase angle.

It is also naive to think that surface effects will only distort the nonfaradaic impedance and will have no effect on  $R_{\text{CT}}$  as assumed in the above model. It is more realistic that surface effects will affect the parallel combination of  $C_{\text{DL}}$  and  $R_{\text{CT}}$  giving rise to skewed (14,15) or distorted (16) arcs. The simple equivalent circuit used in this presentation is, however, a useful approximation that enables qualitative interpretation of much of the published data.

**Polarization.** Since the work of Fricke (10), the term polarization has been used to describe just about anything associated with the electrode–electrolyte interface—frequency-dependence, nonlinearity, noise, and so on. Polarization has been defined as “the departure of the electrode potential from the reversible value upon the passage of faradaic current” (7).

Under equilibrium conditions, the electrode potential  $E$  is equal to its reversible potential  $E_{\text{rev}}$ . When a dc or faradaic current,  $i_{\text{dc}}$ , is applied to the electrode interface, it must flow through the resistance  $R_{\text{CT}}$ , which is in parallel with  $C_{\text{DL}}$ . From Ohm’s law, the voltage dropped across this charge transfer resistance will be equal to  $i_{\text{dc}}$  multiplied by  $R_{\text{CT}}$  (Fig. 6). The electrode potential  $E$  is now given by:

$$E = E_{\text{rev}} + i_{\text{dc}}R_{\text{CT}} \quad (6)$$

The electrode, therefore, is no longer operating at its equilibrium or reversible value  $E_{\text{rev}}$ . This change in the

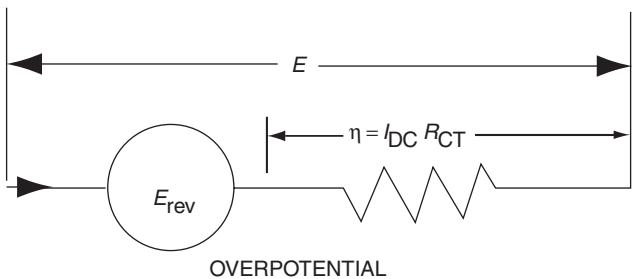


**Figure 6.** Polarization, the departure of the electrode potential from its reversible value upon the passage of faradaic current.

electrode interface's potential from its equilibrium value is termed polarization. The degree of polarization is measured by the additional voltage dropped across  $R_{CT}$ , (or overpotential,  $\eta$ , as it is termed in electrochemistry) where:

$$\eta = /E - E_{rev}/ \quad (7)$$

An ideal nonpolarizable electrode would have a value of  $R_{CT}$  equal to zero and, hence, would exist no resistance to faradaic current. The nonfaradaic impedance would effectively be shorted out and the total interface impedance would be zero. In this case, current would pass freely across the interface unimpeded. Measured biosignals, for example, would be unattenuated and undistorted. A perfect electrode system! The electrode potential would always remain constant at its reversible value.

A perfectly polarizable electrode would not permit the flow of any dc or faradaic current as the charge-transfer resistance in this case is infinite. Such an electrode is sometimes termed a blocking electrode. No faradaic charge would cross the interface, even for large overpotentials, and the electrode couples capacitively with the tissues/electrolyte in this extreme case (Fig. 7).

Real electrodes are, however, neither perfectly polarizable nor perfectly nonpolarizable. Any net current flow across an electrode-electrolyte interface will experience a finite faradaic impedance across which an overpotential will develop.

An electrode system that has a very low value of  $R_{CT}$  lets current traverse the interface almost unimpeded, wastes little energy at the interface, has a relatively small overpotential, and has a relatively nonpolarizable electrode system. Such electrode systems are highly sought after, especially when recording small biosignals from the body surface.

Electrodes made of noble metal come closest to behaving as perfectly polarizable electrodes. As these metals are inert, they tend not to react chemically with the surrounding electrolyte or tissue. Noble metals are, therefore, generally used in the construction of implant electrodes where chemical reaction with surrounding tissues must be avoided in order to minimize tissue toxicity problems. Little steady current can pass in such cases as the charge transfer resistance for these electrodes is therefore very large (Fig. 7). The small current that does pass represents the charging and discharging of the double-layer capaci-

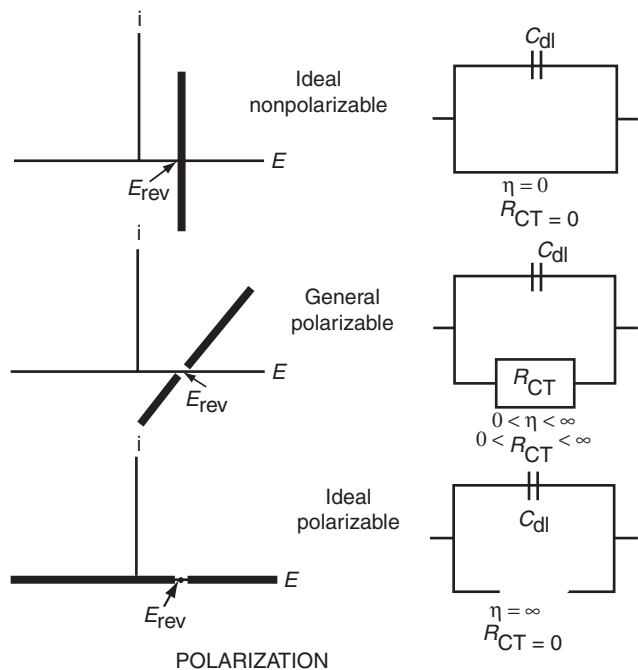


**Figure 7.** The dc current–voltage plots for Ideal Nonpolarizable, General polarizable, and Ideal Polarizable electrode interfaces.

tance. A problem, therefore, exists when designing implant electrodes. For a biocompatibility point of view, one requires a noble, hence polarizable, electrode system, whereas from an electrical performance point of view, one requires a nonpolarizable system. A compromise is achieved by using a polarizable electrode and roughening the surface of the electrode, thus decreasing the large interface impedance.

**Transient Response and Tissue Damage.** The response of the electrode system to sine waves of varying frequencies has been considered above (Complex Impedance and Bode plots) as this is a very useful tool in analyzing circuits or, in this case, electrode systems. Equally relevant is the response of an electrode system to voltage and current steps or pulses, as these will approximate therapeutic stimulation applications.

It must be borne in mind that the conversion from electrical to ionic current takes place at the electrode-tissue interface. Based on the simple equivalent circuit model, current can flow either through the parallel resistance or through the double-layer capacitance.

Current flowing through the parallel resistance involves faradaic charge transfer reactions. At the anode, the electrolysis of water and the oxidation of organic compounds can occur. The oxidation of the electrode itself can also occur, which results in the dissolution of metal. At the cathode, hydrogen ions are reduced to form hydrogen gas, which results in a change in pH near the electrode. The new chemical by products in all of these reactions may lead to tissue damage and, hence, faradaic charge transfer reactions must be avoided (17,18). Current must not, therefore, be allowed to flow through  $R_{CT}$ .

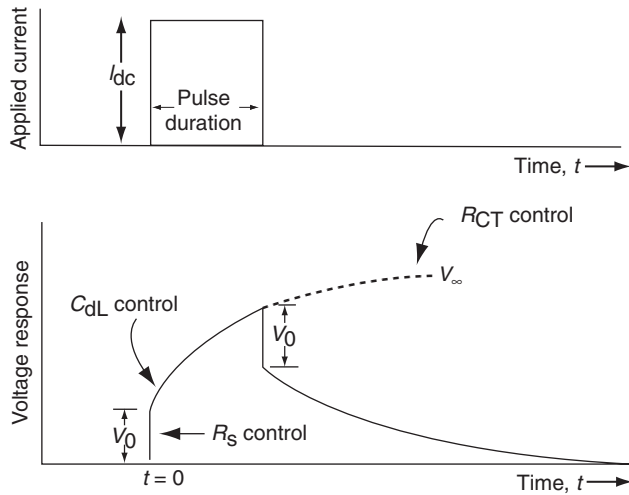


**Figure 8.** Voltage response to a pulse or step in current.

For current flowing through the double-layer capacitance, no charge actually crosses the electrode-tissue interface. Instead, ions in the tissue are attracted or repelled by charges on the electrode, resulting in transient pulses of ionic current. As no net current flows through the interface and electrochemical reactions are not involved, capacitive current is relatively safe. One must therefore seek, as far as possible, to couple capacitively with tissue when seeking to stimulate tissue without causing trauma.

If one applies a pulse of current of amplitude  $I_{dc}$  at time  $t = 0$ , the voltage response of the electrode-interface equivalent circuit model and, it is believed, the electrode-patient system is as shown in Fig. 8.

$$V(t) = I_{dc}R_{TOTAL} + I_{dc}R_{CT}(1 - \exp[-t/R_{CT}C_{dl}]) \quad (8)$$

At  $t = 0$ , the applied current flows unopposed through the capacitor and, hence, only sees the series resistance  $R_{TOTAL}$ . The initial voltage response is, therefore,

$$V_0 = I_{dc}R_{TOTAL} \quad (9)$$

The voltage response is then observed to gradually increase from  $V_0$ . The initial increase in voltage with time is inversely proportional to the magnitude of the capacitance.

For long pulse durations, all of the current will flow through the resistances  $R_{CT}$  and  $R_{TOTAL}$ . The total resistance seen by the current is, therefore,

$$Z_{(t=\infty)} = R_{TOTAL} + R_{CT} \quad (10)$$

and the limit voltage  $V_\infty$  is given by

$$V_\infty = I_{dc}(R_{TOTAL} + R_{CT}) \quad (11)$$

The voltage response will reach this limit value  $V_\infty$  in a time period of approximately five time constants,  $T$ , where  $T = C_{dl}R_{CT}$ .

If a perfect step in voltage,  $V_{dc}$ , is applied to the electrode system or the three-component model, the

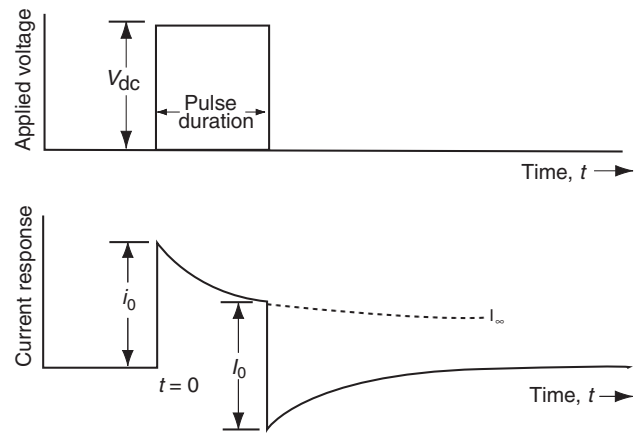


**Figure 9.** Current response to a pulse or step in voltage.

current response is as shown in Fig. 9 and given by the equation

$$I(t) = V_{dc} \left\{ \left( \frac{1}{R_{TOTAL} + R_{CT}} \right) \right\} + \left( \frac{R_{CL}/R_{TOTAL}}{R_{CT} + R_{TOTAL}} \right) \exp \left[ - \frac{R_{CT} + R_{TOTAL}}{R_{CT}R_{TOTAL}C_{dl}} t \right] \quad (12)$$

At the beginning of the voltage step, the resultant current jumps to a relatively large value  $I_0$ , where

$$I_0 = V_{dc}/R_{TOTAL} \quad (13)$$

As time passes, the resultant current decreases exponentially with an initial slope inversely proportional to the capacitance  $C_{dl}$ . Eventually, the current will reach a limiting value of  $I_\infty$ , where

$$I_\infty = \frac{V_{dc}}{R_{TOTAL} + R_{CT}} \quad (14)$$

**Tissue Damage.** The rise in voltage response or the decrease in current response is often attributed in the literature to a mysterious phenomena called polarization. It is, in fact, nothing more than the transient response of a simple three-component circuit model.

When one applies pulses to an electrode-tissue interface (either for implanted or surface stimulation), the applied or resultant current initially flows into the patient via the double-layer capacitance. No reactions are associated with the capacitive flow of current and, hence, few undesirable effects exist when using short duration pulses (i.e. with a duration less than one time constant). As the pulse duration is increased, however, progressively more current flows through the parallel charge transfer resistance and the patient is more at risk due to the reaction byproducts, which is especially true if the pulse is applied for a length of time longer than five time constants giving the voltage or current response time to level off and reach its steady-state value of  $V_\infty$  (or  $I_\infty$ ). At this point, most of the current is flowing through the charge-transfer resistance and charge is therefore injected into the tissues via a faradaic process. The byproducts of the electrochemical reactions involved in

the charge-transfer process will diffuse into the skin or tissue, causing chemical injury (19). As the leveling off of the voltage response is indicative of pure charge transfer control, this feature must be avoided at all costs by either avoiding long duration pulses or by using electrode systems with very long time constants,  $T = C_{dl}R_{CT}$ . In both cases, charge will be largely applied to the body via relatively safe capacitive processes.

It may not always be possible to use sufficiently short pulse durations to avoid tissue damage and still achieve therapeutic effect. It must also be noted that even when using short pulses where the current or voltage response has not leveled off, some current still flows through  $R_{CT}$  and a faradaic charge-transfer reaction takes place, with the associated, albeit reduced, problems (18). Over extended periods of stimulation, the byproducts will accumulate in the tissues. In the past, however, the applied waveforms found experimentally to minimize electrode and tissue damage are consistent with the basic goal of minimizing the flow of faradaic current across the electrode interface (20) and thus ensuring little, if any, net transfer of charge. Decreasing the duration, amplitude, and rate of current pulses have all been suggested as each ensures  $C_{dl}$  control of the transients and thus avoids, to some extent at least, the undesirable faradaic processes.

An alternative to using short pulse durations is to use electrode systems with long time constants [i.e., with a large value of  $R_{CT}$  (faradaic charge-transfer resistance) or  $C_{dl}$  (double-layer capacitance)]. As we have seen, noble metals react with difficulty with surrounding tissues and thus have large values of  $R_{CT}$  (19). For a given pulse duration, they tend to couple capacitively with tissue. The reactions on both anode and cathode are reversible, involving surface oxygen, and this reversibility explains the observed identical nature of anodic and cathodic waveforms (19). As a result, noble electrodes are widely used for physiological stimulation. Unfortunately, noble metals give rise to large interface impedances. From a biocompatibility point of view, one requires a noble (hence, large impedance) electrode system, whereas from an electrical performance point of view, one requires a low impedance system. A compromise is achieved by using such polarizable electrode materials and roughening the surface of the electrode, thus decreasing the large interface impedance. Roughening the electrode surface gives rise to a significant increase in the interface capacitance, thus increasing further the time constant ( $T \uparrow = C_{dl} \uparrow R_{CT}$ ) and ensuring that the voltage or current response is even more dominated by the highly desirable capacitive processes while decreasing the interface impedance.

It would be a gross oversimplification to attempt to demystify biomedical electrode design by stating that all high performance biomedical electrodes simply have rough surfaces. However, a significant element of truth exists in the statement. For example, terms like activated, sintered, and porous have been used to describe implant electrodes for cardiac pacing and indicate that the electrode fabrication process results, deliberately or otherwise, in a rough-surfaced electrode. It could be argued that it is

often the surface finish rather than the electrode metal that gives rise to the favorable electrical properties reported, especially the low interface impedances.

Most electrical stimulation electrodes rely, to some extent, on faradaic mechanisms at the interface between the metal and the tissue. Even in the case of noble metal electrodes with short pulse durations, byproducts of the electrochemical reactions involved will accumulate over time in the tissues when a signal is applied in one direction (monophasic) and will eventually give rise to irritation. With surface stimulation, for example, early designs of electrodes incorporated thick pads of electrolyte-impregnated lint in order to distance the patient's skin from the electrode-electrolyte interface and the undesirable byproducts. Obviously, with implanted electrodes, that short term solution is not possible.

In particular, monophasic anodic pulses must be avoided as they will cause corrosion problems. Additionally, for most applications, cathodic stimulation has a lower threshold than anodic stimulation. Even in the case of monophasic cathodic pulses, however, current flows in only one direction and the chemical reactions at the interface are not reversed.

Biphasic waveforms are preferred in most electrotherapies as the byproducts of the forward reaction are thought to be recaptured by the reverse reaction (21). In using charge balanced waveforms, it is often believed that because no net charge transfer exists across the electrode-skin interface, no net flow of potentially harmful byproducts into the skin. Unfortunately, the electrochemical reaction that occurs to enable the flow of current during the first phase is not necessarily that involved in the second. Byproducts of the first reaction are therefore not always recaptured and may escape from the interface into the patient (22). However, it must be pointed out that the use of charge balanced biphasic waveforms does indeed greatly minimize the problem and, hence, its widespread use in a range of surface and implant applications. Additionally, surface biphasic stimulation is found to be more comfortable than monophasic.

**Limit Voltages and Currents of Linearity.** Although the non-linearity of the skin's electrical properties has been investigated under a range of conditions, the phenomenon is still far from well understood. "There appears to be, so far, no model available which accounts for both the linear and nonlinear behavior of the electrodes in the frequency and time domains" (23). It is an important feature of an electrode as 'it appears...that electrodes often introduce nonlinear characteristics that are erroneously ascribed to the biological system under study (24).

Schwan proposed empirical relationships for the limit current of linearity and the limit voltage of linearity.

**Limit Current of Linearity.** If has been observed that electrode-tissue interface impedance nonlinear behavior is first evidenced at low frequencies. As the applied current amplitude is increased, progressively higher frequency points are affected. Schwan proposed a limit current of

linearity  $i_L$ . He observed that the relationship between the angular velocity of a given impedance point and the current amplitude required to drive it into nonlinearity (deviate by more than 10% from its linear, small-signal value) was well expressed by the empirical relationship

$$i_L = B \omega^\beta \quad (15)$$

where  $B$  is a constant particular to the electrode system and  $\beta$  is the fractional power that appears in equation 5.

Schwan and others (25–28) have observed that this empirical relationship is valid for many electrode systems over wide frequency ranges.

The presence of  $\beta$  (a parameter describing the frequency dependence of the linear interface impedance) in a relationship describing the nonlinearity of the system was found most intriguing.

The solution to this mystery is quite simple when it is approached from the right direction. Generally, researchers have assumed that the observed nonlinear behavior is attributable to the high frequency  $Z_{CPA}$  impedance (Eq. 5), which they observe under linear, small-signal conditions and over the limited frequency ranges they use. However, in parallel with  $Z_{CPA}$  is the charge transfer resistance  $R_{CT}^0$ , which, in the linear range, has a very large value  $R_{CT}^0$ , where

$$R_{CT(0)}^0 = \frac{RT}{nF} \frac{1}{i_0} \quad (16)$$

As a result, its contribution is either not observed or ignored.

The value of the charge-transfer resistance can be derived from the Butler–Volmer equation and is very nonlinear, decreasing rapidly with applied signal (ac or dc) amplitude. Compared with  $R_{CT}$ ,  $Z_{CPA}$  is relatively linear.  $R_{CT}$  is therefore the source of the observed nonlinear behavior.

As the applied current amplitude is increased, the charge transfer resistance decreases rapidly, causing the diameter of the impedance locus to decrease. As the low frequency end of the arc is dominated by the charge transfer resistance, the effects of such nonlinearity will be first evidenced at these frequencies. Low frequency points are therefore the first to deviate significantly (by more than 10%) from their small-signal, linear values, as observed by Schwan and others. As the applied signal amplitude is further increased, the diameter of the impedance locus decreases further, and progressively higher frequencies are affected (29,30).

Simplistically, it can be shown that the following approximations can be made over limited ranges of frequency or applied signal amplitude:

- Approximate relationship between applied current and  $R_{CT}$

$$i \propto 1/R_{CT} \quad (17)$$

- Approximate relationship between  $R_{CT}$  and the frequency at which nonlinearity occurs

$$R_{CT} \propto \omega^{-\beta} \quad (18)$$

Then, by cancelling  $R_{CT}$ , in the above two equations,

- Approximate relationship between applied current and the frequency at which nonlinearity occurs

$$i_L \propto \omega^\beta \quad (19)$$

as found by Schwan. The presence of  $\beta$  in the expression of an electrode system's nonlinear behavior is therefore simply due to the presence of a very nonlinear resistance in parallel with a relatively linear, frequency-dependent  $Z_{CPA}$ . A more accurate calculation based on the equivalent circuit model outlined above and the Butler–Volmer equation was published (29).

**Limit Voltage of Linearity.** Schwan and others (25,28) also postulated that the electrode–electrolyte interface impedance becomes nonlinear at a certain limit voltage,  $V_L$ , which they found to be independent of the frequency of the applied signal.

Using the Butler–Volmer equation and the equation for the impedance of the equivalent circuit model, the voltage limit of linearity can be calculated for a range of frequencies (31). It can be shown that the charge-transfer resistance decreases pseudo exponentially with applied voltage amplitude, initially causing low frequency impedance points on the locus to deviate from their small-signal values (32,33).

At very low frequencies, such that  $\omega \rightarrow 0$ , the voltage limit of linearity,  $V_L$ , approximates to the voltage at which the charge-transfer resistance decreases by 10% from its small-signal value, which occurs at  $V_L = 40/n$  mV, where  $n$  is the number of electrons per molecule oxidized or reduced (31).

As the applied voltage is increased above this low frequency limiting value, the charge transfer resistance further decreases and affects progressively higher frequency points (i.e., become nonlinear). The derived log ( $f$ ) versus  $V_L$  plot is found to be a straight line over a wide range of frequencies.  $V_L$  is observed to increase only very slightly with frequency, which would agree qualitatively with Onaral and Schwan's results (28), where  $V_L$  increased from 106 to only 129 mV over the frequency range of 10 mHz–100 Hz for platinum electrodes in saline, which would also explain why, in the past,  $V_L$  has been assumed constant and independent of the applied frequency.

**Electrode Metals.** As biocompatibility is of great importance in implants, implant electrode materials are generally confined to those that are essentially inert and do not react with the surrounding tissues. As cardiac pacing electrodes were among the first implanted and have had a long, generally successfully and well-researched history, most conclusions drawn on the suitability of materials for implant electrodes are based on pacing electrodes.

Implant electrodes are and have been generally made from noble metals such as gold, platinum, iridium, rhodium, and palladium. Platinum has been the most widely used as it has excellent corrosion resistance and produces relatively low polarization (34). Platinum, however, is mechanically relatively soft and for many applications is

alloyed with much harder iridium, producing platinum–iridium. Other noble metal alloys that have been used include gold–platinum–rhodium, platinum–rhodium, and gold–palladium–rhodium.

Passive metals, such as titanium, tantalum, zirconium, tungsten, and chromium, have been successfully implanted. Titanium has been widely used because it forms a nonconducting oxide layer at the surface. This coating prevents charge transfer at the electrode interface. Titanium, therefore, exhibits a high resistance to corrosion. Stainless steel is similar in that it acquires a protective oxide layer that renders it inert. Although stainless steels were used in early pacing electrodes, they do not appear to have the required corrosion resistance for long-term use. Stainless-steel pacing electrodes were discontinued after the 1960s because of unreliable corrosion resistance (34,35).

Some early pacing electrodes were made of Elgiloy (an alloy of Fe, Ni, CO, Cr, and MO from Elgin Watch Co.) However, Elgiloy has marginal corrosion resistance and produces a relatively high polarization overvoltage. It was discontinued in the 1980s. Carbon is an inert, nonmetallic element that has similar electrochemical characteristics to noble metals and continues to be used successfully as an implant electrode. Materials such as zinc, copper, mercury, nickel, lead, copper, silver, silver chloride, iron, and mild steel have been found toxic to body tissues and are normally not used.

Biocompatibility has been defined as the ability of a material to perform with an appropriate host response in a specific application (36). Strictly speaking, no such thing as a biocompatible material exists as an implant's biocompatibility will also depend on a range of variables including its shape and surface finish.

Stimulation threshold is a key parameter in implant stimulation electrode design. When activated vitreous carbon electrodes were first introduced in pacing electrodes, they were found to have relatively low chronic thresholds. These thresholds were thought to be the result of the superior biocompatibility of the carbon electrode. Other researchers similarly interpreted the low thresholds observed for their new exotic materials such as indium oxide, titanium nitride, and semimetal ceramics. Stokes (34), however, concluded that "material selection appears to have little or nothing to do with threshold evolution—as long as the material is biocompatible and reasonably corrosion resistant. Thus our experiments with biocompatible materials such as carbon, titanium, platinum, iridium oxide, and many more have all produced about the same results when tested as polished electrodes, all other factors held equal". Stokes went on to point out "while the bulk properties of an electrode material are important, it is the electrode-tissue interface that determines the electrode's performance. In fact, the surface microstructure of the electrode is critical" (34). It would appear that the microstructure of an electrode surface may affect cellular adhesion and activation, thus reducing the foreign body response. It is, therefore, the surface structure of many of the new materials (resulting from their fabrication process) that gives rise to the observed positive effect on threshold evolution over time, rather than the biocompatibility of the bulk material.

Another advantage of porous and microporous implant surfaces is their reduced interface impedance. Although interface impedance is generally less critical for implanted stimulation electrodes, many such electrodes (e.g., implanted pacing electrodes) are used to monitor biosignals as well as to deliver the required stimulation impulses. Decreased interface impedance helps in this regard.

Implanted biosignal monitoring electrodes require stable potentials as well as low interface impedances to minimize biosignal recording problems. These metals have high positive standard electrode potentials ( $E^{\circ}$  in Eq. 1) and are the lowest ones on the electromotive series. As noble metal electrodes do not tend to react chemically with the electrolyte, the Nernst equation is not defined and the measured potential is often influenced more by any traces of impurities on the surface than by the intrinsic properties of the metal itself. The electrode potential can drift randomly, especially immediately following implantation. It may fluctuate widely under apparently identical circumstances, which is an inherent disadvantage of noble materials.

External biosignal monitoring electrodes can generally use high electrical performance nonnoble materials such as silver–silver chloride without fear of biocompatibility problems (2). Silver–silver chloride has been found to be an excellent electrode sensor material as, when it is in contact with a chloride gel, it has the following characteristics:

1. A low, stable electrode potential.
2. A low level of intrinsic noise.
3. A small value of charge transfer resistance (i.e., it is relatively nonpolarizable).
4. A small interface impedance.

A silver–silver chloride electrode is generally made by the deposition of a layer of silver chloride onto a silver electrode. Silver chloride is a sparingly soluble salt and, thus, effectively provides the silver electrode with a saturated silver–chloride buffer, which facilitates exchanges of charge between the silver electrode and the sodium chloride environment of the gel and human body. The system behaves as a reversible chloride ion electrode, and the Nernst potential, in this case, depends on the activity (which is closely related to concentration) of the environment chloride ions and not on that of the silver ions. The potential of this electrode is, therefore, quite stable (as well as small) when the electrode is placed in an electrolyte containing Cl as the principal anion—as is the case in the human body and electrode gels (2).

Electrical noise (potential fluctuations) can occur spontaneously at the electrode interface without any physiological input. Ag/AgCl electrodes have been shown to be particularly stable and resistant to noise (37).

A silver–silver chloride electrode has a relatively large value of exchange current density (2) (Eq. 4) and, hence, a very low value of charge transfer resistance,  $R_{CT}$ . Charge is transferred across the interface with relative ease and little voltage is dropped across the interface. The electrode therefore operates close to its equilibrium or reversible

potential. Ag-AgCl electrodes are, therefore, relatively nonpolarizable.

When a smooth-surfaced electrode is chlorided, the AgCl deposit can give rise to a very rough surface and thus to relatively very low interface impedances (37,38).  $K$ , the magnitude of the interface pseudocapacitance (Eq. 5), is observed to decrease following the deposition of an AgCl layer (39). However, although AgCl facilitates the interfacial electrochemistry, it is very resistive having a resistivity of around  $10^5$ – $10^6 \Omega\text{-cm}$  (2). As the layer thickness increases, the series resistance,  $R_{\text{TOTAL}}$  will therefore increase. This series resistance dominates the very high frequency interface impedance, and the latter will also increase with chloride deposit. Therefore, an optimal layer thickness exists, for a given frequency, that decreases the interface impedance and yet does not significantly increase the series resistance,  $R_{\text{TOTAL}}$  (29). The optimal silver chloride layer thickness consequently depends on the frequency range of interest (40).

Tin-stannous chloride, a material somewhat similar to silver–silver chloride, was used in some biosignal electrodes (41).

Electrode material and high electrical performance is generally less critical for external stimulation electrodes such as TENS and external pacing electrodes (current density distribution is the key concern). The majority of commercially available TENS electrodes are molded from an elastomer such as silicone rubber or a plastic such as ethylene vinyl acetate and loaded with electrically conductive carbon black. Mannheimer and Lampe (42) pointed out that the only tangible disadvantage with having a large electrode interface impedance is that more power will be required from the stimulator to drive the stimulating current through the electrodes into the patient.

Graphite-loaded polyesters and similar materials are used in external pacing electrodes, for example. Some are constructed using tin as the metal layer. In early electrodes, the combination of tin and the chloride-based gel gave rise to pitting of the metal. Improvements made to the gels and the use of high purity tin have effectively removed this problem.

Although silver–silver chloride has been and still is used in some external electrostimulation electrodes, it should be used with care. Silver chloride is deposited electrolytically and can therefore be either removed by the passage of current or a thicker, high resistance layer deposited, depending on the polarity of the electrode, which can be a significant problem in iontophoretic transdermal drug delivery and may cause problems in multifunction pads, which include a silver–silver chloride layer to enable distortion-free monitoring of the ECG through electrodes designed to deliver the pacing or defibrillation impulses.

## The Skin

**Structure of the Skin.** The skin is a multi layered organ that covers and protects the body. It is made up of three principal layers—the epidermis, the dermis, and the subcutaneous layer. (*Note:* In the literature, variations exist in the terminology used to denote these layers.)

The epidermis, the outermost layer, is around  $100 \mu\text{m}$  thick, depending on body site. It is the strongest layer, providing a protective barrier against the outside hostile environment. Unlike any other organ of the body, the epidermis renews itself continually. It can be subdivided into several layers, with the basal layer forming the innermost layer and the stratum corneum the outermost layer. Cells in the basal layer constantly multiply and, as they are pushed up toward the skin's external surface, the cells undergo changes. Eventually, layers of compacted, flattened, nonnucleated, dehydrated cells (called corneocytes) form the stratum corneum. These dead cells are continuously being shed and are replaced from the underlying epidermal layers. The intercellular spaces between corneocytes are occupied by arrays of bilaminar membranes with the morphological features of polar lipids (43). This matrix appears to serve to bind the cells and the stratum corneum has been described in terms of corneocyte bricks surrounded by lipid mortar (44). On average, the stratum corneum comprises around 20 cell layers thick and has a thickness of around  $10$ – $15 \mu\text{m}$ . Thickness will, however, vary with the number of cell layers making up the stratum corneum and the state of hydration. On some body areas, it can be several hundred micrometers thick. The epidermal layer is traversed by numerous skin appendages such as hair follicles, sebaceous glands, and sweat glands.

The underlying layers of the epidermis are, in contrast, a relatively aqueous environment. The transition from an essentially nonconductive, lipophilic membrane (the stratum corneum) to an aqueous tissue (viable epidermis and dermis) gives rise to the skin's barrier properties.

The dermis is the second layer of the skin and, with an approximate thickness of  $2 \text{ mm}$ , is considerably thicker than the epidermis. It is formed from a dense network of connective tissue made of collagen fibers, giving the skin much of its elasticity and strength. Embedded in the dermis are blood vessels, hair follicles, sebaceous and sweat glands, and several types of sensory nerve endings.

The final layer of the skin (the subcutaneous layer) is found beneath the dermis layer. It contains structures of connective tissues and enables the skin on most parts of the body to move freely across the underlying bone structures. It is one of the body's areas for fat storage and acts as a cushion to protect delicate organs lying beneath the skin.

## Skin Impedance

**Electrical Properties of the Skin.** As the stratum corneum is relatively nonconductive, it presents a high impedance to the transmission of electric currents. As a result, the impedance of the skin is the largest component of the overall interelectrode impedance (Fig. 10). Nonetheless, due to the stratum corneum's dielectric properties and its thinness, it permits capacitive coupling between a conductive metal electrode placed on the skin surface and the underlying conductive tissues. One can imagine the relatively nonconductive stratum corneum sandwiched between the conductive electrode and the conductive tissues underlying the stratum corneum forming a parallel-plate capacitor. The stratum corneum's electrical impedance is, therefore, often represented by a simple capacitor,  $C_{\text{SP}}$ . (The subscript SP refers to Skin and Parallel.)

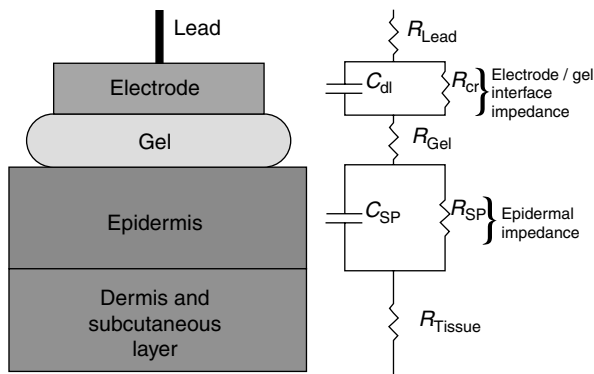


**Figure 10.** Schematic representation of the skin and its equivalent circuit model.

Some ions do, however, manage to cross the stratum corneum via paracellular pathways and through the skin's appendages (hair follicles, sweat ducts, sebaceous glands, imperfections in the integrity of the skin). As skin appendages extend through the stratum corneum barrier they can act as shunts to the interior. The flow of ionic current can be represented electrically by a large resistance,  $R_{\text{SP}}$ , in parallel with  $C_{\text{SP}}$ .

The underlying layers of the epidermis are, in contrast, relatively conductive and can be collectively represented by a tissue resistance,  $R_{\text{Tissue}}$ .

A simple equivalent circuit model of the overall electrode-gel-skin system is therefore shown in Fig. 10 and includes the electrode lead resistance,  $R_{\text{Lead}}$ ; the electrode-gel interface impedance (the double-layer capacitance,  $C_{\text{dl}}$ , in parallel with the charge transfer resistance,  $R_{\text{CT}}$ ); the gel resistance,  $R_{\text{Gel}}$ ; the skin impedance (the parallel combination of a capacitance,  $C_{\text{SP}}$  and a resistance,  $R_{\text{SP}}$ ), and the underlying tissue resistance,  $R_{\text{Tissue}}$ .

It must be borne in mind that this equivalent circuit model is a simplification of the rather complex electrical properties of the skin. For example, it has been found experimentally (45,46) that the capacitance of the skin is better described by an empirical, constant phase angle impedance,  $Z_{\text{CPA}}$ , where

$$Z_{\text{CPA(S)}} = K_S(j\omega)^{-\alpha} \quad (20)$$

[which is similar to the empirical expression for the pseudo capacitance often used to represent the nonideal capacitive properties of the electrode interface's double-layer capacitance (Eq. 5)].

$K$  has units of  $\Omega \cdot s^{-\alpha}$ . The parameter  $\alpha$  is constant such that  $0 \leq \alpha \leq 1$ . The fractional power,  $\alpha$ , of the capacitive impedance has been found to be related to the degree of hydration of the stratum corneum (47). If the epidermal layer behaved as a simple capacitance,  $\alpha$  would equal unity. The actual value of  $\alpha$ , normally around 0.8–0.9, is a measure of the deviation from this ideal behavior.

The use of  $C_{\text{SP}}$  will, however, be sufficient for this present review. The lead resistance, the gel resistance, the tissue resistance, and the electrode-gel interface impedance are all relatively small in comparison with the large skin impedance. Skin impedance, therefore, generally dominates and will be studied in more depth.

**The Skin's Parallel Capacitance,  $C_{\text{SP}}$ .** It was suggested above that the electrode-skin interface can be approximated by a capacitor with the stratum corneum forming the dielectric layer sandwiched between the electrode and the underlying tissues that form the conductive plates. It can be seen from Eq. 2 that the skin's capacitance will increase as the thickness of the stratum corneum decreases, its dielectric constant increases, or the area of the electrode increases.

The number of cell layers in the stratum corneum can range from 12 to 30 (48). Epidermal thickness can, therefore vary greatly for different body sites within the range of about 10 to well over 100  $\mu\text{m}$  (49). The stratum corneum can be, for example, as thick as 400–600  $\mu\text{m}$  in the palm and plantar areas and as little as 10–20  $\mu\text{m}$  on the back, legs, and abdomen (50). The value of the capacitance of the skin is related to the thickness and composition of the stratum corneum and has a typical value in the range 0.02–0.06  $\mu\text{F} \cdot \text{cm}^{-2}$  when measured using electrodes with "wet" electrolyte gels several minutes following electrode application (51,52). As the stratum corneum is typically at least 10 times as thick on the palms of the hands and soles of the feet as compared with other body areas, the skin capacitance at these points is considerably smaller than at other sites on the body. The stratum corneum on the face and scalp is not as thick as on other body parts and is characterized by large capacitance values.

Dark-skinned subjects have stratum corneum layers that are more dense and contain more layers of cells than fair-skinned subjects (48). Not surprisingly, they are characterized by skin capacitances that are much lower (skin impedances, Eq. 3, much higher) than those for fair-skinned subjects. One should therefore take care when assessing a new electrode system or associated device that they are tested on a range of subjects and skin sites. What may work well on a subject with low skin impedance in a warm and humid environment may be found later to fail on a high impedance subject, especially in a cold or dry environment.

**The Skin's Parallel Resistance,  $R_{\text{SP}}$ .** Although the stratum corneum does not easily allow foreign substances to traverse it, some current, carried by ions, manages to flow through it. The difficulty or resistance, this current experiences in passing through the skin is represented in the equivalent circuit (Fig. 10) by the parallel resistance,  $R_{\text{SP}}$ .

The skin's resistance is highly dependent on the presence and activity of sweat glands and on the presence of other appendageal pathways. An average human skin surface is believed to contain between 200 and 250 sweat ducts on every square centimeter (53). The density of sweat glands varies greatly over the body surface with a value of approximately 370 per  $\text{cm}^2$  on the palms of the hands and the soles of the feet and a value of approximately 160 per  $\text{cm}^2$  on the forearm (49). The diameter of the ducts can range from 5 to 20  $\mu\text{m}$ . It is, therefore, not surprising that  $R_{\text{SP}}$  is reported to vary greatly from patient to patient, from body site-to-body site, and with time. The measured values of  $R_{\text{SP}}$  are much smaller on areas with high densities of sweat glands, such as the palms of the hands (in spite of the thicker stratum corneum layer), especially when the

glands are active in response to thermal or psychophysiological stimuli.

An average human skin surface is reported to contain between 40 and 70 hair follicles per square centimeter (53). The presence of a high density of hair follicles (which act as low resistance shunts) gives rise to a very low value of skin parallel resistance,  $R_{SP}$ . However, this observation is counterbalanced by the difficulty in making firm mechanical and electrical contact to hirsute body sites or patients. In such cases, the skin impedance is very large at best. Generally, the electrodes fall off and, hence, require the shaving of the skin site prior to electrode application.

Observed intersite and interpatient variations in skin impedance tend to be due to large variations in  $R_{SP}$ . In the low frequency range, dominated by  $R_{SP}$ , regional differences in skin impedance were observed by Rothman (54), Lawler et al. (55), and Rosell et al. (56). Low frequency skin impedance was observed to decrease in the following order: thumb, forearm, abdomen and, smallest of all, forehead. Similarly, Almasi and Schmitt (57) observed the low frequency skin (10 Hz) impedance to decrease in the order of outer forearm, leg, inner forearm, back, chest, earlobes, and forehead. The forehead appears to have a very low skin impedance value (58), presumably as a result of the stratum corneum on the face and scalp being thinner than that on other body parts (48) and the presence of a high density of sweat glands. Almasi and Schmitt (57) plotted their average impedance values for the body sites on a complex impedance plot and found that most of the points lay along a "smooth common locus of monotonically increasing phase angle and impedance magnitude." This behavior was successfully interpreted by McAdams and Jossinet (32), who showed that such frequency loci were formed when the skin's parallel resistance varied greatly from site to site while the skin's capacitance remained relatively constant. Two body sites did not fit the locus and, hence, the physical explanation; these sites were the palm and fingertips. These body sites have much larger epidermal thicknesses and, hence, have skin capacitance values much smaller than other body sites.

One must be very careful when assessing different electrode designs or gels. Testing different electrodes on different patients is certain to give misleading results due to the intersubject variations, unless, of course, large numbers of subjects are used and statistically significant differences are observed.

$R_{SP}$  varies greatly over time due to a number of parameters including room temperature and psychophysiological stimuli. The latter effect is exploited in so-called lie detectors. Schmitt and Almasi (59) reported that a considerable daily variation exists in a given subject, and seasonal changes have also been reported (60). Testing a range of electrodes on the same subject but on different days is, therefore, not optimal either, as day-to-day variations in skin impedance, especially fluctuations in  $R_{SP}$ , will nullify the validity of this approach. For example, Searle and Kirkup (61) found that the diurnal variations on a given subject for a given electrode was much larger than any difference between the range of electrode designs they tested in any one recording session. It should be further noted that the electrode test sites should be allowed to

recover for several days between experiments to enable the skin to recover. For example, peeling off an adhesive electrode will remove some of the underlying stratum corneum. Any electrode subsequently tested on the site will benefit from this prior skin stripping (see below).

Electrode designs must, therefore, be compared *in vivo* by testing them at the same time on the same subject. One must still bear in mind the significant differences in skin impedance that exist over the subject's body, as outlined above. Even testing the electrodes at the same time on a limb of a given subject remains problematic. The different skin sites involved, even if located close together, will give rise to significant differences in the measured electrode-skin impedances, which may be wrongly attributed to the electrode designs or gels under test. Searle and Kirkup (61), for example, showed that testing a range of dry electrode metals on the inner forearm gave rise to potentially very misleading results. Electrodes placed closer to the wrist gave rise to lower impedances due to the presence of a higher concentration of sweat glands.

Electrodes must therefore be repeatedly tested at the same time, under the same conditions, varying their relative positions in order to clearly establish their relative performances. McAdams et al. developed a four-channel impedance monitoring system to enable the simultaneous comparison of electrode designs/gels (62).

**Skin Potential Motion Artifact.** A potential difference  $E_S$ , given by the Nernst equation, exists across the epidermis as a result of ionic concentration differences. This potential varies from patient to patient, from site to site, and depends on gel composition (if used) and skin condition.

The skin surface is normally negative with respect to the inside of the body. Skin potential becomes more negative when sweat glands are active, and palmar and plantar surfaces, with their higher sweat gland concentrations, are the most negative. Increasing gel concentrations of NaCl or KCl also render the site more negative. The parameter  $E_S$  has a typical value of 15–30 mV (63).

The dependence of the skin potential on the thickness of the epidermal layer is important to many ECG recording applications. If the thickness of the layer is changed by stretching or pressing down on the skin, the skin potential can vary by 5–10 mV compared with, for example, the 1 or 2 mV ECG signal. As these fluctuations generally result from patient movement, they are termed motion artifact. Motion or skin-deformation artifact is a serious problem during exercise cardiac stress testing of patients on treadmills or exercise bicycles, during ambulatory monitoring, and while monitoring patients lying in bed (64,65) (Fig. 11).

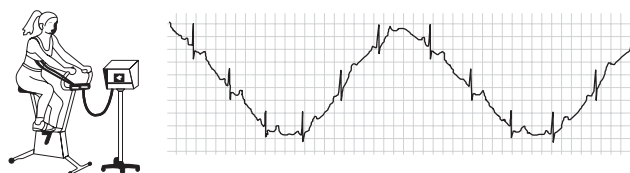


**Figure 11.** Disturbance of biosignal due to patient movement. (Redrawn from Ref. 65.)

Abrading or puncturing the skin is often used in stress testing to remove or bypass the problem source. Although skin potential increases with gel concentration, artifact gradually decreases with time as the conductive electrode gel soaks into the skin and renders the stratum corneum more conductive. High concentration gels are often used for short-term diagnostic applications where the risk of skin irritation is outweighed by the need for clear traces.

In general, hydrogel-based electrodes (see below) should not be used for stress testing or in other monitoring applications that are likely to suffer motion artifact problems. Hydrogels tend not to hydrate the skin and, hence, do not actively attack the source of the problem. The same comment applies for dry (gel-less) electrodes.

In stress testing and ambulatory event monitoring, modified electrode locations are used to avoid muscular or flabby areas of the body and thus minimize skin deformation (and EMG) artifact. Stress loops are formed in the connecting leads, which are taped to the patient and used to avoid direct pull on electrodes and the underlying skin. The use of foam-backed electrodes tends to absorb any pull on the electrode and minimizes artifact.

**Electrode Gels and Their Effects.** Dry electrodes are successfully used in some monitoring applications. Suitably designed gel-less electrodes have advantages when used in the home environment where the patient may not remember or have the time to apply gel electrodes prior to use (66).

For many home-based monitoring applications, electrodes are manufactured from noncorroding materials such as stainless steel, which can be repeatedly washed and reused. Unfortunately, such polarizable materials give rise to poor electrical performances. In order to ensure good, stable electrode potentials, silver–silver chloride electrodes should be used (see below).

Jossinet and McAdams (67) demonstrated that the impedance of a dry electrode decreases pseudoexponentially due to the gradual buildup of sweat under an occlusive, gel-less electrode and the resultant progressive hydration of the underlying skin. Searle and Kirkup (61) reported that the decrease in skin impedance of dry electrodes is polyexponential and requires two time constants, one very short (~45 s) and the other almost 10 times longer (~450 s), possibly indicating two different processes at work.

Given that the surface of the skin is irregular, a flat dry electrode will initially only make contact with a few ‘peaks’ on the skin surface. Therefore, a smaller effective contact area exists than one would otherwise expect. However, as sweat builds up under the occlusive, dry electrode, a better contact with the skin will result in a relatively rapid increase in the measured value of  $C_{SP}$ . Human sweat contains a small amount of sodium chloride [~0.1–0.4% NaCl (49)], and hence serves as a weak electrolyte. It is suggested by the author that this accounts for the shorter time constant. (The longer time constant is probably indicative of the progressive hydration on the underlying skin resulting in a gradual decrease in  $R_{SP}$ .) As will be outlined below,  $R_{SP}$  is observed to decrease with a time constant of around 10 min in the presence of an electrolyte gel, which

agrees quite well with the 7.5 min observed by Searle and Kirkup (61).

Before leaving gel-less electrodes, it should be pointed out that in certain applications that employ very high frequency signals, such as electrical impedance tomography (EIT), the use of a gel pad may not be needed as it will contribute a small but significant contact resistance to the desired measurement (5). In such instances, the use of a very thin spray of moisture onto the electrode surface prior to its firm application to the patient’s skin may be all that is required. Profiled dry electrodes firmly pressed onto the skin may also be adequate for certain home-based biosignal applications. If skin impedance is a problem with standard button electrode designs, this can be addressed by increasing the electrode area in the noncritical axis. For example, long, narrow, dry electrodes are used for precordial ECG recording, which enable a large contact area while ensuring sufficient interelectrode distances on the chest (66).

Electrode gels serve (1) to ensure a good electrical contact between the electrode and the patient’s skin, (2) to facilitate the transfer of charge at the electrode-electrolyte interface between the two kinds of charge carrier (electrons in the electrode and ions in the gel), and (3) to decrease the large impedance of the stratum corneum.

Two main types of electrode gel exist, viz. wet gels (often described as pastes, creams, or jellies) and hydrogels.

Wet gels are generally composed of water, a thickening agent, a bactericide/fungicide, an ionic salt, and a surfactant (68). The ionic salt is present to achieve the appropriate electrical conductivity of the gel, which will depend on the specific application. As the major portion of ions present in tissue fluids and sweat are sodium, potassium, and chloride ( $Cl^-$ ), in order to ensure biocompatibility, the ionic salts most commonly used in electrode gels are NaCl (sodium chloride) and KCl (potassium chloride). High concentrations of these salts tend to be better tolerated by the body than other salts. The ions in the gel serve not only to ensure electrical conductivity of the gel but to decrease the skin impedance by diffusing into the skin due to the existing concentration gradient. A relatively high concentration of electrolyte will also decrease the value of the charge transfer resistance (thus rendering the electrode more nonpolarizable).

When a standard pregelled wet electrode is applied to the skin, the gel rapidly fills up the troughs on the electrode and skin surfaces, thus ensuring maximum effective contact area. The skin capacitance,  $C_{SP}$ , is therefore observed to initially increase rapidly in value following electrode application and then to remain relatively constant (32). [A similar effect was probably noticed by Searle and Kirkup (61) as a result of sweat accumulation under a dry occlusive electrode.] Although  $C_{SP}$  does not exhibit a strong time dependence, it does vary with the electrolyte composition and concentration (49), increasing with increasing concentration (69).

Following electrode application, the skin’s parallel resistance,  $R_P$ , generally decreases with time in a pseudo exponential manner as the ions in the gel diffuse through the skin rendering it more conductive (32,70) (see Fig. 12).

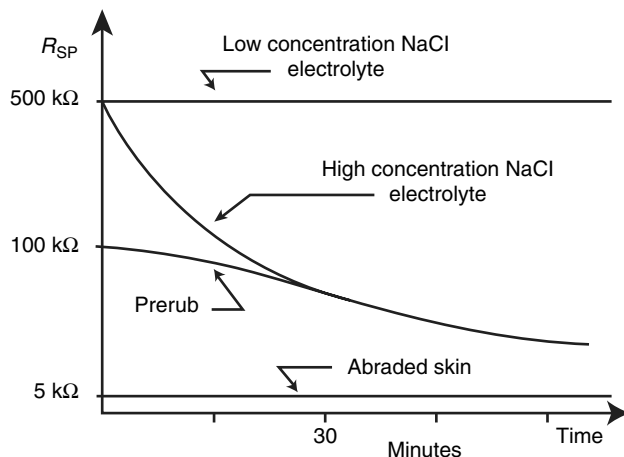


**Figure 12.** Variation of skin resistance with time for a range of gel concentrations and skin preparation techniques (1).

It has been observed, however, that when a cold gel is applied to a skin site, the measured value of  $R_{SP}$  is observed to initially increase (32,56), which is attributed to the cold gel causing the sweat pores to contract. Once the gel and skin has warmed up, the value of  $R_{SP}$  is observed to decrease as the electrolyte ions diffuse through the epidermal layer.

The skin temperature effect should be borne in mind when assessing a range of electrode designs. If, for example, the patient/subject removes his/her shirt just before the tests, the electrodes tested at the start of the experiment will have an advantage (i.e., smaller skin impedance) over those tested later as the uncovered skin sites will gradually cool down with time following removal of the shirt. Meaningful *in vivo* assessment of electrodes is not straightforward, and wrong conclusions can very easily be made by the unaware or the unscrupulous.

The time constant for the skin's parallel resistance,  $R_{SP}$ , appears to be inversely proportional to the concentration of the gel. The decay has a time constant of around 10 min (1), thus indicating that it takes almost 1 h for the electrode-skin impedance to decrease to its lowest value. For example, 50/60 Hz interference, linked to mismatch of electrode-skin impedances, is often observed experimentally to decrease with time. One should, therefore, where possible, apply the electrodes to the patient first, for example, before setting up the rest of the measurement system, to enable the skin impedance to decrease as much as possible.

High salt concentrations give rise to a more rapid diffusion of ions into the skin and a more rapid decrease in the skin's parallel resistance,  $R_{SP}$  (1,32) (Fig. 13). Such aggressive gels tend to be used in short-term biosignal monitoring applications such as stress testing, where instant, high quality traces are required (71). Biological tissues cannot tolerate long-term exposure to salt concentrations, which depart significantly from physiological levels [ $\sim 0.9\%$  NaCl for body fluids and around 0.1–0.4% NaCl for human sweat (49)]. Aggressive gels (5% NaCl) should not be used, for example, for the long-term monitoring of bed-ridden patients or for the monitoring of neonates. In the latter case, the incompletely formed skin is very susceptible to

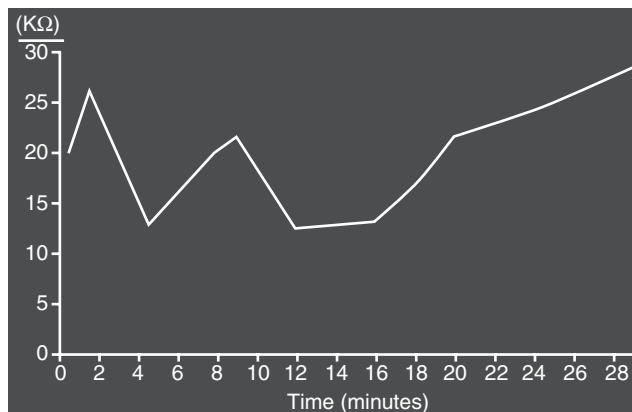


**Figure 13.** Variation of skin resistance with time for a hydrogel-based electrode. Fluctuations are due to variations in subjects state of relaxation/arousal (32).

skin irritation problems. In any monitoring application, aggressive gels should not be used in combination with skin abrasion (see below). It is especially to be avoided in longer term monitoring applications where the removal of the body's defensive barrier coupled with the long-term exposure to an aggressive gel will lead to severe discomfort to the patient.

The second kind of electrode gel commonly used in electrode systems are hydrogels. Hydrogel-based electrodes have recently become popular for numerous biomedical applications including resting ECG. Hydrogels are solid gels, which originally incorporated natural hydrocolloids (e.g., Karaya gum a polysaccharide obtained from a tree found in India) (68). The use of natural hydrocolloids give rise to variable performances and, in some cases, an unattractive color. Synthetic (e.g., polyvinyl pyrrolidone) hydrocolloids are now widely used.

The use of such solid gels entails numerous advantages when they are used in conjunction with screen-printing or similar technologies. The use of an adhesive hydrogel pad dispenses with the need of the standard gel-impregnated sponge, gel-retaining ring, and surrounding disk of adhesive foam that are used in wet-gel electrode designs. It is possible to construct thin, lightweight, highly flexible electrode arrays with accurately defined electrode/gel areas, shapes, and interelectrode distances (72,73).

Hydrogels also tend to cause less skin irritation compared with wet gels. A simplistic explanation of the advantageous/disadvantageous features of hydrogels is that hydrogel serves principally to ensure a good electrical contact between the skin and the electrode and that they do not significantly affect (compared with wet gels) the properties of the stratum corneum.

The impedance of the gel layer can be represented by a simple resistance in series with the impedances of the skin and the electrode plate-electrolyte interface. The magnitude of the gel resistance will depend on the composition and concentration of the gel and on the dimensions of the gel layer. Hydrogels are generally more resistive than wet gels. Typical resistivities for wet gels are of the order of 5–500 Ω·cm (the higher the salt concentration, the lower the

resistivity) compared with 800–8000  $\Omega\cdot\text{cm}$  for hydrogels (the higher resistivity hydrogels tend to be used in cardiac pacing electrodes). Wet ECG electrodes, for example, have a gel layer thickness of around 0.3 cm and typical areas of 3  $\text{cm}^2$ . The resistance of a wet gel layer is, therefore, generally in the range 0.5–50  $\Omega$ . Although hydrogels have higher resistivities, this disadvantage is generally compensated for by the use of larger gel areas, which need not necessarily entail the use of a larger overall electrode area as the adhesive hydrogel may not require the use of a large surrounding disk of adhesive foam. Another way to compensate for hydrogel's inherent disadvantage is to decrease the gel layer thickness, a variable generally ignored in electrode design even though it can have a significant effect on electrical performances. Many commercial hydrogels used in biosignal monitoring electrodes have layer thicknesses of around 1 mm (compared with around 3 mm for pregelled wet electrodes) and, coupled with larger areas of around 7  $\text{cm}^2$ , can lead to hydrogel pad resistances in the range 10–100  $\Omega$  (5).

It is suggested that further improvements can be made to the performances of hydrogel electrodes (and wet electrodes) by the use of even thinner gel layers. It must be borne in mind that gel-layer resistance is not solely determined by the dimensions and properties of the gel pad. When a large area gel pad is used in conjunction with a small area sensor, the dimensions of the smaller sensor will largely determine the magnitude of the gel-layer resistance, the overlapping section of gel pad carrying relatively little current, which is important in both biosignal monitoring and electrostimulation applications.

Hydrogels, being hydrophilic, are used for wound dressings in order to absorb exudate. They are, therefore, poor at hydrating the skin and will even absorb surface moisture. With hydrogel electrodes,  $R_{SP}$  is observed to fluctuate with sweat gland activity and the subject's state of mental arousal, decreasing during increased activity and gradually increasing again as the hydrogel absorbs the excess surface moisture (74,75). In contrast,  $C_{SP}$  remains relatively constant after a slight initial increase (32).

Hydrogels are therefore not only more resistive than wet gels, but they hydrate the skin less effectively and give rise to higher skin impedances (i.e., higher values of  $R_{SP}$  and lower values of  $C_{SP}$ ). Typical values of  $R_{SP}$  for hydrogels can be as high as 15  $\text{M}\Omega\cdot\text{cm}^2$  compared with a high of 5  $\text{M}\Omega\cdot\text{cm}^2$  for wet gels (75). Once again, this disadvantage can be overcome, at least partially, by the use of larger hydrogel pad areas. An additional way of increasing the value of  $C_{SP}$  is the use of thinner hydrogel pads (32).

**Skin Preparation Techniques.** In the clinical environment, the skin site is often degreased using an alcohol wipe prior to electrode application, which probably removes some of the loose, outermost cells of the stratum corneum and the poorly conducting lipid substances from the surface of the skin (55). However, the use of alcohol wipes may initially increase the impedance of the skin by dehydrating the outer layers of the skin (76). Motion artifact also may increase initially following application of alcohol to the skin (64). When wet gel electrodes are applied to alcohol-wiped skin, the gel will eventually penetrate the degreased skin

more readily once the electrode has been on the skin for several minutes, leading to a more rapid decrease in skin impedance and possibly to a decrease in motion artifact, which may not be the case, however, in the case of hydrogel electrodes, which do not actively hydrate the skin. The use of an alcohol wipe accompanied by vigorous rubbing should result in low initial impedances due to the additional mild abrasion.

A related method of rapidly decreasing skin impedance is to prerub the skin site with a high concentration electrolyte, thus forcing the gel into the outer layers of the skin, resulting as in a significant decrease in  $R_{SP}$  (Fig. 12) and an increase in  $C_{SP}$ , especially when accompanied by vigorous rubbing. Arbo-prep cream is supplied for this purpose and it is claimed to reduce skin resistance by up to 90% (from 40 or 50 to 4 or 5  $\text{k}\Omega$ , according to an advertisement). Some commercial gels such as Hewlett-Packard's Redox paste contain abrasives such as crushed quartz, which, when rubbed into the skin prior to electrode application, greatly reduce skin impedance. Such aggressive gels should only be used in short-term biosignal monitoring applications such as stress testing where high quality traces are required.

The outer layers of the stratum corneum can also be removed by rubbing the skin with abrasive pads especially designed for this purpose, which can give rise to a major decrease in  $R_{SP}$  (Fig. 12) and an increase in  $C_{SP}$ .

Unomedical, for example, markets a small disposable skin preparation abrasive pad that, when adhered to the finger tip, can be used to dramatically reduce skin impedance. A Skin Rasp, which resembles a strip of Velcro, is marketed by Medicotest for this purpose. The Quinton Quick-Prep Applicator, rotates the abrasive center of the Quick-Prep electrodes, causing a marked decrease in skin impedance. ECG electrodes are often supplied with abrasive pads built into the electrode release backing.

In skin stripping, the stratum corneum is progressively removed by repeatedly applying and removing adhesive tape to and from the skin (55,77). Skin stripping can greatly decrease skin impedance as a consequence of a dramatic decrease in the value of  $R_{SP}$  and an increase in  $C_{SP}$ . As the outermost layers of the stratum corneum are the most resistive, the most significant decrease in skin impedance is achieved with the first few stripplings (77). Therefore, no need exists for the complete removal of the stratum corneum, which would obviously be clinically unacceptable due to the discomfort (pain, bleeding, or irritation) caused to the patient during and following the recording. The more the skin is abraded for a given gel composition, the sooner discomfort develops and the more severe the irritation. The level of irritation also varies with the salt concentration and the additives present in the gel.

As pointed out above, abrading or stripping the skin is often used in stress testing to decrease motion artifact (63) as well as the 50/60 Hz noise induced by any mismatch of the contact impedances. High concentration gels are also often used for such demanding applications, rapidly soaking the skin and, thus, effectively removing the source of the problem.

The use of both skin abrasion/stripping and an aggressive gel will, however, maximize the potential for severe

skin irritation problems. These approaches should not be used together. Even with the use of mild gels, it is probably unwise to abrade the skin for long-term monitoring applications. The increased length of exposure of the abraded skin to the gel will be conducive to skin irritation. Somewhat surprisingly, long-term monitoring electrodes are sometimes commercially supplied with integral abrasive pads, which is not only risky but probably unnecessary as the use of a suitable mild gel would eventually decrease the skin impedance without the need for skin abrasion.

## ELECTRODE DESIGN

### External Biosignal Monitoring Electrodes

**Historical Background.** In 1887, Augustus Waller, using Etienne Jules Marey's modification of the capillary electrometer, obtained surface ECGs (as opposed to recording directly from the exposed heart of an animal) of one of his patients, 'Jimmy'. The patient turned out to be his pet dog. Waller used two buckets of saline to measure the canine ECG, one for the front paws and one for the hind paws (78–80).

Waller eventually succeeded in recording the first human ECG in 1887 using the capillary electrometer (Fig. 14) (81). However, he initially concluded "I do not imagine that electrocardiography is likely to find any very extensive use in the hospital. It can at most be of rare and occasional use to afford a record of some rare anomaly of cardiac action" (82).

It was, therefore, left to a more visionary and tenacious Dutchman, Willem Einthoven, to establish the clinical relevance of this strange new trace and to develop and commercialize a clinically acceptable system based on the string galvanometer. Einthoven's achievement was truly awesome. However, it must be pointed out that he did build (very significantly, it is conceded) on the work of earlier pioneers. The electrode system used, for example, was



**Figure 14.** Human subject connected to capillary electrometer via large area bucket electrodes (81).

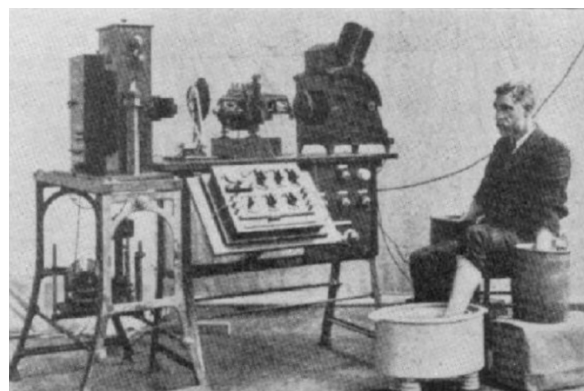


**Figure 15.** Early commercial ECG machine and electrodes (84).

Waller's bucket electrode, whereas the moving photographic plate recording technique was originated by Marey (83).

The input impedance of Einthoven's galvanometer was such that very low contact impedances were necessary, hence, the very large bucket electrodes (Fig. 15) (84). Obviously, the range of applications was somewhat limited.

Realistically, only one's limbs could be conveniently placed into the buckets. Hence, the use of limb leads exists in electrocardiography, even to the present day. It is, therefore, important to note several points. Present state-of-the-art is often based on historical quirks rather than on a profound scientific basis. The monitoring device and amplifier determined the electrode size, design, and location of the electrodes, which in turn determined the clinical application and the presentation of the physiological data.

Einthoven's device in its early form could not be used for the monitoring of bed-ridden patients or for ambulatory monitoring. These applications had to wait for improvements to be made to the amplifiers, which then enabled the use of smaller electrodes that could be more conveniently attached in other anatomical locations. However, the early monitoring locations and the form of the signals observed became accepted as standard and there is often considerable resistance to novel monitoring scenarios (e.g., smart clothing), which require or are based on different lead systems and present physiological data in a different format to that familiar to the clinician.

In the 1920s vacuum tubes were used to amplify the electrocardiogram instead of the mechanical amplification of the string galvanometer, which lead to smaller, more rugged systems that were transportable (Fig. 16) (84). The input impedances of the new ECG monitors were larger, and the large metal buckets could be replaced by smaller metal-plate electrodes (still large compared with present-day electrodes) (83). These advances enabled bedside monitoring, and, by the 1930s, some ECG devices could be carried to the patient's home. Not unsurprisingly, the new plate electrodes were attached to the limbs, both for historical and practical reasons. The metals used were chosen for their availability and ease of machining (Fig. 17). They included German silver, nickel-silver,

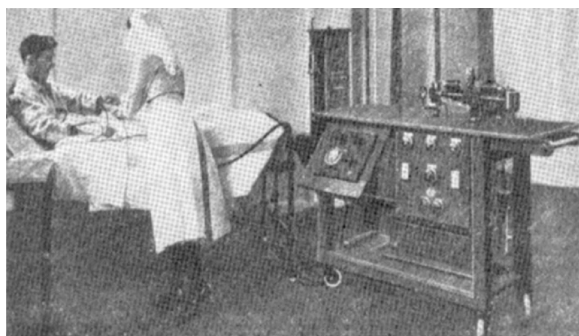


**Figure 16.** Mobile ECG used to monitor bed-ridden patient in hospital ward circ. 1920 (84).

and nickel-plated steel. The foil plates were used in conjunction with moistened pads of paper toweling, lint, cotton gauze, or sponge and were generally held in place with rubber straps. Around 1935, conductive gels were developed to replace the soaked pads. A wide range of gel ingredients were assessed, and it was noticed that the presence of an abrasive in the gel greatly reduced the skin impedance (5).

They also noted that slightly abrading the skin before applying the electrolyte helped achieve very low skin impedances.

A dry version of the plate electrode was reported by Lewes (85). The multipoint stainless-plate electrode resembled a large nutmeg grater that penetrated the skin when firmly strapped onto the limb or applied to the skin with a slight rotary movement, thus resulting in a very significant reduction in skin impedance.

Modern versions of the limb plate electrode still exist. Some have a convenient spring clip mechanism, which dispenses with the need for the rubber strap.

In the 1930s, clinicians, some using electrodes held on the chest by the patient himself or by another member of clinical staff, experimented with precordial leads and established their clinical value (86). In 1938, the American Heart Association and the Cardiac Society of Great Britain defined the standard positions and wiring of chest leads V1–V6 (87).

Research then focused on the development of electrodes that could be conveniently attached to the chest to enable convenient routine clinical measurements. Several designs



**Figure 17.** Metal plate limb electrode.

involved a rubber bulb, which was used to create suction sufficient to hold the metal electrode on the chest. One of the first suction electrodes was developed by Rudolph Burger in 1932 for the precordial leads (88). The suction electrode shown in Fig. 18a (85,89) is one developed by Ungerleider (89). Another more recent system incorporated the multipoint electrode of Lewes (85) into the suction head (Fig. 18b). The most popular suction electrode design, widely used around the world and still in use today, was developed by Welch (90) and often called the Welch or Suction cup/bulb electrode (Fig. 19) (3). It consists of a hollow, metallic, cylindrical electrode that makes contact with the skin at its base. A rubber suction bulb fits over the other end of the cylinder. The suction bulb was squeezed while the electrode was held against the skin. Upon releasing the bulb, the electrode is held in place. The suction electrode can be used anywhere on the chest and can even be used on hairy subjects. A single electrode can, if necessary, be used to take a measurement at a given location and then moved to another site.

Although the Welch cup electrode became widely used as a precordial electrode, it could only be realistically used for resting (supine) diagnostic ECG recording. The weight and bulk of the electrode generally rules out its use on upright, ambulatory, or clothed subjects. Since then, more suitable, lightweight, low profile suction electrodes have been developed that are pneumatically connected to remote vacuum pumps (37). Some arrays of suction electrodes are commercially available, for example, for use with exercise bicycles for cardiac stress testing (72).

A method had to be invented to attach small disks of suitable metal and their conductive gel coating to a patient's chest (in the case of ECG) or to other body parts in the case of other biosignal applications, such as EEG and EMG. Simply taping a metal disk to the skin site with a sandwiched gel layer was a method often used (91).

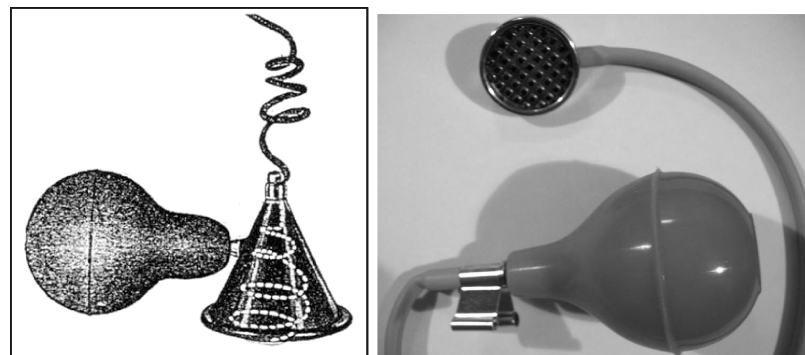


**Figure 18.** Early designs of suction precordial electrode (a) Ungerleider (89). (b) Lewes (85).

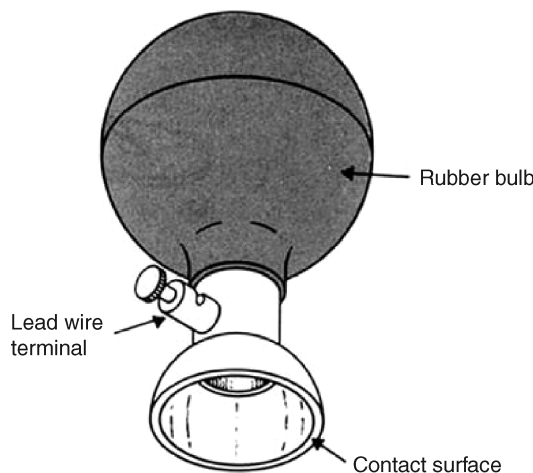


**Figure 19.** A metallic suction electrode is often used as a precordial electrode on clinical electrocardiographs (3).

Conically formed metal disk electrodes were and often still are used for EEG recordings (Fig. 20). The base of the metal cone is attached to the patient's scalp using elastic bandages, wire mesh, or more recently, using a strong adhesive such as colloidon. Aperture exists in the apex of the cone to enable the introduction into the recessed electrode of electrolyte gel or to enable the abrasion of the underlying skin by means of a blunt hypodermic needle. The cone electrodes were often made of gold as it has high conductivity and inertness, desirable in reusable electrodes. More recently, Ag/AgCl has been used.

Early plate electrode designs were presumably very messy and gave rise to considerable artifact problems. The observed artifacts were attributed to disturbance of the double-layer region at the electrode/skin (or, more precisely, electrode/electrolyte) interface [termed the electrokinetic effect by Khan and Greatbatch (94)]. When the electrode moves with respect to the electrolyte, the distribution of the double layer of charge on electrode interface was thought to change and cause transient fluctuations in the half cell potential or give rise to a streaming potential.

Recessed or floating electrodes were introduced in an effort to protect the electrode–gel interface from such mechanical disturbance and resultant movement artifact.

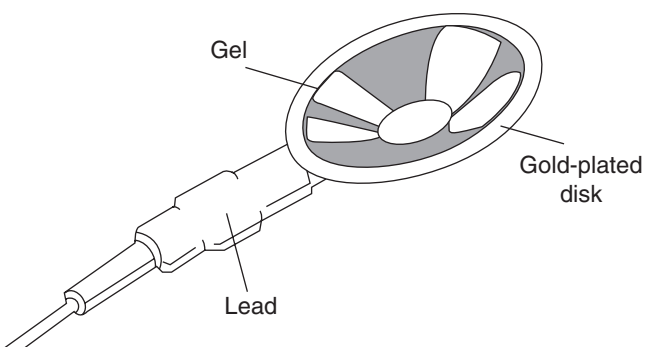


**Figure 20.** Conically formed metal disk EEG electrodes.

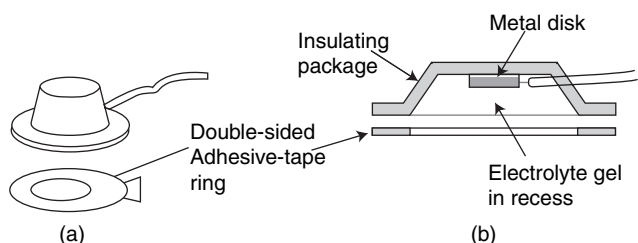


**Figure 21.** Examples of a floating or recessed biosignal electrode. (a) Recessed electrode with top-hat structure. (b) Cross-sectional view of the electrode in (a)(3).

A metal disk was recessed in a plastic housing that was filled with electrolyte gel prior to application to the patient. The top hat-shaped container was adhered to the skin by means of an annulus of double-sided adhesive tape, (Fig. 21) (3). Later a gel-impregnated sponge was used to ensure good electrical contact between the electrode disk and the skin surface. The electrode disk was, therefore, not in direct contact with the skin, which was found to reduce motion artifact. At first, various metal plates were used as the electrode conductor, then a sintered Ag/AgCl disk with preattached wire ensured better performances for more demanding applications.

**Modern Disposable Electrodes.** The top hat housing was eventually replaced with a smaller retaining ring or plastic cup and the electrode was held in place by means of a surrounding disk of adhesive foam. The plastic cup holds the gel-impregnated sponge in place and stops the gel from spreading beyond the set boundary, either during storage or use on the patient. Low cost Ag/AgCl-plated plastic eyelets (part of a snap fastener) are used in these disposable electrodes and the leads are connected to the electrodes via the electrodes' snap fastener studs. The rigid retaining ring was, however, uncomfortable as it did not allow the electrode to conform optimally to body contours. It was eventually removed in many modern disposable electrodes and the recess is now often formed by a hole in the adhesive foam layer. The backing label serves to hold the snap and eyelet in place as well as to present the company's logo (Fig. 22). The resultant electrode structure is much more flexible and more comfortable to wear.

The use of a snap fastener-style connection in disposable electrodes has one significant drawback for certain applications. The male stud protruding from the back of the electrode and the female connector required on the connecting lead results in a relatively heavy, large-profile electrode/connector interface, which is less than optimal for applications such as neonatal and pediatric monitoring. The use of such electrodes in long-term monitoring of bed-ridden patients could lead to considerable discomfort and the heavy connection could also give rise to significant motion artifact problems. The integrated lead design seeks to overcome these disadvantages. A thin, highly flexible lead wire is bonded directly to the back of a specially designed Ag/AgCl-coated eyelet, which results in a very low profile, lightweight electrode-connector system much used in neonatal and pediatric monitoring and attractive for long-term monitoring applications (Fig. 23).

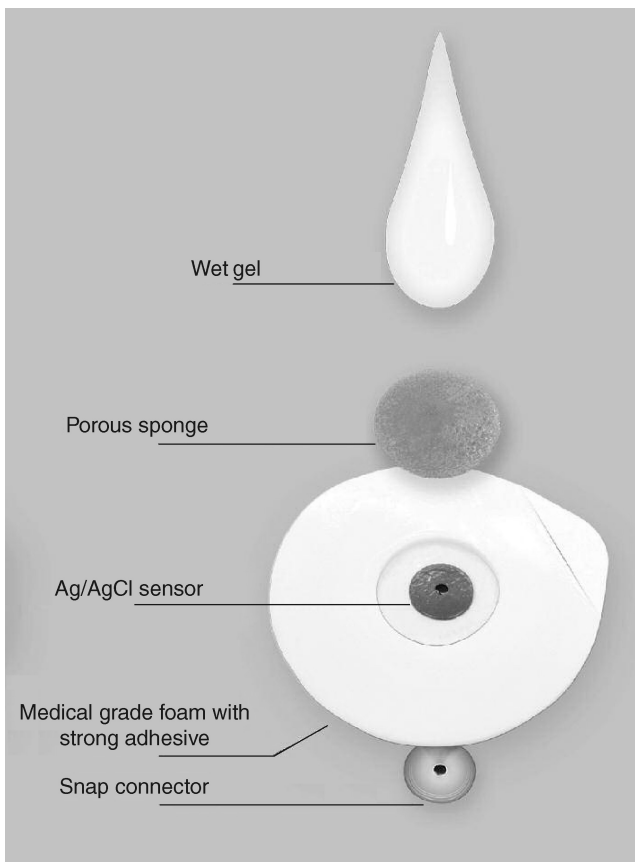


**Figure 22.** Modern wet gel disposable electrode. (Courtesy of Unomedical A/S.)

In an effort to decrease motion artifact, many electrode designs feature an offset center. The connector, often in the form of a snap fastener, is separated from the gelled sensor by a strip of metal or similar conductive layer. The connector is thus 1 or 2 cm away from the metal-gel-skin interface, and it is possible to connect the lead to the electrode or to pull on the connector without pulling directly on the gelled, skin site, thus causing artifact problems. This design appears well suited for stress testing applications although arguably less so for long-term monitoring of bed-ridden patients due to the bulky connector. The invention was patented by Manley (93) and the concept



**Figure 24.** An example of an off-set connector electrode. (Courtesy of Unomedical A/S.)

has been commercially exploited very successfully by Ambu A/S.

More recently, many other manufacturers supply electrodes with offset connectors (Fig. 24). Leadlock have developed an electrode that incorporates a slit in the foam backing. Once the electrode has been applied to the patient and the lead connected to it, part of the foam backing is used tape down the lead, locking it in place and minimizing direct pull on the connector and underlying electrode/skin interface.

A wide range of backing materials now exists, and some are better suited for specific monitoring applications, types of patients, skin types, and so on. Given the great variety of materials, adhesives, and designs used, the following comments are generalizations.

Open-cell foam layers, made from a plastic such as polyethylene, are much used and have thicknesses typically in the range 1–2 mm. They have a 10–100 µm coating of a pressure-sensitive adhesive, generally a polymeric hydrophobic substance (68,94). Adhesive foams generally give rise to firm adhesion, are resistant to liquids, and tend to cushion lead pull, thus giving rise to less artifact. They are, therefore, generally well-suited to cardiac stress testing and similar applications. However, as they are occlusive and generally have a relatively aggressive adhesive, they can give rise to more skin irritation and they must be used with caution for neonatal and long-term monitoring.

Porous, breathable layers, such as nonwoven clothes or tapes, have the advantages of being soft, stretchable, and conformable with the skin. (Note: The term micropore, although sometimes used loosely to describe any breathable backing material, is strictly a 3M product.) Porous layers tend to cause less mechanically induced trauma to the skin, which can occur with more rigid materials and is due to shearing of underlying skin layers. As they are highly air permeable and use milder adhesives, porous tapes cause less skin irritation and are well suited for long-term monitoring. Larger backing areas tend to be required. The gelled center can, however, pull away from the skin as a result of the stretchable backing. Ambu A/S

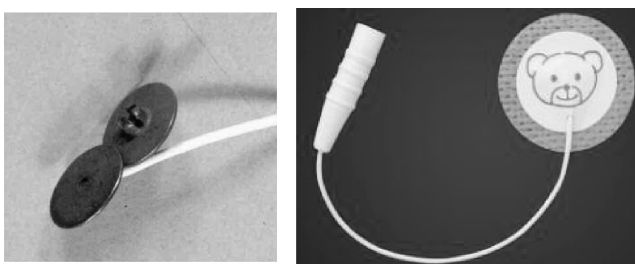


**Figure 23.** (a) Specially designed Ag/AgCl-coated eyelet with bonded lead. (b) Low profile, lightweight pediatric electrode with bonded lead. (Courtesy of Unomedical A/S.)

use a central ring of adhesive around the gelled eyelet to minimize this problem.

As we have already seen, wet (as opposed to solid gels) vary in composition and concentration depending on the application. Aggressive gels with higher concentrations of electrolyte or including abrasive particles are used for short-term, demanding monitoring applications such as cardiac stress testing. Mild gels are used in pediatric and neonatal applications due to the increased vulnerability of the patient's skin. It should be noted that no matter how hypoallergenic a gel or an adhesive is claimed to be, some patients will experience some form of skin reaction to one of the components.

**Solid Conductive Adhesive Electrodes.** The growing monitoring market has led to the development of even lower-cost disposable electrodes. Solid conductive adhesive or hydrogel electrodes were first introduced by LecTec Corp around 1980 (95). Hydrogels are composed of a hydrocolloid, alcohol, a conductive salt, water, and a preservative. The hydrocolloid use can be either natural (e.g., Karaya gum) or synthetic (e.g., polyvinyl pyrrolidone) (68). Early hydrogel electrodes were based on the natural hydrocolloid, Karaya, which comes from the bark of a tree. The rather unaesthetic appearance of these early gels and the variations in their electrical and mechanical properties limited their widespread acceptance. The use of synthetic hydrocolloids, with their more attractive appearance and performances, has led to the recent revolution in electrode design.

Solid adhesive gels reduce the number of electrode parts required, dispensing with the need of a gel-impregnated sponge or a surrounding disk of adhesive tape, which gives rise to small-area, low profile electrodes suitable for neonatal monitoring, especially when coupled with integrated leads as discussed above (Fig. 23b).

Tab solid adhesive electrodes are now widely used for many biosignal monitoring (and stimulation) applications. Thin, highly flexible metallic/conductive foils or printed conductive ink layers are laminated with solid, adhesive hydrogels. A section of the foil or printed layer is left uncovered. Once the electrodes are cut out, the exposed conductive tab acts as a means of connection, the leads being connected via alligator clips (Fig. 25). Electrode design is therefore very simple and manufacturing costs are low. These flexible, low profile electrodes are best used for short-term, resting diagnostic monitoring. Tab electrodes are not suitable for ambulatory or long-term monitoring as the tab connection will cause the electrode to peal off quite easily when pulled from any angle other than directly downward. Also, hydrogels are hydrophilic and tend to absorb moisture, lose their adhesive properties over time, and fall off the patient if an additional adhesive backing is not used. Hydrogels, being solid, do not leave a messy residue on the skin requiring cleaning. Tab electrodes are also repositionable and are reusable (on the same patient!) in certain home monitoring applications.

When used with an adhesive backing layer, the hydrophilic hydrogels tend to be relatively nondrying (a significant problem with pregelled wet electrodes) and their electrical properties may even improve as they absorb



**Figure 25.** Hydrogel-based tab electrode with connector. (Courtesy of Unomedical A/S.)

moisture. As they do not actively hydrate or otherwise affect the skin, they tend to be relatively nonirritating compared with wet gels.

Some disadvantages exist, however, associated with hydrogels. Hydrogels are more resistive than wet gels and, hence, the gel pad resistance will be higher, which can be compensated for by using larger hydrogel pad areas and thinner layer thicknesses as compared with those used with wet gels. Although the area of the solid adhesive gel in a tab electrode, for example, is considerably larger for this reason than that in a standard disposable wet gelled electrode, the absence of a surrounding adhesive layer results in the tab electrode having a smaller overall area.

Hydrogels, being hydrophilic, are poor at hydrating the skin and may even absorb surface moisture. They, therefore, give rise to larger skin impedances. This disadvantage can also be overcome, at least partially, by the use of larger hydrogel pad areas. Hydrogels are also more expensive than wet gels but generally lead to less expensive electrodes due to the simpler designs involved.

Hydrogels are more sensitive to motion artifact as they do not actively hydrate the skin. They are, therefore, not well-suited for stress testing.

The use of such solid gels entails numerous advantages when they are used in conjunction with screen printing technology (73,96), especially for body surface mapping and similar applications. It is possible to construct thin, lightweight, highly flexible electrode arrays with accurately defined electrode/gel areas, shapes, and interelectrode distances for a wide range of novel stimulation and biosignal recording applications. As the solid gel will not spread between electrodes, it is possible to position electrodes very close together without electrical shorting (Fig. 26).

**Wearable Electrodes for Personalized Health.** The recent and continuous trend toward home-based and ambulatory monitoring for personalized healthcare, although exciting and potentially leading to a revolution in healthcare provision, necessitates even more demanding performance



**Figure 26.** Cardiac mapping electrode harness.

criteria for the monitoring sensors (97,98). Many groups around the world are seeking to incorporate electrodes into clothing in order to monitor military personnel, firefighters and eventually the average citizen who wishes to monitor his or her health. Systems already exist on the market (e.g., Life Shirt) that resemble waistcoats into which one plugs-in standard ECG electrodes and other sensors. These sensors are removed and replaced periodically by the subject and, hence, require the knowledgeable involvement of the motivated wearer, presently military personnel, athletes, rescue workers, and so on.

For the more widespread use of wearable monitoring systems, especially by the average citizen, the system must be very easy and comfortable to use and require no preparation—literally as simple as putting on their shirt. Electrodes must, therefore, (1) require no prepping, (2) be located in the correct location once the smart garment is put on, (3) make good electrical contact with the skin, (4) not give rise to motion artifact problems, (5) not cause discomfort or skin irritation problems, and (6) be reusable and machine-washable. Although much work has been carried out in this novel area, it is not surprising given the above list of required performance criteria that the electrodes/sensors tend to form the bottleneck in the success of the overall monitoring systems. One must, therefore, not simply choose an electrode with as conductive a metal element as possible. Unfortunately, it would often appear that the associated electronic systems are first developed and the electrode design is left to the end, almost as an afterthought. The author would, therefore, suggest

that researchers start with the desired biosignal and establish the optimal body site(s) and electrode design for the given application before developing the rest of the monitoring system. This process may involve the use of novel lead or montage electrode positions in order to conveniently pick up artifact-free signals. Although this method will necessitate clinicians interpreting nontraditional waveforms, it will at least enable feasible monitoring and, as it involves novel body sites and electrode designs, it may well be patentable. After all, if it is not patented and commercialized, it will not benefit the patient.

One of the most promising smart garments is that developed under a European Fifth Framework programme called WEALTHY (Wearable Health Care System) (Fig. 27). WEALTHY is a wearable, fully integrated system, able to monitor a range of physiological parameters including electrocardiogram, respiration, posture, temperature, and a movement index. Fabric electrodes are made using conductive fibers woven into the stretchable yarn of the body-contour hugging garment and connections are integrated into the fabric structure (Fig. 27b). Various membranes are being assessed to ensure optimal electrode-skin contact and minimize skin irritation. The garment is comfortable and can be worn during everyday activities. It is washable and easy to put on.

#### External Electrostimulation Electrodes

**Historical Background.** The evolution of external stimulation electrode design shares some of the key landmarks as the development of biosignal monitoring electrode and, hence, this section will be somewhat shorter.

From the mid-1700s, when electrostatic generators were used to deliver arguably therapeutic impulses to various parts of the body, handheld (by the practitioner) electrodes had to be designed capable of delivering the impulses to the patient without shocking the practitioner who was holding them against the body part in question. The electrodes used tended to be simply long metal rods insulated with wooden handles (Fig. 28) (99). Although the electrodes were initially terminated in a simple metallic sphere, more exotic terminations were soon invented as these were observed to lead to different therapeutic effects on the body by means of the variations in the streams of the electric fluid. A modern parallel would be the use of different pencil electrodes (ball, loop, and needle) in electrosurgery for different effect.



**Figure 27.** (a) The WEALTHY physiological monitoring vest with integrated sensors. (b) An early version of the fabric electrodes.

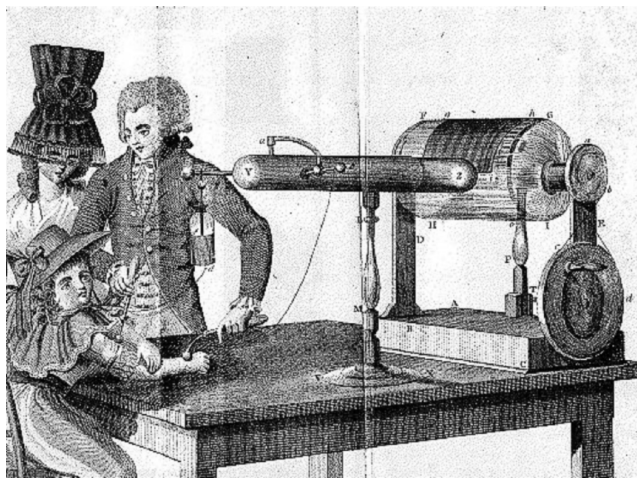


**Figure 28.** Early electrostatic generator and handheld electrodes (99).

Around 1800 came the discovery of Galvanism (dc current) and Voltaic Piles (early batteries). Numerous examples exist of practitioners using their handheld probe for localized effect, and the second contact to the patient was made by means of a container of water into which the patient put a hand or foot (Fig. 29) (100).

Following the discoveries of self-and mutual induction (~1830), Guillaume Duchenne made great contributions to the clinical application of the new Faradic current. At that time, much interest existed in the localization of what became known as motor points. It was common to combine the prevailing interest in acupuncture and use needles to stimulate muscles and nerves under the skin, termed electropuncture (83). Duchenne was not happy with this approach and developed his own electrodes for localized electrification. His electrodes were in various shapes (disks spheroids, and cones) covered with leather

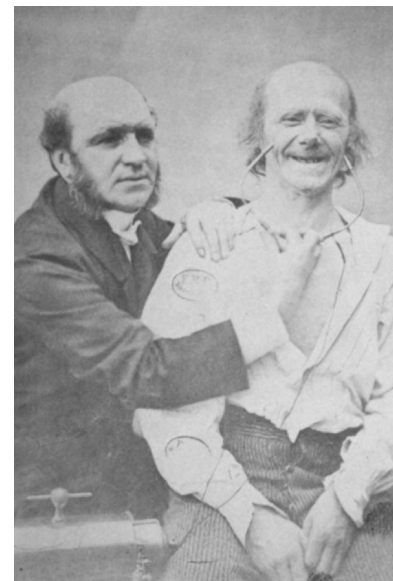


**Figure 30.** Duchenne's moistened conical electrodes for localized electrification (101).

moistened with salt water prior to application (101). (Fig. 30).

During the 1900s, as with biosignal monitoring electrodes, electrostimulation electrodes involved the use of simple metal buckets or receptacles, filled with water or another electrolyte, into which the subject introduced their foot or hand, especially in early iontophoretic applications. Obviously, the range of applications was somewhat limited. Metal probes were still manually pressed against skin for short-term applications. The electrodes were either gelled before application or had moistened chamois coverings similar to those used by Duchenne. In the 1950s, early external pacing and defibrillator electrodes, termed paddles because of their shape, consisted of bare metal disks made of noncorrosive material and were simply pressed against the patient's chest (102) see Fig. 31.

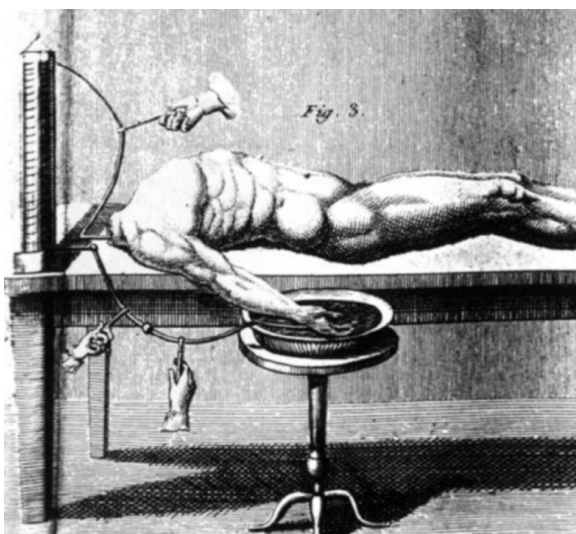


**Figure 29.** Container electrode. Used on the dead and the living (100).

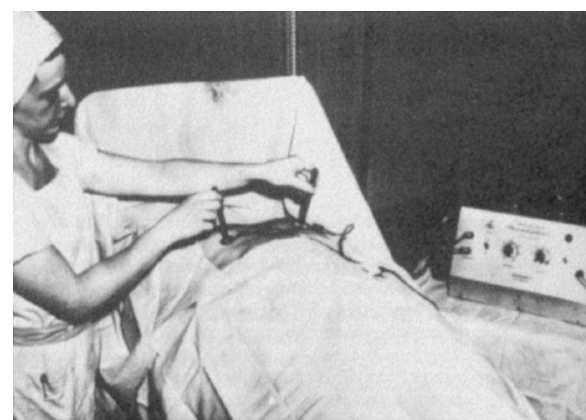


**Figure 31.** Early pacing equipment and handheld electrodes (102).

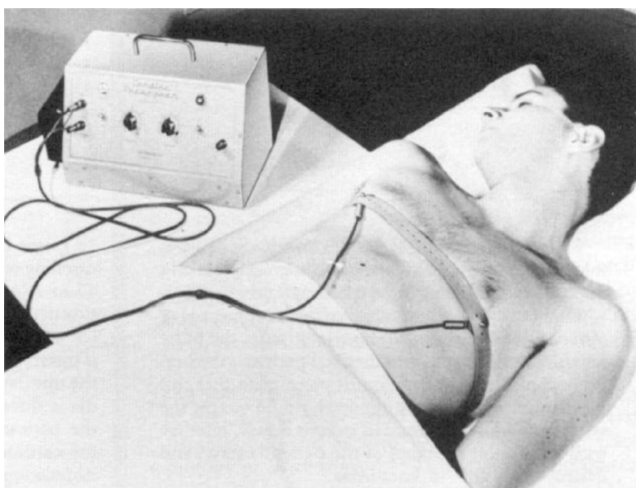


**Figure 32.** Early pacing equipment and metal-plate electrodes (103).

Rigid metal plate electrodes were eventually held in place with rubber straps on the limbs and even the thorax (Fig. 32) (103). Some of these electrodes were and still are made with rigid stainless-steel plates (104). The foil plates were generally used in conjunction with moistened pads of paper toweling, lint, cotton gauze, or sponge. The pads were moistened by the therapist prior to electrode application with water or electrolyte. Such electrodes could be easily reused by simply washing and regelling the electrode. Being rigid, however, these plate electrodes did not always make optimal contact with the body surface and gave rise to current density hot spots. External cardiac pacing at this time, for example, was very painful (83).

Malleable metal foil electrodes were the next evolutionary step in electrode design. Malleable electrodes have been made using a range of metals including tinplate lead and aluminium foils (105). Such electrodes had the advantage of being able to conform, to some extent, with body contours, thus ensuring a better, more comfortable contact between the electrode and the patient than was the case with rigid plates. Wrinkles in malleable metal foil could, however, encourage preferential current flow through small areas of the gel and into the patient.

More convenient, disposable pregelled foil electrodes were then developed for a range of external electrostimulation applications. The metal foil was laminated onto an adhesive foam backing. A gel-impregnated sponge layer was located on top of the metal layer and the complete electrode is attached to the patient by means of the surrounding layer of adhesive backing foam.

Unfortunately, the wet gel in these disposable pregelled electrodes tended to pool to one side, depending on how they were stored, giving rise once again to current density hotspots. More recently, the gel-impregnated sponge layer has been replaced by a conductive adhesive gel layer, as it does not have the potential for pooling to one area during storage and it does not squeeze out under pressure (68) (Fig. 33).

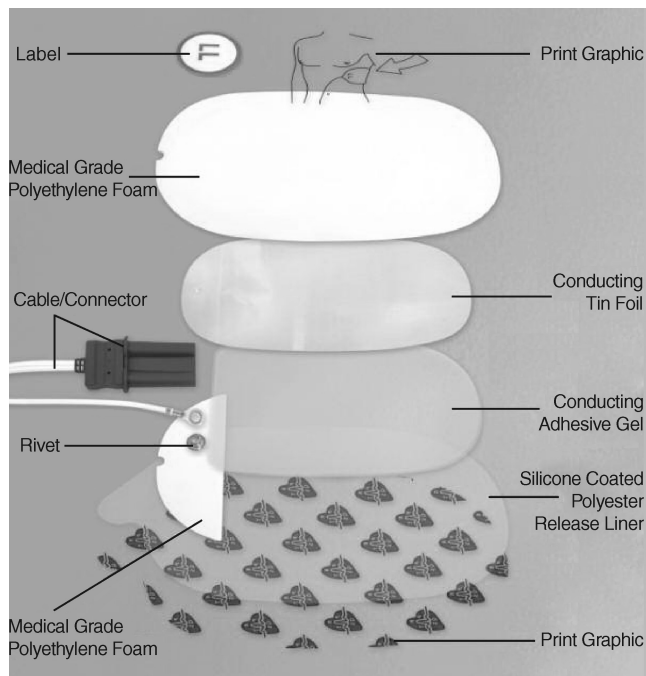


**Figure 33.** Construction of a modern external pacing or defibrillation electrode (courtesy Unomedical A/S).

**Current Density Considerations.** The distribution of current density under an electrode is an important parameter when designing and using electrostimulation electrodes. In the simplest case, current density (the amount of current per unit of conduction area) is inversely proportional to the electrode/skin contact area. For a given current, the current density under a small-area electrode will be higher and more localized than that under a large-area electrode. Generally, an optimal electrode area exists for a given therapeutic application, based on a range of criteria including the anatomical position and size of the nerve/muscle/organ and the relative positions and sizes of the electrodes. Small electrodes are, therefore, well suited to target precisely known points such as motor points. If a small electrode is used in conjunction with a large-area electrode, the effect is more pronounced under the smaller of the two. In such monopolar stimulation, the small electrode is often used as the active electrode to target the therapeutic effect. The larger electrode is simply used to complete the electrical circuit and is termed the indifferent or dispersive electrode. The use of two equally sized electrodes is termed bipolar stimulation. In TENS, for example, bipolar stimulation is often used to stimulate large muscle groups sandwiched between the (large) electrodes. Too large an area of electrode, however, may cause the current to spread to neighboring tissues.

High current densities can cause tissue injury due to, among other things, heating effects. The passage of electricity through any conductor will cause the dissipation of heat within that conductor. The amount of heat generated in a tissue depends on spatial and temporal patterns of current density and tissue resistivity (49).

The total energy dissipated at an electrode–skin interface is given by the formula:

$$E = I^2 R t \quad (21)$$

where

$E$  is energy dissipated (J)

$I$  is root-mean-squared (rms) electrode current (A)

$t$  is the duration of current flow (s)

$R$  is the real part of the impedance at the electrode site ( $\Omega$ ).

The change in temperature at the skin,  $\Delta T$ , site is proportional to the energy dissipated and, hence,  $\Delta T$  is proportional to  $I^2 R t$ . When skin or muscle tissue is heated to about 45 °C for prolonged periods, thermal damage can result. For short durations (i.e., <5 s), a temperature rise approaching 70 °C would be needed to cause heat damage.

As the electrode–skin resistance,  $R$ , is not generally known for a given site, it is often found convenient to use a heating factor (HF), where

$$\text{HF} = I^2 t \quad (\text{A}^2 \cdot \text{s}) \quad (22)$$

Assuming uniform current density distribution under an electrode, it is possible to calculate the minimum area of electrode necessary to achieve therapeutic effect and avoid tissue trauma (42). In theory, the applied currents flowing through standard dispersive electrodes used for electro-surgery, for example, will generally not give rise to sufficiently high overall current densities to cause thermal damage. However, analysis shows that current density distribution is not uniform under a stimulation electrode and that localized hotspots can occur and cause considerable pain and trauma to the patient when applying apparently safe therapeutic impulses (49). At best, in cases such as TENS, the applied current may have to be limited to less

than therapeutic values due to the patients discomfort (68).

Many potential sources exist of accidentally high current densities. Wrinkles or breaks in the metal electrodes, gel squeezing out from under the electrode or drying out, electrodes partially peeling off the skin, poor electrode application, and so on can encourage preferential current flow through small areas of the gel and into the patient. However, current density hotspots can also occur due to poor electrode design, and a considerable amount of research has been and is being spent investigating this important problem.

In this presentation, stimulation electrodes have been divided into conductive electrodes and resistive electrodes in order to facilitate the review of the various design features.

With highly conductive metal electrodes, such as those used for external cardiac pacing, defibrillation, or electro-surgery, current density hotspots are observed to occur under the perimeter of the electrode, often evidenced in the past by annular-shaped burns to the patient (49,106).

Current density hotspot problems are now often studied using thermal imaging cameras. Thermograms of the patient's skin (or a substitute such as pig skin) are taken immediately following the application of a given series of pulses and the removal of the electrode under test (Fig. 34). Increases in skin temperature reflect the magnitude of the current density at a particular point (107).

Wiley and Webster (108) showed that current flow through a circular electrode placed on a semi-infinite medium could be solved analytically. They found that for an electrode of radius,  $a$ , and total current,  $I_0$ , into the electrode, the current density into the body as a function of radial distance from the center,  $r$ , was given by:

$$J(r, 0) = \frac{J_0}{2[1 - (r/a)^2]^{1/2}} \quad (\text{A} \cdot \text{cm}^{-2}) \quad (23)$$

where  $J_0 = I_0/\pi a^2$ , (i.e., a hypothetical uniform current density).

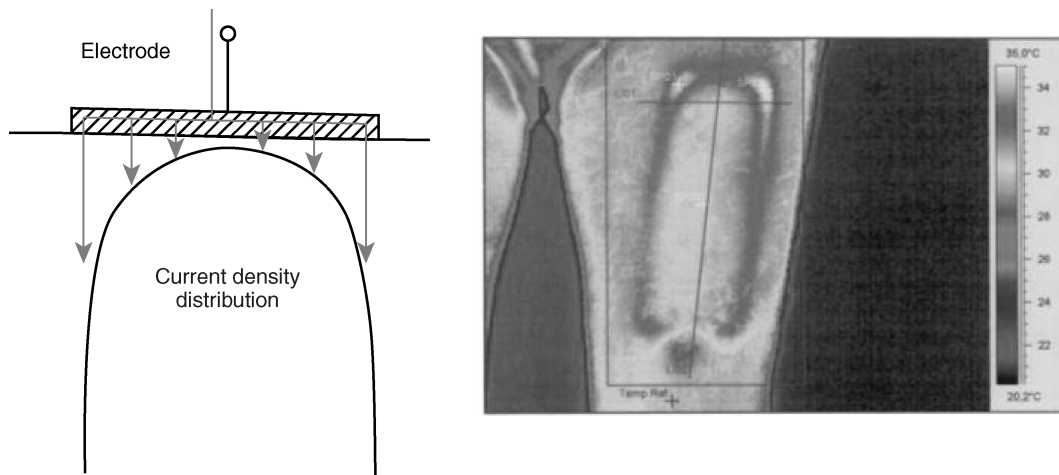


**Figure 34.** (a) Schematic representation of the current density distribution under a conductive electrode plate. (b) Thermal image of the skin under an electrosurgical electrode following testing.

As a result of the approximations made in deriving this simple equation, the value of current density at the edge (when  $r=a$ ) would theoretically approach infinity. More realistically, the current density at the perimeter can be around three times higher than that at the center of the electrode (109) (Fig. 34). The above equation shows that the middle portion of the electrode is relatively ineffective in carrying the current as half the total current flows through an outermost annulus 0.14 a wide or one-seventh of the radius.

Efforts in this area concentrate on encouraging more of the current to flow through the central portion of the electrode.

A main concern in the design of the conductive stimulation electrodes used for external cardiac pacing, defibrillation, or electrosurgery is the decrease in the high current densities observed at the edges.

In TENS, relatively resistive conductive rubber is often used and the opposite problem develops. When current is introduced into the conductive rubber (via a small metallic connector), it tends to flow into the skin immediately under the connector rather than laterally through the resistive electrode. Efforts in this area concentrate on encouraging the current to flow laterally through more of the electrode surface.

### Modern Electrode Designs

**Conductive Electrodes.** Electrosurgery, external cardiac pacing, and defibrillation share a common problem: Electrodes tend to deliver or sink a substantial portion of the outgoing or incoming current through their peripheral area as opposed to providing a uniform current density along their surface. This problem is referred to in the literature as the fringe, edge, or perimeter effect.

Many suggestions have been made to reduce this edge effect observed with metal electrodes, including:

1. Increasing overall area of the electrode. Obviously, an increase in electrode area will lead to a decrease in current density (110,111). However, it is generally not practical to use very large electrodes as the applied electrical field must be sufficiently focused to stimulate the targeted tissues and them alone. Also, a strong commercial interest exists in decreasing the size of the electrodes to save money and to facilitate packaging and storage of the electrodes.
2. Avoiding sharp edges in the metal plate (110,111). It has long been observed that square or rectangular electrodes with angular edges concentrate the electrical field at their corners, giving rise to current density hotspots in these locations. Using round electrodes or rectangular ones with rounded edges have been found advantageous in this regard.
3. Making the gel pad slightly larger than the electrode to enable the electric field lines to spread out before reaching the skin (111) (Fig. 35). Using a gel pad much larger than the size of the metal plate has less effect than would be expected as the perimeter of such a large gel pad will carry little current and the additional gel is electrically redundant, which

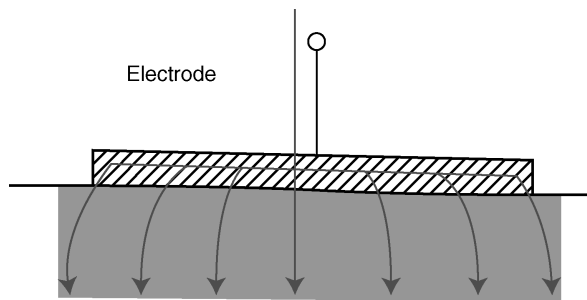


**Figure 35.** Schematic representation of the current density distribution under an electrode plate coupled with a larger gel pad. Current is allowed to spread out beyond the boundaries of the metal plate, thus minimizing the edge effect.

arguably applies to some of the snap connection electrodes used in TENS that do not have an additional current dispersing element.

4. Increasing the overall resistance or thickness of the gel layer in order to give the current more time to spread out evenly through the gel (110,111). It is well-known that, in applications such as external cardiac pacing, the use of relatively resistive gels decreases the pain and burning to the patient's chest. Krasteva and Papazov (110) suggest that the use of a layer of intermediate resistivity, comparable with that of the underlying tissues, optimally improves the distribution. However, in other applications such as external defibrillation, a high resistance gel pad would lead to energy wastage and a decrease in the desired therapeutic effect. Taken to its logical conclusion, this approach results in the coating of the electrode metal plate surface with a dielectric film. Such capacitive electrodes have been shown to give rise to nearly uniform current densities (107).
5. Increasing the resistance or thickness of the gel at the edges. Kim et al. (112) proposed covering the electrode metal with resistive gel of increasing resistivity as one moved out from the center toward the periphery, according to a specific relation with respect to the electrode radius. Although an intriguing concept, the commercial manufacture of such an electrode system is not yet feasible.
6. Making the electrode conductive plate progressively more resistive toward the peripheral edge of the electrode. Wiley and Webster (108) suggested subdividing the electrode plate into concentric segments and connecting external resistors to the individual segments. The connected resistors had progressively higher resistances toward the periphery in order to equalize the currents in the separate segments. A simpler system that has been successfully commercialized was patented by Netherly and Carim (113). A resistive layer is deposited on the outer edge of the electrode conductive plate, thus forcing more current to flow through the central portion of the electrode (Fig. 36). Krasteva and Papazov (110) demonstrated theoretically that a high resistivity perimeter ring

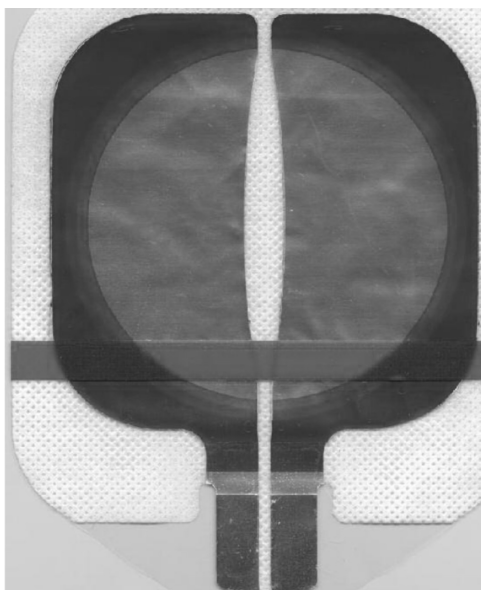


**Figure 36.** 3M's electrosurgical dispersive electrode. Note the green lossy dielectric material deposited around the peripheral edge of the electrode.

decreased the maximum periphery current by 12% without increasing the total interface resistance, hence the resistance to the defibrillation current.

Another related approach to this problem starts with a resistive graphite-based conductive layer and progressively builds up multilayered (at least two) coatings of more conductive silver/silver chloride toward the center of the electrode (114). The perimeter resistance is approximately 200 times that of the center, this is the technique exploited in Medtronic EDGE system electrodes for defibrillation, noninvasive pacing, and ECG monitoring (Fig. 37). It is claimed that the design distributes the current density evenly over the entire surface area of the electrode, rather than concentrating it at the edges.

7. Scalloping or otherwise shaping the edges of the metallic plate so that the length of the perimeter is



**Figure 37.** Medtronic's EDGE system electrode.



**Figure 38.** An electrostimulation electrode with cut-out metal plate in an effort to increase peripheral edge. The green sponge impregnated with gel has largely been removed to facilitate inspection of the underlying plate.

increased and, hence, the peripheral current density is decreased. Over the years, various designs have incorporated this concept. For example, it has been shown that using a figure-eight design rather than a rectangular metal plate reduced the maximum temperature (reflective of current density) by 30–50% (107). An alternative design is shown in Fig. 38. Caution is advised with this approach as the formation of fingers in the metal layer may serve only to concentrate the current at the tips of the fingers, and one could be effectively left with a reduced peripheral area.

8. Making holes in the central portion of the metal plate in order to provide internal peripheral edges to block the lateral flow of current. Some early claims were made that holes in the metal layer improved current density under the electrode. Presumably, it was believed that the holes blocked the current from flowing from the connector to the edge of the metal plate, forcing it to flow into the patient at the edges. It is the authors belief that such holes in the metal plate achieve little apart from further decreasing the area of the electrode and, if anything, increasing the current density at the edges. This impression appears to be confirmed by the work of Krasteva and Papazov (110), who investigated electrode structures with openings in the metal plate for skin breathing.

The author has suggested that the use of concave slits in the metal layer rather than circular holes may well have a favorable effect on current density distribution with the concave internal peripheral edges effectively blocking the lateral flow of current, forcing the trapped current to flow into the gel and, thus achieving a more uniform current density distribution over the surface of the conductive layer (115). Early work on the project with an industrial

partner appeared promising, but the work was never completed.

**Resistive Electrodes.** A TENS electrode system appears relatively simple and generally comprises a conductive plate, an ion-containing gel, a means of attachment to the skin, and a means of connection to the stimulators lead. Mannheimer and Lampe (42) pointed out, however, that of all the component parts of the overall TENS system, the electrode–skin interface has probably been the least understood and the most problematic. In addition to influencing the effectiveness of the treatment, poor electrode design can give rise to electrically, chemically, and mechanically induced skin irritation and trauma to the patient.

Initially, electrodes originally designed for ECG and other biosignal monitoring applications were used with TENS units, and some still are. Larger, more suitable electrode designs were eventually developed in order to reduce the current densities under the electrodes, to reduce skin irritation problems, and to increase stimulation comfort (116).

A large percentage of commercially available TENS electrodes are now molded from an elastomer (e.g., silicone rubber) or a plastic (e.g., ethylene vinyl acetate) and loaded with electrically conductive carbon black (Fig. 39) (3). Very few irritation or allergic reactions have been reported for conductive rubber electrodes as they do not generate the corrosion products often observed with metal electrodes (42). The great advantage of such electrodes is that they can be molded into almost any size or shape and a wide range of choice exists in the market. They can be made sufficiently thin to have high flexibility and, thus, are able to conform with body contours, making them suitable for a wide range of TENS applications.

Conductive rubber electrodes are often used in conjunction with an electrolyte gel and attached to the patient using elastic straps or custom-cut disks or patches of adhesive tape. Expanded polyester foam tends to give the most secure adhesion. However, as this backing is occlusive, the use of foam can give rise to skin irritation

problems. Breathable, cloth-like fabrics allow the transmission of air and moisture and generally cause less skin irritation problems. Cloth-like materials tend to stretch, however (an advantage when it accommodates skin stretching due to movement), which can lead to the electrode working loose and making poor contact with the skin, possibly resulting in current density hot spots.

Wet gels can squeeze out from under parts of the electrode and give rise to increased current densities in other areas. The use of hydrogel minimizes this problem source (68). Conductive, adhesive pads of solid hydrogel help ensure firm electrical contact between the electrode and the skin, reduce the incidence of current density hotspots, and often simplify the design of the electrode. As a large surrounding disk of adhesive tape is not required, the electrode size can be reduced to the active electrode area. These solid gel pads can be, depending on the application, replaced, refreshed, or simply reused in various semi- or totally-reusable electrode systems. In some applications, the gel pads can be removed and the conductive rubber electrode cleaned and regelled with a fresh gel pad for further use. In other cases, the electrode can be intermittently reused, on the same patient, by rehydrating the gel pad. Such reusable electrodes are ideal for home-based patient use.

One disadvantage with such conductive rubber electrodes is that they are relatively resistive. More power is required to drive the stimulating current through the resistive electrodes into the body and achieve the desired stimulation. Therefore, some reduction in battery life may occur which is generally not a significant problem, however.

A more serious problem involves current density distribution under the resistive electrode. When current is applied through the conductive rubber (via a small metallic connector), it tends to flow into the skin immediately under the connector rather than laterally through the resistive electrode, thus giving rise to a current density hotspot under the connector, which effectively, is the opposite problem to that encountered when using highly conductive electrodes.

Efforts to overcome this problem include incorporating conductive elements in the rubber to more evenly to help spread the current over the entire interface surface. Some electrodes have a thin metallic layer coated onto the back of the conductive rubber, which appear to give rise to the most uniform current density profiles (68).

The growing home-based market has led to the great variety of low cost disposable and reusable electrodes that are generally based on solid adhesive gels. Some electrodes are made using conductive cloth-like materials, thin metallic foils, aluminized carbon-filled mylar, or wire strands. Electrical connection is generally made to these electrodes via alligator clips, snap fasteners, or pin connectors. Many of these hydrogel-based electrodes can be trimmed to the desired size or shape by simply cutting with a pair of scissors. The current density profiles under these electrodes will very much depend on the relative resistivities of the metal and gel layers as well as on the actual design.

Snap fastener designs resembling standard ECG electrodes and are available with hydrogel pads or sponge

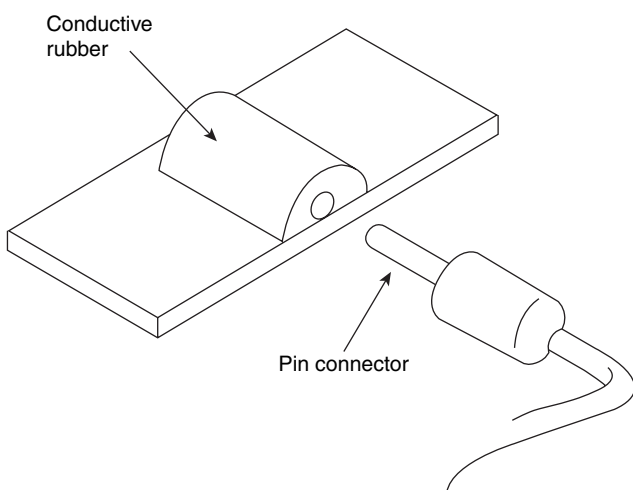
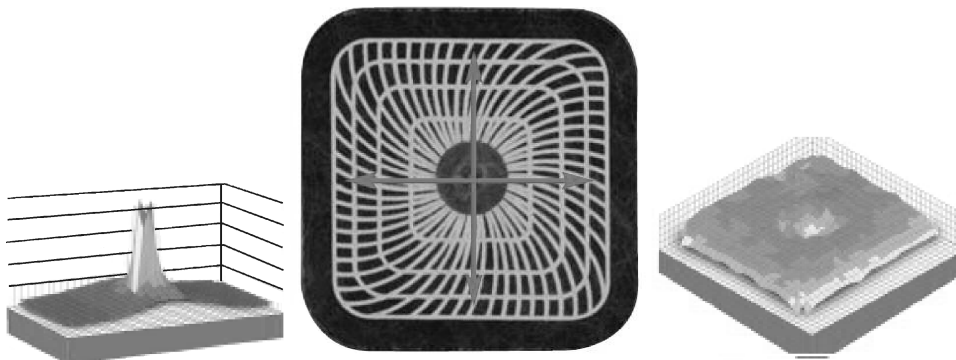


Figure 39. Carbon-filled silicone rubber electrode (3).



**Figure 40.** (a) Current density distribution under a conventional snap electrode. (b) Axelgaard's UltraStim snap electrode with current controlling grid. (c) Current density distribution under Axelgaard's UltraStim snap electrode. (Courtesy of Axelgaard Ltd.)

disks containing low chloride wet gels (to minimize skin irritation). These desists may require an additional current-dispersing element to ensure that the current spreads out beyond the immediate confines of the eyelet electrode (68). Axelgaard Lts UltraStim Snap Electrodes feature a highly conductive grid pattern printed on to a conductive flexible layer and coated with a moderately conductive adhesive gel layer. The conductivity of the conductive pattern is controlled through the use of various grid designs with preselected line widths and spacing as well as thickness and ink compositions (117). The pattern is thus used to control and optimize the spread of electric current over the surface of the electrode with an intentional current drop off toward the edge of the electrode (Fig. 40).

It is interesting to note that considering current density under conductive and resistive electrodes leads to a similar optimal design. To improve conductive electrodes, one places a resistive layer between it and the patient. To improve a resistive electrode, one puts a conducting layer either behind or in front of the resistive layer. Such sandwich electrode designs appear promising for a range of electrostimulation applications.

**Garment Electrodes.** A range of researchers in the TENS, FES, and body-toning areas of electrostimulation are endeavoring to incorporate electrodes in to body hugging garments to enable the convenient and accurate application of a (large) number of electrodes to the body part to be stimulated. The use of a large number of electrodes can enable, for example, several muscle groups to be stimulated together or sequentially in a coordinated manner to achieve a more natural movement of a limb. Garments are already on the market that resemble tight-fitting cycling shorts and have integrated wires and connectors for the attachment of standard TENS (or similar) snap electrodes prior to application. Other, more challenging designs include the integration of reusable electrodes into a stretchable garment.

### Implant Electrodes

Implantable monitors/stimulators and their electrodes are used, or are being developed, for a wide range of applications, including cardiac pacing and defibrillation, cochlear implants; urinary control, phrenic nerve stimulation for

respiration control; functional electrical stimulation of limbs; vagal stimulation for control of epilepsy, spinal stimulation for chronic pain relief, deep-brain stimulation for Parkinsons disease or depression, bonehealing, and several visual neuroprostheses.

Implanted monitoring electrodes are used to more accurately pick up the desired signal while minimizing the contributions of extraneous signals. Implanted stimulation electrodes deliver the applied waveform more selectively to the targeted tissue, making the therapy more effective and, as the stimulation electrode is generally implanted away from cutaneous pain receptors and afferent nerve fibers, more comfortable for the patient. One significant drawback, however, is the greater potential for damage from improper electrode design, installation, and use.

The design of an implant electrode will depend greatly on the anatomical structure it is to be implanted against, into, or around. Electrodes can be or have been implanted in, on, or near a given muscle; in, on, or around a given nerve; in, on, or around a given bone; in, on, or around the spinal cord; and in or on the surface of the cerebellar cortex.

A review of all of these designs is beyond the scope of this chapter. The reader is referred to the appropriate chapters in this Encyclopedia.

To facilitate this overview of some of the key design possibilities, two main application areas will be concentrated on: muscular and neural electrodes. Muscular (especially cardiac) electrodes, using more traditional electrode fabrication, are presented in a separate section. Neural electrodes will be largely covered in the section on newer microelectrodes constructed using thin-film and similar techniques. These categories are very loose and a considerable degree of overlap obviously exists between applications and the various electrode fabrication techniques. Once again, the reader is referred to the appropriate chapters in this Encyclopedia for more detailed descriptions of electrodes and their fabrication for specific applications.

Cardiac electrodes are the most important example of muscular electrodes. As cardiac pacemakers and defibrillators have the longest and most successful track records as implantable devices, much of the science underpinning the newer (and future) implantable devices (muscular, neural, and other) has been developed by the cardiac implant pioneers. Key contributions were made in the areas of implant electrodes, biomaterials, and powersources, to

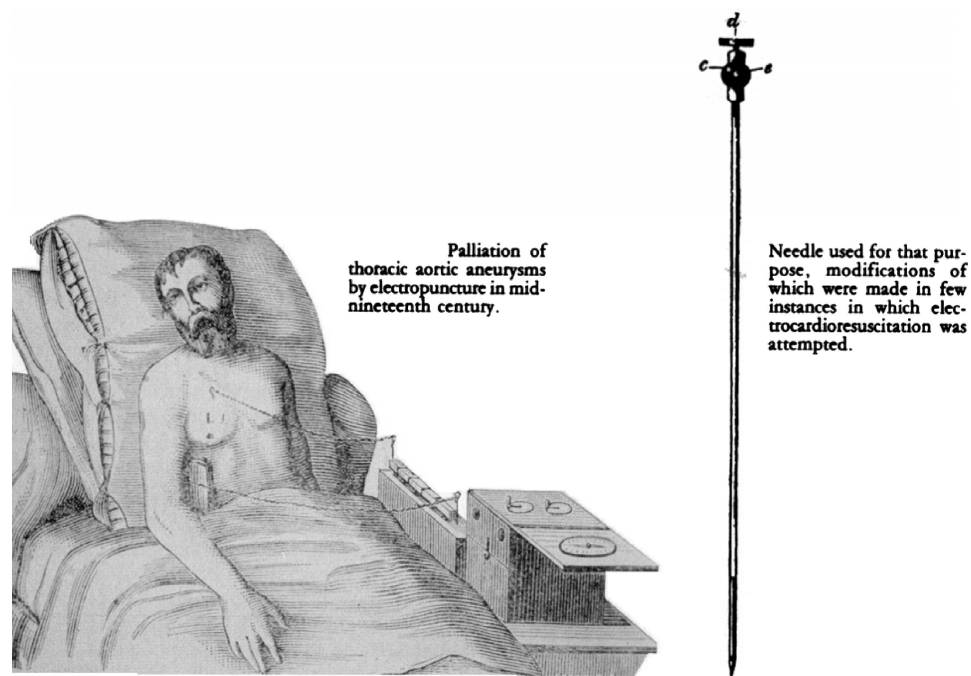


**Figure 41.** Kimer's electropuncture of the heart (103).

name but a few. The present review of electrodes is, therefore, largely based on cardiac electrodes. However, ideas can be gleaned from this area and, once suitably customized, applied to others with success. The advantageous aspects of biphasic impulses (discovered in the 1950s, arguably earlier) is a good example of something being rediscovered in a range of stimulation applications over the past few decades.

**Historical Background.** Implant stimulation electrodes, or at least percutaneous stimulation electrodes, predate the earliest biosignal monitoring electrodes. In the early 1800s, there appeared a renewal of interest in acupuncture in Europe that had been introduced into Europe in the second half of the eighteenth century by Jesuit missionaries. In 1825, Sarlandière was the first to apply an electric (galvanic) current to thin metal needle electrodes (derived from acupuncture needles) thus creating electropuncture for the application of current to specific points on or in the body (98,118).

Electropuncture soon became the accepted method of stimulating muscles, nerves, or organs beneath the skin (83). Electropuncture of the heart was first attempted by Kimer in 1828 without recorded success (Fig. 41) (103). This technique was then abandoned for several decades. Meanwhile, W. Morton successfully introduced the use of ether as an anesthetic in 1846. Eventually, chloroform was found to be more suitable although cardiac arrest was a frequent complication of chloroform anesthesia in those early days. In 1871, Steiner overanesthetized horses, dogs, cats, and rabbits to produce cardiac arrest. He reported successfully applying an intermittent galvanic current to a percutaneous needle in the heart to evoke rhythmic contractions. Terms such as galvano and farado puncture soon started to appear in the literature (103).

In the early 1900s, cardio-stimulating drugs such as epinephrine were injected directly into the heart of sudden death victims by means of a large needle inserted through the chest wall to restore automatic activity. It was eventually established that one of the key factors in the occasional success of these intracardiac injection procedures was the actual puncture of the heart wall rather than the medication administered. Based on this observation, Hymen went on to build the first hand-cranked, spring-driven artificial pacemaker (119). He used transthoracic needle electrodes plunged into the atrium and even introduced the concept of using a bipolar needle arrangement as in having the two electrodes so close together that only a small pathway is concerned in the electric arc established by the heart muscle, an irritable point is produced (103).

In the 1950s, Lillehei, Weirich, and others pioneered the use of cardiac pacing for the management of heart block accidentally resulting from cardiac surgery and for other emergency cardiac treatment. Slender wire electrodes were implanted into the myocardium before closing the chest with the connecting leads thus exiting through the chest wall. Pacing impulses could then be delivered through these wires for a week or so until the heart healed. Once the heart had recovered, the electrodes were pulled out. Early versions of these electrodes consisted of silver-plated braided copper wires insulated with polyethylene or Teflon (103,120).

In 1958, Furman and Schwedel reported the first instance of transvenous pacing of the heart. They inserted a unipolar catheter electrode into the right ventricle of the patient through a superficial vein and paced the heart via the endocardial surface. The electrode used was a solid copper wire with a bare terminal tip (120). The electrode was withdrawn once the patients heart resumed its own idioventricular rhythm. Although the cardiac pacing employed by Lillehei et al. and by Furman and Schwedel

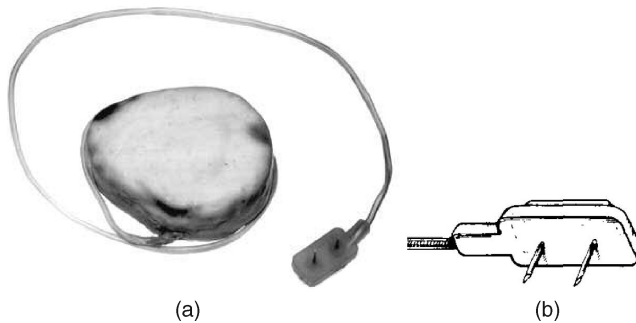


**Figure 42.** (a) Chardack, Gage, and Greatbatch's wholly implantable pacemaker and the Hunter-Roth bipolar intramyocardial electrode (83) (b) Diagram of an early Hunter-Roth lead with two bipolar myocardial pin electrodes (35).

was much better tolerated than the external stimulation of Zoll, perielectrode infection was a major drawback as was the transport of the external pacemaker. The development of an implantable pacemaker, therefore, became the goal of several groups around the world.

In 1958, Senning and Elmqvist successfully implanted the first Pacemaker without leads emerging from the patient's chest to invite infection. The implanted unit was powered by cells that were recharged from outside the body using a line-connected, vacuum-tube radio-frequency generator. The electrodes/leads used were stainless-steel wires. The second version of the unit failed due to a lead fracture one week following implantation. It was then decided to abandon pacemaker therapy for this patient until better leads were developed (120).

At that time, many of the electrodes used were unipolar. The active electrode tended to consist of the bared tip of an insulated wire implanted in the myocardium whereas the indifferent electrode was a similar wire implanted subcutaneously in the chest wall. Unfortunately, the stimulation threshold was observed to rise following implantation during longer-term pacing. This increase in threshold was thought to be due to the development of scar tissue around the active electrode. Hunter and Roth developed a bipolar electrode system in 1959. This electrode consisted of two rigid, 0.5 cm long, stainless-steel pins attached to a silicone rubber patch. The cathode-anode pins were positioned into myocardial stab wounds surgically created for the purpose and the pad was then sutured to the epicardial surface (35). The lead wire was a Teflon-coated, multistrand stainless-steel wire with an outer sleeve made from silicone rubber tubing (121).

In 1960, Chardack, Gage, and Greatbatch successfully produced a wholly-implantable battery-powered pacemaker (Fig. 42a). Initially, they used a pair of multistrand stainless steel wires in a Teflon sleeve with the bare ends sutured to the myocardium (35). Other metallic formulations were tried, such as solid wire, silver wire, stainless steel, orthodontic gold, and platinum and its alloys (122).

They eventually adopted the Hunter-Roth intramyocardial electrode (Fig. 42a and b). Considerable surgery was required as the pacemaker had to be implanted into the abdomen and the electrodes were sutured to the heart wall. The bipolar electrode did, however, dispense with the need of a dispersive chest electrode and the associated pain it caused (103). Stimulation thresholds tended to stabilize at much lower levels with this electrode (120), which enabled successful pacing for many months.

Breakage of lead wires, due to metal fatigue, was a major concern. One of the main problem areas occurred at the point where the two metal components were welded together (121). Corrosion also occurred at the small-area stainless-steel anode, causing cessation of pacing within a few months.

Chardack et al. (123) devised a replacement for the Hunter-Roth electrode based on a continuous helical coil of platinum-iridium (Fig. 43). The electrode was simply a few turns of the coiled lead wire, exposed and extended to enable fibrous tissue to grow between the spirals and firmly anchor the electrode in place. The use of a helical coil greatly increased flexibility and decreased the number of fatigue failures, as did the use of one continuous wire (without a join) for both lead and electrode. The use of the same metal for lead and electrode also had the advantage of preventing corrosion from galvanic action. Additionally, platinum-iridium is more corrosion resistant than the metals used in many electrodes prior to Chardack's electrode.

The sutureless screw-in lead was later introduced by Hunter in 1973 (35). The screw-in electrode was simply rotated into the myocardium and did not require a stab wound or sutures for insertion. The electrode was effectively the means of attachment. As this corkscrew electrode tended not to dislodge, it dominated pacing for a long time and is still used today for many epicardial implants (Fig. 44).

A thoracotomy was required to attach many of the above electrodes to the heart, which complicated surgical procedure and resulted in a 10% early mortality (122). The first so-called modern pacemaker, which combined an implanted generator and a transvenous lead, was developed simultaneously in 1962 by Parsonnet and Lagergren (124,125). The endocardial catheter electrodes could be

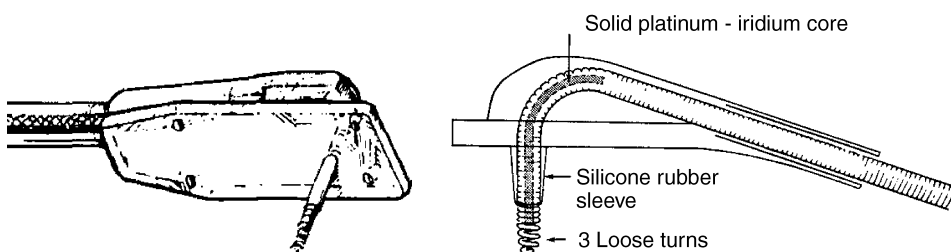


**Figure 43.** The "Chardack" electrode (a) (35) (b) Chardack et al. (123).

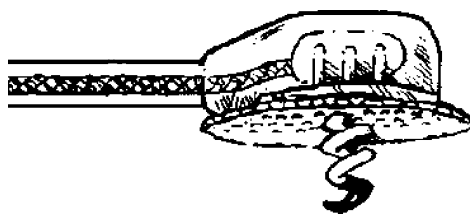


**Figure 44.** The corkscrew myocardial electrode (35).

installed under local anesthesia, and this approach virtually eliminated early mortality. As they did not require the opening of the chest cavity, the use of catheter leads opened the field of pacemaker implantation to non-surgeons in later decades.

To minimize the risk of venous perforation, the electrode leads were made flexible by winding bands of stainless steel around a core of textile fibers (120). The electrode was a small stainless-steel cylinder at the end of the catheter.

As time passed, the transvenous route progressively evolved over the myocardial approach, so much so that, at present, the transverse route is almost exclusively used for pacemaker implantation.

Cardiac pacing has been the earliest and most successful example of implanted electrodes and associated hardware. Many present and future developments in other implanted electrostimulation (and biosignal recording) areas are and will be based, to a large extent, on the pioneering work carried out in the pacing area.

**Some Modern Electrode Designs.** With the early transvenous leads, the stimulation threshold was observed to greatly increase if the electrode pulled away even slightly from the myocardium. A wide variety of active fixation devices was therefore invented. These devices included springs, deployable radiating needles, barbs, hooks, claws and screws designed to anchor the electrodes by actively penetrating the myocardium (35,126). The “Bisping” transvenous screw-in electrode is the most popular, as it allows

the screw helix to be extended from the tip once the lead has been successfully threaded through the vein and located against the desired part of the heart (Fig. 45). It can be used as a combined anchor and electrode. The screw can be retracted allowing for an easier extraction of the lead, when necessary. (Note: A similar design of electrode is used for detecting the fetal electrocardiogram during labor. The intracutaneous needles are screwed in to the fetus' presenting scalp. Similar designs are also used in EEG monitoring.)

A wide variety of passive fixation devices were also invented. Various tines, flanges, and other soft, pliant projections were formed at the distal end of the lead, generally as an extension of the silicone or polyurethane lead insulation, and designed to passively andatraumatically wedge the electrode between endocardial structures such as trabeculae (Fig. 46). In some designs, the electrode has the form of a closed-loop helical coil that, when twisted clockwise, becomes lodged in the trabeculae (126).

Early electrodes had smooth metal surfaces. Techniques were then developed to roughen the surface in the hope of encouraging tissue in-growth, thus locking the electrode in place, minimizing mechanical irritation and excessive fibrous encapsulation, and ensuring low chronic stimulation thresholds. Studies found that porous electrodes did indeed achieve better fixation, thinner fibrous capsules, and stable thresholds.

A variety of porous electrode tips have been developed including totally porous structures such as CPIs meshed screen electrode and electrodes whose surfaces had been textured using a range of techniques (Fig. 47). Porous surfaces have been generated by coating metal surfaces with metallic granules, by sintering metal spheres to form a network of cavities, and by laser-drilling the surface of electrodes (126).

Not only does roughening improve electrode fixation and threshold stability, it has been found to have a very advantageous effect on interface impedance. From a stimulation point of view, one is keen to use a small-area electrode to increase current density at the small tip and

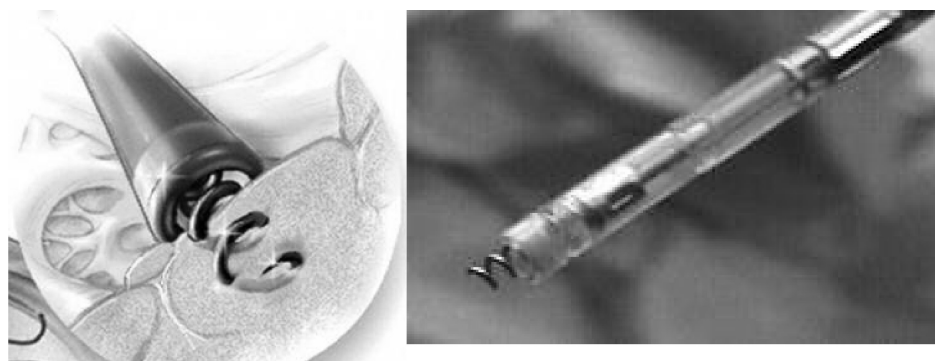


**Figure 45.** The “Bisping” transvenous screw-in lead with the helical screw electrode extended. [From S.S. Barold's The Third Decade of Cardiac Pacing (35).]



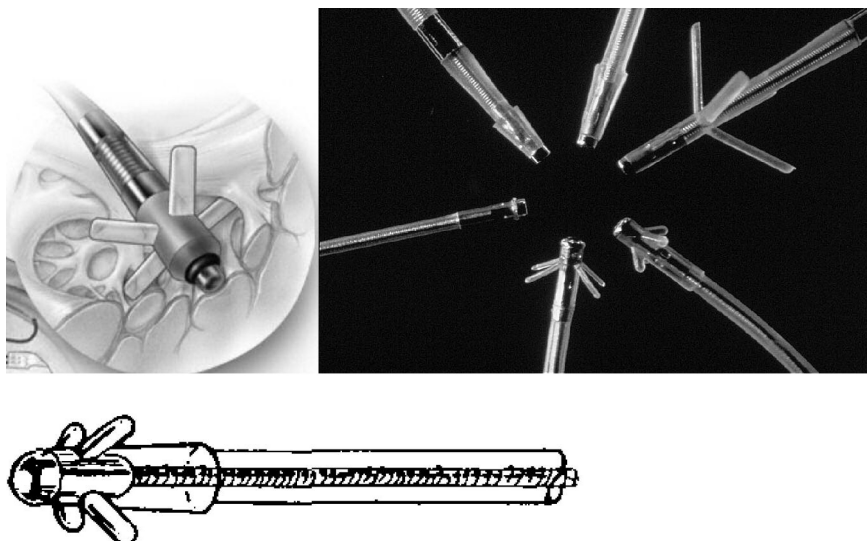


**Figure 46.** Transvenous lead with silicone rubber tines (35).

thus decrease stimulation threshold. A small-area electrode also has a high pacing impedance that can decrease current drain on the generator and thus prolong implant life (35). However, one would also like to have a low sensing impedance in order to avoid excessive attenuation of the cardiac signal. Two ways that exit these conflicting criteria can be optimized, modifying the electrode surface or modifying its design.

Roughening the surface of a small-area electrode increases its effective area without changing its geometric or outer envelope surface area (35). Many electrode systems have been developed that incorporate this concept—electrodes with terms such as activated, porous, and sintered in their company's description. These electrodes have been found to be effective in lowering the electrode interface impedance under small-signal sensing conditions. [Note: the electrode–electrolyte interface is very nonlinear and, hence, smaller under stimulation.] Unfortunately, the reduction in interface impedance has been erroneously interpreted as rendering the electrode nonpolarizable. As stated previously, the word polarization appears to be used in a rather vague manner and has been used as the explanation of, among other things, the nonlinearity of the interface impedance as well as its frequency- and

time-dependence. The fact that the current or voltage response to a step in voltage or current is not a simple step has been attributed to polarization. The observed transient responses are merely due to the presence of the double layer capacitance (see Figs. 8, and 9). Roughening the surface of an electrode effectively increases the area of the interface and the value of  $C_{dl}$ , which in turn results in an increase in the response's time constant ( $T = R_{CT}C_{dl}$ ). The observed response thus looks stretched out along the time axis. This flattened response has been mistaken for that of a purely resistive, nonpolarizable electrode. At any rate, roughening the surface of the electrode almost gives us the best of both worlds, a noble or inert electrode with a low interface impedance.

Another way of achieving a small simulation surface area (high current density) while ensuring a large-sensing surface area (low interface impedance) is to modify the design of the electrode.

The porous electrode of Amundson involved a hemispherical platinum screen that enclosed a ball of compacted 20  $\mu\text{m}$  diameter platinum–iridium fibers (127). As electrolyte could penetrate this three-dimensional (3D) or multi-layered electrode, the design resulted in a major increase in

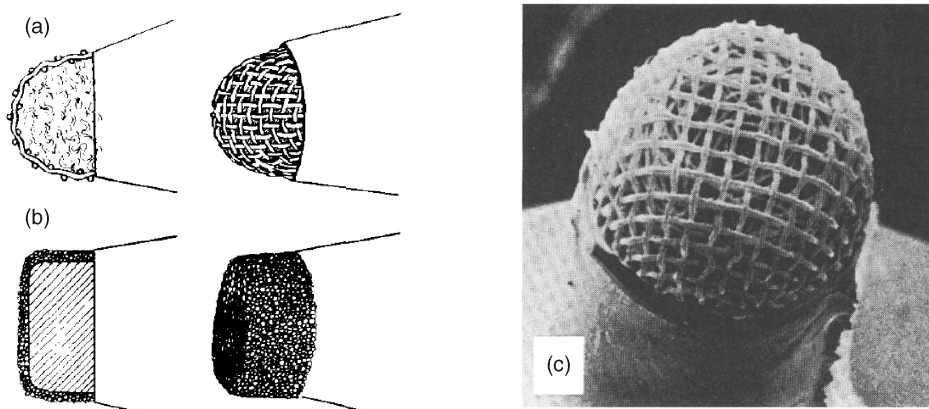


**Figure 47.** (a) Cross-section of a totally porous electrode (35). (b) Cross-section of a porous surface electrode (35). (c) Photo of totally porous electrode (126).

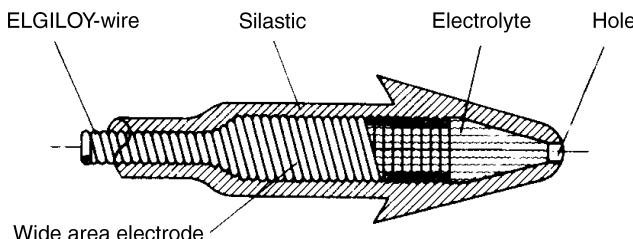


**Figure 48.** The differential current density (DCD) electrode (129).

effective surface area as well as promoting tissue in-growth and long-term stability of thresholds. Lagergren et al. (128) introduced the birdcage design, which also exploited some of these features (126).

One interesting example of a modified design by Parsonnet et al. involved the use of an electrolyte-filled hollow electrode, called a differential current density (DCD) electrode (129). The actual stimulating electrode is the mouth of the electrolyte filled pore, which can be small to provide high current density at the point of contact with tissue (Fig. 48). The inside of the hollow electrode chamber has a large metallic surface (a helical coil forming a cylinder) and thus gives rise to a low electrode-electrolyte interface impedance.

Figure 48 appears to be an electrode design that could readily be customized and used in a wide range of monitoring or stimulation applications. The electrode-electrolyte interface is effectively recessed and protected from any disturbance, a further advantage to those already listed above.

Several other designs exist that aim to achieve a similar effect by manipulating the current density distribution around an electrode tip. Electrodes with complex shapes have irregular patterns of current density with localized hotspots at points of greatest curvature (126). It is possible to exploit these areas of high current density for stimulation purposes while the larger overall surface area gives rise to a low interface impedance (130). A hollow, ring-tipped electrode (effectively similar to the DCD electrode) has a large current density at its annular mouth while having a large electrode-electrolyte interface area. Such electrodes are reported to have better stimulation thresholds and sensing characteristics than hemispherical designs and have proved popular. Several manufacturers have combined this ring-tip design with increased surface porosity (126). Other related designs include a dish-shaped

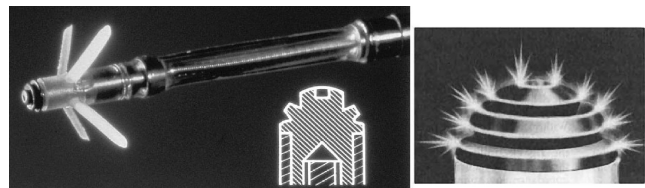


**Figure 49.** The target tip electrode. Microporous, plantinized platinum electrode. The target appearance is due to shallow grooves separated by peaks. (Courtesy Medtronic, Inc.)

electrode for edge-focusing of current (with laser-drilled pores for interface impedance reduction) and a grooved hemispherical platinum electrode coated with platinum black particles (target-tip electrode, Fig. 49) (126,130).

Steroid-eluting electrodes were introduced in 1983 in an effort to minimize the growth of connective tissue. The first-generation electrode was made of titanium, with a platinum-coated porous titanium surface (Fig. 50). The electrodes incorporated a silicone core that was impregnated with a small quantity an anti-inflammatory corticosteroid (34). Upon implant, the steroid is gradually eluted into the interface between the lead electrode and the endocardium, reducing the inflammation and fibrosis that would normally occur. Steroid-eluting leads are characterized by a lower long-term capture threshold. Similar improvements in capture thresholds have been achieved (131,132).

Most cardiac electrodes now involve the combination of drugs and complex surface structures at the macro and micro scales.

For newer applications, such as Cochlear implant electrodes, an array of electrodes is involved. In some such multielectrode applications, one may be interested not only in the current density profiles under the surfaces of the individual electrodes, but in the interplay between the electrical fields produced by the electrodes in the array in the hope of achieving more effective stimulation or more effectively imitate physiological stimulation. For example, the Clarion hi-focus electrode system of Advanced Bionics Corp. incorporates 16 electrodes in a flexible array that are designed to deliver improved focused stimulation to the auditory nerve (133).

**Microelectrodes.** Over the past few years, exciting developments have taken place in areas of biomedical

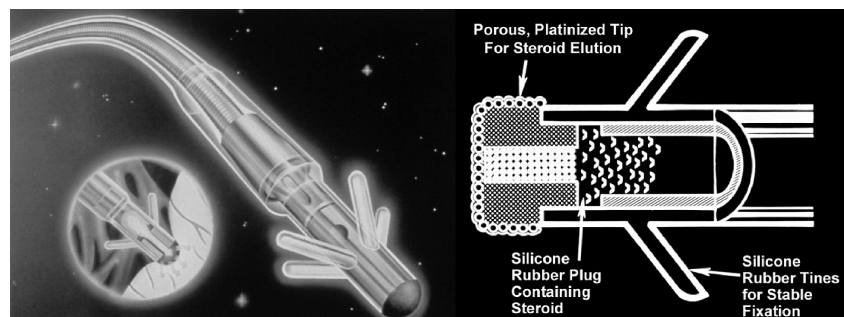


**Figure 50.** (a) Steroid-eluting electrode. (b) Cross-sectional diagram of an early design of steroid-eluting electrode. Behind the electrode is the silicone rubber plug compounded with steroid. (Courtesy Medtronic, Inc.)

engineering that involve implantable devices for the recording or stimulation of the nervous system.

In the previous section, we saw the success in commercializing pacemakers. Other implant devices that have also reached the patient in clinical routine practice or research settings include Cochlear implants to restore hearing; deep-brain stimulators to alleviate symptoms of Parkinson's Disease and depression; vagal nerve stimulators to minimize the effects of epilepsy; as well as FES systems to restore or improve function in the upper extremity, lower extremity, bladder and bowel, and respiratory system (134,135). Other areas of research that are likely to come to fruition within the next few years include various visual prostheses to restore functional vision in the profoundly blind and the exploration of the brain-computer interface (134,136,137).

Much of the early research in these areas started around the 1960s (135). Where possible and appropriate, surface and percutaneous electrodes were first used to establish the feasibility of the given recording/therapy. Early implant electrodes involved fine metallic wires or small disks placed near, in, on, or around the targeted muscle or nerve. The fabrication of these electrodes was time-consuming and the electrode properties were not very reproducible given the variations in areas, surfaces, inter-electrode distances, and so on, which was particularly a problem when several electrodes were to be used in an array. As the demands on human implantable diagnostic/stimulation devices increases, an increased need for a larger number of smaller-area electrodes with well-defined and reproducible surfaces and dimensions generally occurs. Although, due to their high level of specificity, muscle-based electrodes will continue to be used, new electrode designs tend to concentrate more on direct nerve stimulation as this may provide more complete muscle recruitment and the same electrode may successfully recruit several muscles, thus reducing the number of electrode leads required (135). Electrodes are, therefore, needed that can interface electrically with the neural system at the micrometer scale (136).

For example, the goal for a high resolution retinal prosthesis is a 1000-electrode stimulating array in a  $5 \times 5$  mm package (137). If this area of research is to be clinically successful and if the other areas are to continue to improve, microelectrodes must be (and are being) manufactured using the thin-film technologies associated with

the IC circuit industry. Microfabrication involves either material deposition or removal. Either rigid silicon wafers or flexible polyimide substrates act as platforms for the microelectrodes and associated circuitry. The deposited films (for connectors, leads, electrodes, or insulation) are produced by electroplating, evaporation, and sputtering. The layers can be photo-patterned and etched to sub-micrometer resolutions and finally encapsulated in biomaterials such as diamond-like carbon, bioceramic, or a biocompatible polymer. Processes such as photolithography, reactive ion etching (RIE), CMOS processing, MEMS processing, focused ion beam patterning, and AFM lithography can be used to achieve the desired microelectrode design.

The benefits of a microfabrication approach include a high degree of reproducibility in physical, chemical, and electrical characteristics. Microfabrication is a high yield, low cost process once the design and processing sequence have been developed. Additionally, precise control of the spatial distribution of electrode sites exists, which may be of interest when seeking to optimally stimulate or record from a target site. A high packing density of electrode sites for a given implant volume is also readily achievable using photolithographic techniques. The possibility exists of incorporating the interface circuitry directly on the micro-sensor platform thus reducing the need for complex interconnections.

The widespread availability of silicon micromanufacturing techniques has enabled the fabrication of a range of silicon-based wedge- or needle-shaped electrodes to allow penetration of the nervous tissue. 3D arrays of such structures have been developed for insertion into, for example, the cortex to detect local potentials (134).

1D arrays of electrodes are fabricated using lithographic patterning and deposition of thin-film metal leads and electrodes onto not only silicon, but also glass and even flexible polyimide substrates (136). Much of the work on silicon-based microprobe fabrication has been pioneered at the Center for Integrated Sensors and Circuits at the University of Michigan.

A 3D electrode array can be fabricated by assembling a range of 1D probes (such as those shown in Fig. 51). As each probe has multiple recording sites along its length, the complete volume of the tissue under study can be assessed, giving rise to very dense sampling. The Michigan Probe has evolved a large number of single-shaft, multishaft, and 3-D-stacked microelectrode arrays (136).

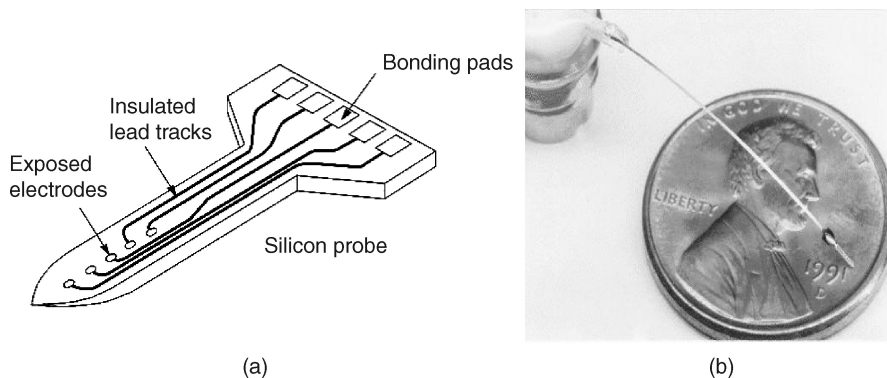


**Figure 51.** (a) Multielectrode silicon probe. [After Drake et al. (138).] (b) Michigan micromachined multielectrode probe for recording and stimulation of central nervous system.

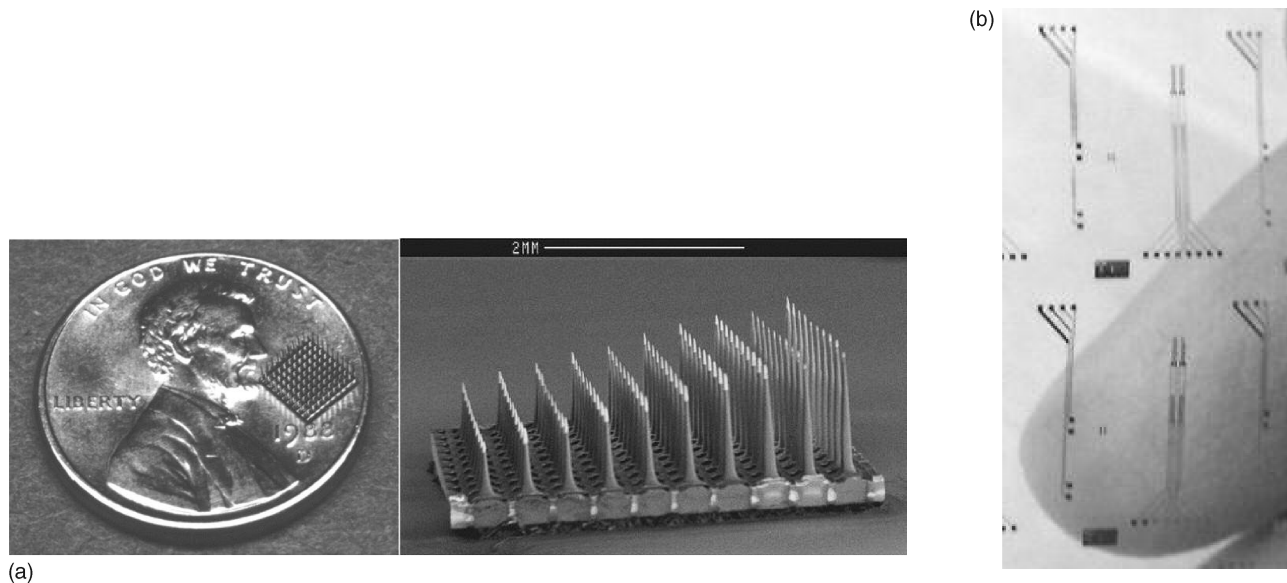


**Figure 52.** (a) Utah electrode array shown on a U.S. penny to convey size. (b) Modified Utah electrode array in which the length of the needles is uniformly graded (134).

Recent improvements in silicon microtechnology have made it possible to create not only planar microelectrodes but also penetrating brush electrode structures for *in vivo* measurements. In contrast to the University of Michigan's planar devices, the 2D and 3D cortical multimicroelectrode arrays developed at the University of Utah are fabricated out of a single solid block of silicon. Etching of the block results in a  $10 \times 10$  array of needles, each 1.0–1.5 mm long, arranged on a  $4.2 \times 4.2$  mm base. The metal and insulation layers are then applied, creating 35–75  $\mu\text{m}$  long platinum recording tips (134,136,139) (Fig. 52a).

This design has the advantage of placing a relatively large number of recording sites in a compact volume of the cortex. However, with a single recording site on the end of each needle set at a fixed depth into the cortex, this version of the Utah array is classified as a 2D array as all the electrodes are in the same plane (140). The Utah probe can achieve high-density sampling by spacing many needles close together but does not have multiple sites along each shaft. When the length of the needles in such an array is graded (the array is said to be slanted, Fig. 52b) or the needles have some other distribution of lengths, these arrays are termed 3D as the electrode tips are no longer in the same plane. These designs are thought to give the better spatial selectivity (134,136).

Implanting such needle or brush electrode systems is obviously associated with damage of the tissue. Moreover, the stiffness of many systems may lead to damage of nervous tissue, especially if relative movement exists between the sharp needles and the delicate tissues. Breakage of the brittle needle is also a concern. Considerable efforts are therefore being directed at miniaturizing the width of the needles or at introducing more flexible materials.

For example, some versions of the Michigan Probe consist of four parallel, dagger-like probes connected to a micro-silicon ribbon cable. The ribbon cable is semiflexible

and allows the probes to move up and down with the cortex as it pulses (139).

In the development of subretinal stimulating arrays using current silicon micromanufacturing techniques, it has been pointed out that a planar, rigid implant is likely to mechanically damage the compliant, spherical retina (137). Concerns have also been expressed regarding the use of penetrating microelectrodes, the relative micro-motion between the array and the retina potentially provoking mechanical damage and a significant encapsulation response (134). The ideal retinal-stimulating electrode would therefore have the flexibility to match the curvature of the retina and the next generation of electrode arrays are likely to be constructed on flexible substrates.

Microelectrode arrays on flexible substrate have been demonstrated in a range of applications including the European project "Microcard", Si-Based Multifunctional Microsystem needle for Myocardial Ischemia Monitoring. Initially, work centered on silicon-based microprobes to monitor the electrical impedance of tissue, tissue temperature, pH, and local ionic concentrations of potassium, sodium, and calcium. These parameters were found to vary considerably when, for example, a heart undergoes an ischaemic phase, thus establishing the clinical value of the technique and device, (140).

In the course of the silicon probe development, it was foreseen that the brittle nature of silicon could make intact probe removal difficult. Additionally, the rigid needle could cause damage to the delicate tissues. The thrust of the project thus changed to the development of flexible, polymer-based probes.

Thin-film devices for the measurement of tissue impedance and ion concentrations were manufactured on flexible polyimide substrates (Fig. 53a) (141). Gold thin-film electrodes were deposited using an improved photolithography process for 1  $\mu\text{m}$  resolution. Polyimide insulation

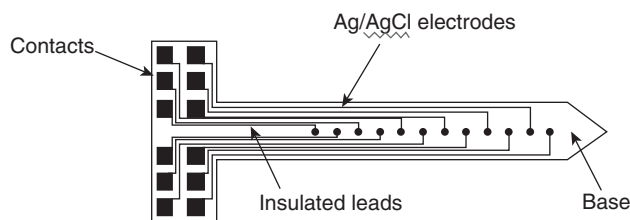


**Figure 53.** Microfabrication of sensors onto flexible substrates. 1D probe electrode array. [After Mastrototaro et al. (141).]

layers were spin-coated onto the PTFE surface after suitable conditioning, and they proved to be insulating and continuous.

Electrochemical characterization of the gold thin-film impedance electrodes showed them to possess high interface impedance. Pt and IrO oxide coatings were electrochemically applied to the gold thin-film surface and resulted in a drastic reduction in interface impedance for monitoring or stimulation applications (142).

Encircling neural electrodes may be of a cuff or spiral design. The term cuff electrodes applies to those devices that engulf the entire circumference of a nerve. First model, which rather stiff, carried only one or two electrodes and they were made using a platinum foil electrodes that were located on the inside of a cylinder of silicone rubber, which was wrapped around a nerve (Fig. 54b). (136). It is generally recommended that the diameter of the cuff be 50% larger than the nerve diameter to avoid nerve compression and necrosis due to swelling and fibrous tissue ingrowth. Cuff electrodes do however have a long and successful track record in a range of FES applications (143).

The spiral electrode is a loose, open helix that is wound around the nerve (143). The open design can accommodate swelling and is very flexible. A version of this electrode is marketed by Cyberonics for use with their vagus nerve stimulator (Fig. 54b). New designs of nerve cuff electrodes seek to reshape the geometry of the nerve to more selectively stimulate or record from particular nerve fascicles. Efforts are also directed at controlling the electrical fields generated by the electrode arrays to better focus the stimulation (135).

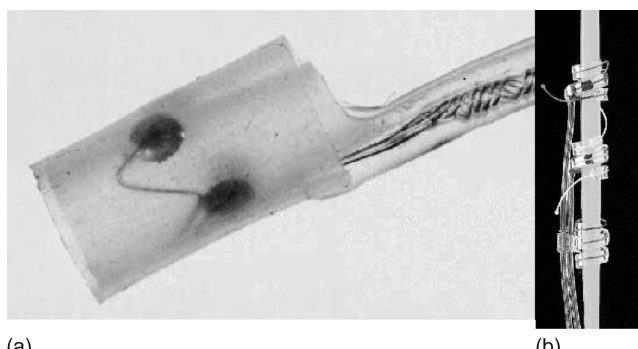


**Figure 54.** (a) Neural cuff electrode. (b) Spiral electrode (Cyberonics).

As part of a European project NEUROS, NIBEC developed a flexible thin-film-based stimulation and sensing cuff electrode for FES-related application. IrO, Pt, and Au electrodes were deposited onto a polyimide substrate. In order to facilitate implantation and ensure good contact between nerves, fascicles and electrode surface was self-curling. Polyimide resin with a thermal expansion coefficient differing from that of the polyimide substrate was chosen so that the curing process gives rise to a residual stress and curl in the device. The diameter of the electrode cylinder could be made less than 1 mm.

Diamond-like carbon (DLC) encapsulation was deposited onto the device using a plasma-enhanced chemical vapor deposition (PECVD) process. Adhesion to the polyimide substrate was found to be satisfactory following the addition of a silane adhesion layer at the interface (144,145).

With the aid of micofabrication techniques, one can control the area and properties of the electrodes and greatly decrease them in size. However, as electrode area decreases, the interface impedances increase with resultant difficulties in making accurate measurement. The key to success in this case is in the choice of electrode design, material, and electrode surface topography.

A similar concept to Chardack's differential current density pacemaker electrode was suggested for use in thin-film electrodes. The metal electrode is housed within a hollow chamber (Fig. 55). The chamber is filled with electrolyte and has a small aperture to enable electrical contact with tissues (146). As the metal-electrolyte interface is relatively large, the interface impedance is relatively small. The interface is also protected from mechanical disturbance (similar to the floating electrode) and, hence, should suffer from less artifact. As the small aperture determines the area of contact with the tissue, the effective stimulation or recording area is very small.

Other 3D designs with etched meshes should be assessed for their potentially larger interfacial areas.

Once again, surface roughness is an important factor in decreasing interface impedance and possibly in helping anchor the electrode in position. Rough-surfaced electrodes must be used with caution, depending on the application, in case the surface causes damage to the surrounding tissues. Certain materials and the electrode fabrication processes involved may well result in favorable macro-, micro-, and nano- surface features. Presently, investigators are studying modifications to the electrode surface using such things as nanotubes. Nanotechnology offers much promise for

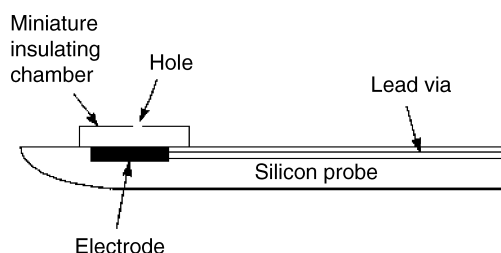


**Figure 55.** Thin-film differential current density electrode. [After Prohaska et al. (146).]

new sensor devices, particularly in the biomedical sector. Not only do individual nanotubes offer the possibility of using them as ultrafine needles for *in vivo* probing at the cellular level, but surfaces can be created with optimal distributions of clusters of nanotubes to maximize performance.

## ELECTRODE STANDARDS

The Association for the Advancement of Medical Instrumentation (AAMI) produce a range of labeling, electrical, and other performance requirements for manufacturers and users to help ensure acceptable levels or product safety and efficacy. Some of the key electrode-related standards are briefly reviewed below.

### Standards For Biosignal Monitoring Electrodes

#### Standards for Disposable ECG Electrodes. ANSI/AAMI EC 12 (2000)

**Introduction.** In an effort to minimize ECG recording problems associated with the performance of electrodes coupled to a standard ECG monitor or electrocardiograph, AAMI has proposed a series of simple bench tests designed to assess pre-gelled, disposable ECG electrodes.

Although originally conceived to assess disposable ECG electrodes, these standards are widely used to assess other biosignal monitoring electrodes, which is a consequence of the lack of other widely accepted standards for these monitoring applications and to the general applicability of the ECG standards to the other applications.

Although AAMI also lays down stipulations for electrode labeling, adhesion testing, and soon, only the electrical performance requirements are reviewed here.

**AC Impedance.** The average value of 10 Hz impedance for at least 12 electrode pairs connected gel-to-gel, at a level of impressed current not exceeding 100  $\mu$ A peak-to-peak, shall not exceed 2 k $\Omega$ . None of the individual pair impedances shall exceed 3 k $\Omega$ .

Low impedance electrodes are desirable to avoid signal attenuation and distortion and to minimize 50/60 Hz interference pickup. High electrode impedances can also give rise to serious burns when the ECG electrodes are used in the presence of electrosurgery or defibrillator discharges. (147).

The impedance of the skin's outer layer, the stratum corneum, is many times larger than that of the metal/electrolyte interface, and hence, the former is of key concern when endeavoring to ensure good electrode performance. The skin preparation technique, the extent of diaphoresis, and the ability of the electrode gel in penetrating and reducing the skin impedance are generally more important than the electrode-electrolyte interface impedance.

The Standards Committee decided that the electrode gel-to-gel impedances should be significantly less than the expected impedance of clean, dry skin to ensure a minimal contribution by the electrode itself to the overall impedance (147). In the UBTL tests carried out on behalf of the

Standards Committee, it was found that the mean 10 Hz impedance of a standard pair of ECG electrodes on unabraded skin was of the order of 100 k $\Omega$ . The AAMI committee chose 2000 k $\Omega$  as a reasonable limit for 10 Hz gel-to-gel impedance to ensure that the electrodes did not contribute significantly to the overall impedance nor to power dissipation in the presence of defibrillation overload and electro-surgery currents.

As the electrode-gel interface impedance is nonlinear and decreases with applied signal amplitude, the standard stipulates that the level of impressed current must not exceed 0.1 mA peak-to-peak when carrying out the test.

In the UBTL tests, it was found that the impedance as measured on abraded skin correlated well (99%) with the impedance measured with the electrodes connected gel-to-gel, whereas the impedance measured with electrodes applied to clean, dry skin correlates very poorly (47%) with the gel-to-gel measurements. Obviously, the bench test simply evaluates the ac impedance performance of the electrode-gel interface and will, therefore, not accurately predict or represent the clinical performance of an electrode on intact skin. For example, cases of electrodes that performed poorly as per the AAMI bench test exist, yet which proved very satisfactory *in vivo*. Conversely, some of the best electrodes according to the bench tests performed relatively badly *in vivo* (148).

**DC Offset Voltage.** After a 1 min stabilization period, a pair of electrodes connected gel-to-gel, shall not exhibit an offset voltage greater than 100 mV.

Ideally, the potentials of both electrodes used to monitor a biosignal should be identical and, thus, cancel each other out. Slight differences in the gels and metals used, however, result in an offset voltage. The potentials of the skin sites further complicate the recording, especially as these latter potentials (and their amplified difference) tend to be much larger. If the overall electrode-skin potential difference is larger than 300 mV, the amplifier may saturate and the biosignal will not be observed.

The UBTL report studied the correlation between gel-to-gel and electrode-skin offset voltages and found that gel-to-gel offsets were in the order of 2.5 times smaller than those recorded *in vivo* for the same electrodes on a patient's skin. As the maximum allowable *in vivo* dc offset should be less than 300 mV, the Committee decided that the limit for gel-to-gel dc offset should therefore be less than 300/2.5 mV (i.e., 100 mV).

Some reviewers of the standard argued that the limit should be reduced to 10 mV as this would help minimize motion artifact problems. The Committee rejected this suggestion, pointing out that no clear evidence exists that links high gel-to-gel offset voltages with motion artifact (largely caused by skin deformation).

**Offset Instability and Internal Noise.** After a 1 min. stabilization period, a pair of electrodes connected gel-to-gel, shall not generate a voltage greater than 150  $\mu$ V<sub>p-p</sub> in the passband (first-order frequency response) of the 0.15–100 Hz for a period of 5 min following the stabilization period.

This standard is concerned with the problem of baseline wander, which introduces a low frequency component into the monitored biosignal making accurate diagnosis difficult. The American College of Cardiology's Task Force on the Quality of Electrocardiographic Records judged that drift rates less than  $400 \mu\text{V} \cdot \text{s}^{-1}$ , although not highly rated, were not considered unacceptable.

The UBTL report detailed several experimental limitations that prohibited their detailed study of *in vivo* dc offset drift. Consequently, no correlational analysis was carried out between dc offset drift measurements made with electrodes applied to human skin and those joined gel-to-gel. They, however, decided to use the factor of 2.5 they had observed between clinical and bench test result for dc offsets, given that the measurement techniques are fundamentally similar. A limit of  $150 \mu\text{V} \cdot \text{s}^{-1}$  was therefore arrived at by dividing the  $400 \mu\text{V} \cdot \text{s}^{-1}$  baseline drift rating by a factor of 2.5. As the test circuit used in the bench test differentiates the offset voltage, the offset instability requirement is specified in  $\mu\text{V}$  rather than  $\mu\text{V} \cdot \text{s}^{-1}$ .

The Committee was contacted and asked to decrease the limit from  $150 \mu\text{V}$  to  $40 \mu\text{V p-p}$  in order to be in line with the AAMI standard "Cardiac monitors, heart rate meters and alarms (EC13)". The working group agreed that this requirement could be made more stringent but refused to decrease the limit to  $40 \mu\text{V}_{\text{p-p}}$ . This requirement is under study and may well be altered.

This calculation involved in reaching the  $150 \mu\text{V} \cdot \text{s}^{-1}$  limit implies that skin potential fluctuations are only 2.5 times larger than those of the electrode–gel interface, which is most unlikely, and problems developing from drifting electrolyte/skin potentials will depend on skin preparation, electrode design, and electrode gel rather than the electrode–gel interface characteristics *per se* (64).

**Defibrillation Overload Recovery.** Five seconds after each of four capacitor discharges, the absolute value of polarization potential of a pair of electrodes connected gel-to-gel shall not exceed 100 mV. Also during the 30 s interval following each polarization potential measurement, the rate of change of the residual polarization potential shall be no greater than  $\pm 1 \text{ mV} \cdot \text{s}^{-1}$ .

It is important that a clinician, having defibrillated a patient, be able to see a meaningful ECG within 5–10 s in order to judge the efficacy of the delivered impulse and to decide if another is required. The offset voltage across the electrode-skin interfaces, which drastically increased as a result of the defibrillation impulse, must therefore return to below 300 mV within 5 s following the discharge. Once again, using the 2.5 factor between bench test and *in vivo* potentials, this requirement translates to a gel-to-gel bench test offset voltage under 100 mV within 5 s of applying an overload of 2 mC (representing the worst possible situation encountered *in vivo* where the defibrillator paddles are placed in immediate contact with the ECG electrodes). Electrodes made of stainless steel, for example, tend to acquire offset voltages of several hundred mV for minutes and, consequently, no ECG trace is observable on the monitor (68).

Following the initial 5 s the ECG must not only be visible on the monitor but must also be recognizable and clinically

useful. Hence, the stipulation that the offset voltage should not drift with time by more than  $\pm 1 \text{ mV} \cdot \text{s}^{-1}$ .

The UBTL results indicate good correlation exists between the results of this bench tests and animal tests, particularly at the higher recovery voltages encountered with non-Ag/AgCl electrodes.

Although only a very low percentage of ECG electrodes are, in fact, subjected to defibrillation impulses *in vivo*, the AAMI committee decided after some deliberation to insist that all ECG electrodes meet the proposed standard as it is impossible to guarantee that a given electrode would not be used in an emergency defibrillation situation.

**Bias Current Tolerance.** The observed dc voltage offset change across a pair of electrodes connected gel-to-gel shall not exceed 100 mV when the electrode pair is subjected to a continuous 200 nA dc current over the period recommended by the manufacturer for the clinical use of the electrodes. In no case shall this period be less than 8 h.

When a dc current passes through the metal-gel interface of an electrode, the electrode potential deviates from its equilibrium value and the electrode is said to be polarized. If the current is maintained indefinitely, the reactants become depleted causing the electrode potential to deviate further, possibly exceeding the limit allowable at the input of the ECG recording device.

Although most modern ECG recorders pass less than 10 nA of bias current through the electrodes, some older models can have bias currents as high as 1000 nA. A number of cardiac monitor manufacturers use dc bias currents to sense high electrode impedances to warn of disconnected leads or poorly affixed electrodes. The standard for cardiac monitors permits input bias currents of up to 200 nA. UBTL, therefore, adopted the 200 nA limit on the dc input bias current suggested for cardiac monitors for the tests. The ability of an electrode to cope with this value of bias current must therefore be demonstrated by not exceeding the AAMI dc offset requirement of 100 mV over the time period recommended by the manufacturer for the clinical use of the electrodes.

The 200 nA current level is generally well-tolerated by Ag/AgCl electrodes. Stainless-steel electrodes rapidly fail this test even at 10 nA with major increases in electrode potential.

**Discussion.** The AAMI standards bench tests are currently the only widely accepted electrode standard tests in use. The tests are simple and inexpensive to set up and have been widely embraced by manufacturers and users for production quality control purposes. One must bear in mind, however, that these tests evaluate only the electrode-gel interface and that they do not include the more important properties of the gel-skin interface. Assessment of the clinical performance of electrode impedance using the proposed bench tests is only relevant if the skin has been suitably abraded. Skin abrasion is not widely used by the clinical community and, hence, the relevance of at least some of the standard tests to the clinical situation is open to question.

Especially several decades ago, fulfillment of the AAMI requirements was commonly quoted as a guarantee

of the high *in vivo* electrical performance of an electrode. An electrode with, for example, a dc offset of 1 mV was widely believed by customers to be a much better electrode than one with an offset of 5 mV. This naivety appears to be on the wane, however, and manufacturers and customers are shifting toward low cost electrodes that score less highly in the AAMI tests but are good enough for a given application.

The author once supplied a leading company with dry metal-loaded polymer electrodes. The company connected the electrodes together and tested them as per the AAMI standards (for pregelled electrodes). Perfect electrical performances were measured given that what was effectively being assessed was metal-to-metal contact. Direct current offsets of 0 mV were obtain. Once the dry electrodes were applied to a patient's skin, a less than favorable result was obtained.

The attitude to adopt, therefore, when interpreting AAMI standard bench tests results for pregelled, disposable ECG electrodes is that electrodes that meet the AAMI standards have a tendency rather than a certainty to perform well *in vivo*. Electrodes that perform better as per the bench tests do not necessarily perform better *in vivo*. They are a useful set of tests nonetheless.

The ANSI/AAMI standard tests were conceived such that the test apparatus needed can be readily assembled by an electrode manufacturer. However, one can buy a convenient-to-use, custom-built electrode tester (as per AAMI standards) called the Xtratek electrode tester ET65A (Direct Design Corporation, Lenexa, Kansas.) (Fig. 56).

Electrocardiograph surface electrode testers also exist for the *in vivo* testing of the quality of (1) the design ECG electrodes, (2) the application of the electrodes, and (3) the skin preparation technique used.

The electrode tester generally measures the ac impedance and dc offset of the electrode-patient system. These measurements can be used, for example, in stress testing to decide if the skin sites have been sufficiently well prepared (i.e., contact impedances are low enough) to proceed with the clinical procedure. They can also be used to detect the presence of loose cables or bad contacts.



**Figure 56.** Early version of the Xtratek electrode tester ET65A. (Direct Design Corporation; Lenexa, Kansas.)

### Standards for Stimulation Electrodes

Although not covered in this article, the following standards exist that stipulate minimum labeling, safety, and performance requirements for the given stimulators. The rationale for the standards is also presented.

- Transcutaneous electrical nerve stimulators ANSI/AAMI NS4.
- Implantable spinal cord stimulators ANSI/AAMI NS14.
- Implantable peripheral nerve stimulators ANSI/AAMI NS15.

### Standards for Automatic External Defibrillators and Remote-Control Defibrillators. ANSI/AAMI DF 80 (2003)

**AC Small Signal Impedance.** The 10 Hz impedance for any of at least 12 electrode pairs connected gel-to-gel, at a level of impressed current not exceeding 100  $\mu$ A peak-to-peak, shall not exceed 3 k $\Omega$ . The impedance at 30 kHz shall be less than 5  $\Omega$ . The rationale for this requirement is based on the performance criteria in ANSI/AAMI EC 12 for disposable ECG electrodes. Interestingly, the permissible gel-to-gel 10 Hz impedance for large-area defibrillation pads is higher than that allowed for small-area ECG electrodes. The gel-to-gel impedance measured at 30 kHz will be largely that of the gel pads as the interface impedances at this frequency will be almost zero.

**AC Large Signal Impedance.** The impedance of an electrode pair connected gel-to-gel, in series with a 50  $\Omega$  load and measured at the maximum rated energy of the defibrillator shall not exceed 3  $\Omega$ . A value of 50  $\Omega$  is thought to represent the typical (rather low) *in vivo* transthoracic impedance between the electrodes. One wants the delivered energy to be dissipated in the patient's chest and not in the electrodes where the wasted energy may give rise to skin burns. The above requirement is therefore thought to provide a reasonable limit on the impedance contributed to the overall impedance by the electrode pair during defibrillation (<6%).

**Combined Offset Instability and Internal Noise.** A pair of electrodes connected gel-to-gel shall generate, after a 1 min stabilization period, a voltage no greater than 100  $\mu$ V peak-to-peak in the pass band of 0.5–40 Hz, for a period of 5 min following the stabilization period. The rationale for this requirement is based on the performance criteria in ANSI/AAMI EC 12 for Disposable ECG electrodes. The frequency range used is more limited in recognition that the cardiac monitor bandwidth is more appropriate in this application.

**Defibrillation Recovery.** The potential of a pair of gel-to-gel electrodes in series with a 50  $\Omega$  resistor and subjected to three shocks at 360 J or maximum energy at 1 min intervals shall not exceed 400 mV at 4 s and 300 mV at 60 s after the last shock delivery. The rationale for this requirement is largely based on the performance criteria in ANSI/AAMI EC 12 for Disposable ECG electrodes. An actual

defibrillation impulse is applied instead of that from a simulation circuit. The offset voltage across the simulated electrode-patient load must return to below 400 mV within 4 s following the discharge (slightly different values, 300 mV and 5 s, are used in ANSI/AAMI EC 12). As the patient's chest is represented by the 50 Ω resistor, no need exists for the 2.5 factor used in ANSI/AAMI EC 12 to correlate bench test and *in vivo* results.

**DC Offset Voltage.** A pair of electrodes connected gel-to-gel shall, after a 1 min stabilization period, exhibit an offset voltage no greater than 100 mV. The rationale for this requirement is based on the performance criteria in ANSI/AAMI EC 12 for disposable ECG electrodes.

**Universal-Function Electrodes.** With conventional defibrillators, it has been customary to use separate pregelled ECG electrodes for monitoring and defibrillator paddle electrodes for defibrillation. The monitoring electrodes are not capable of effectively delivering a defibrillation shock, and the paddle electrodes have only limited monitoring capability. For recent applications, particularly automatic external defibrillation, it is very desirable to use self-adhesive pregelled disposable combination electrodes that perform well in the dual monitoring and defibrillation functions. These electrodes may also be used for delivery of transcutaneous pacing. Hence, combination electrodes may become preferred for defibrillation, and it is appropriate in a standard for defibrillators to consider their use and to outline a few requirements for them.

If the electrodes are designed and intended for use in multiple modes (i.e., monitoring, defibrillation, and pacing) the electrode shall meet all (of the above) requirements after 60 min of pacing at the maximum current output and maximum pacing rate through a pair of gel-to-gel electrodes in series with a 50 Ω resistor.

No general performance standards exist for combination pacing/defibrillation/monitoring electrodes, the (above) requirements define the basic minimum controls necessary to ensure safe and reliable operation.

#### Standards for Electrosurgical Devices. ANSI/AAMI HF 18 (2001)

**Introduction.** Although AAMI lays down stipulations for the testing of a range of parameters, only the key electrical performance requirements for the dispersive electrodes are reviewed below.

**Maximum Safe Temperature Rise.** The maximum patient tissue temperature rise shall not exceed 6 °C when the dispersive electrode carries a current of 700 mA under the test conditions below, unless the device is labeled in accordance with 4.1.4.2 (i.e., for use on infants). For devices labeled for use on infants, the maximum patient tissue temperature rise shall not exceed 6 °C when the dispersive electrode carries a current of 500 mA under the test conditions stipulated in the standard. In monopolar electrosurgical procedures, the dispersive electrode must be able to reliably conduct the required surgical current without generating a significant rise in skin temperature. It is widely accepted that the maximum safe skin temperature

for short-term and long-term exposure is 45 °C, as normal resting skin temperature varies between 29° and 33 °C. Electrodes must not generate skin temperature increases approaching 12 °C. A 6 °C increase in temperature is therefore thought to represent an acceptable upper limit.

The temperature measurement method must have an overall accuracy of better than 0.5 °C and a spatial resolution of at least one sample per square centimeter of the electrode thermal pattern. The thermal pattern must include the area extending 1 cm beyond the geometry of the electrode under test. This degree of special resolution is stipulated as electrosurgical burns may be confined to very small areas and these must be detected. As current tends to flow to the edge of the electrode and spread out further in the skin, the test requires that the surround area of skin is also scanned.

The electrode under test is to carry a current from an electrosurgical generator of 700 mA<sub>rms</sub> for 60 s, unless the device is labeled in accordance with 4.1.4.2, in which case the test current may be 500 mA. A current of 700 mA applied for 60 s yields a heating factor of 30 A<sup>2</sup> s. [Heating Factor =  $I^2t$  (A<sup>2</sup>s).] This value is far in excess of the maximum likely current and duration for a TUR (transurethral resection) procedure. A more realistic heating factor is less than 10 and, hence, the stipulated testing procedure is very conservative.

These tests must be conducted on human volunteers or on a suitably structured surrogate medium. When human volunteers are used, the tester must include a variety of body types in the sample group rather than concentrate on a single body type (thin, average, or thick layers of subcutaneous body fat). If surrogate media are used, the tester must demonstrate that the media are electrically and thermally similar to human volunteers. Human volunteer subjects are the reference standard. Current density distribution under an electrode depends on a wide range of factors, including the electrical properties of the skin and underlying tissues, hence, the need to test a given electrode on a wide range of individuals. The use of a surrogate material, even pig skin, which is commonly used, will not necessarily replicate with sufficient accuracy the clinical performance of the electrode. If a surrogate medium is used, the tester must demonstrate the equivalence of the test medium to human tissue. It is the Committee's view that no adequate surrogate medium has yet been suggested or used that has all of the properties of human tissue for the purpose of determining electrode performance.

Nessler et al. (149) point out that the above experiments are laborious, time-consuming, and expensive to perform. They have developed a new test device, swaroTEST, which includes a surrogate electronic skin, which, they claim, simulates the relevant electrical features of human skin and thus can replace the required volunteer experiments (Fig. 57). The device consists of a 3D resistor network representing the electric features of the skin and muscle tissue, and a temperature-sensing array (one transistor for each cm<sup>2</sup>) to measure the resultant temperature increase after a standardized current load (700 mA hf current during 60 s, proposed in the relevant AAMI HF-18 standard). The authors claim that a comparison of results obtained with their device and those with thermo camera images of

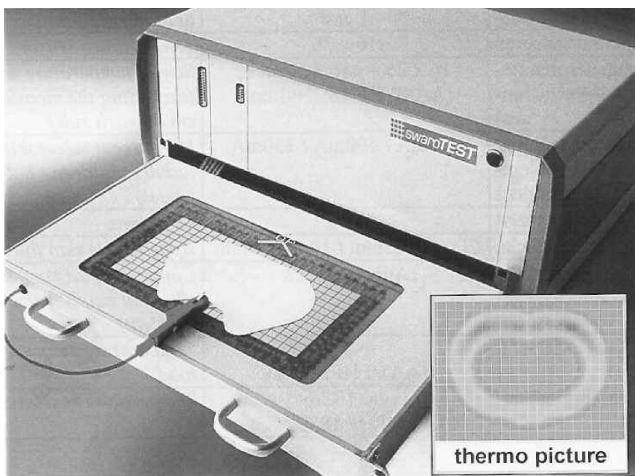


**Figure 57.** Swaro Test device with a measuring board electronic skin to simulate the electrical properties of human skin. It is hoped that this device will replace the human volunteer experiments required for ANSI/AAMI HF 18.

volunteer experiments correspond sufficiently well to justify the acceptance of their test device as a surrogate medium.

**Electrode Contact Impedance.** The electrode contact impedance must be low enough that the dispersive electrode represents the preferred current pathway, thus avoiding skin burns at alternative pathways. For conductive electrodes, the maximum electrode contact impedance shall not exceed  $75\ \Omega$  over the frequency range of 200 kHz–5 MHz when measured as described on a human subject. The frequency range of 200 kHz–5 MHz encompasses the frequency ranges of existing generators. As electrode-tissue impedance increases as applied current decreases, the committee decided on an impedance measuring current of 200 mA as it represents the lower limit of average currents reported for TUR procedures. Under these conditions, a maximum contact impedance value of  $75\ \Omega$  was judged an acceptable for the conductive electrodes.

For capacitive electrodes, the minimum capacitance shall be no less than  $4\text{ nF}$  ( $0.004\ \mu\text{F}$ ) when measured as described. In this case, electrode contact impedance is measured by placing the capacitively coupled dispersive electrode under test on a rigid metal plate larger than the electrode contact area. The test current and frequencies are the same as those specified for conductive electrodes. Their impedance characteristics are described in terms of capacitance as their impedances vary as the inverse of the frequency. The majority of capacitive electrodes that have been found to be clinically acceptable typically have a capacitance value of  $4\text{ nF}$ , hence the minimum acceptable capacitance value specified by the Committee.

## SUMMARY

With external biosignal monitoring electrodes, difficult challenges exist in the exciting new area of personalized

health. Such electrodes must form part of the patient's (or health-conscious citizen's) clothing and must continue to work, day after day, wash after wash, without gelling or preparation of any kind, without suffering from motion artifacts, and without causing skin irritation, which is no mean achievement.

An old monitoring problem still remains to be adequately conquered. A convenient and rapid method of applying many high performance electrodes to the head of a patient for EEG measurement awaits invention. The problem (and that of ECG ambulatory monitoring above) can be side-stepped to some extent by finding new electrode positions (montages or leads) that avoid the most problematic skin sites, hairy head in EEG and muscle and flabby areas in ECG.

For external stimulation, exciting new areas include public access defibrillation. The electrodes and their application to the victim must be almost literally fool-proof, given the seriousness of the possible consequences for all concerned. The electrodes must work after having been stored in the most inhospitable locations and possibly under extreme temperature fluctuations, for example, in the trunk of a car in the desert. In the more mainstream areas of cardiac pacing and defibrillation and electrosurgery, the optimal distribution of current density under the electrodes remains a goal still to be achieved. The solution to this problem offers the hope of decreased electrode areas and the design of truly multifunction pads.

The integration of electrodes into garments for FES and body toning is a relatively new area with considerable possibilities.

At present, implant electrodes and associated technologies already offer amazing potential for the deaf, lame, and even the blind. The development of multimicroelectrode arrays and waveforms that can help optimally shape the electrical fields to facilitate more effective and natural stimulation is a thrilling prospect. The interface properties of the microelectrodes will require further research so as to offset the potentially high interface impedances. Ideas already exploited in cardiac pacing, for example, may prove rewarding when adapted for these areas.

It is hard to overstate the potential of research being undertaken in the area of brain-machine interface. We live in exciting times.

## BIBLIOGRAPHY

### Cited References

1. Gatzke RD. In: Miller HA, Harrison DC, editors. The electrode: A measurement systems viewpoint. Biomedical Electrode Technology. New York: Academic Press; 1974.
2. Janz GJ, Ives DJG. Silver-silver chloride electrodes. Ann NY Acad Sci 1968;148:210–221.
3. Webster JG. Medical Instrumentation: Application and Design. 3rd ed. New York: John Wiley & Sons; 1998.
4. Cheney M, Isaacson D, Newell JC. Electrical impedance tomography. SIAM Rev 1999;41:85–101.
5. McAdams ET, Jossinet J, Lackermeier A, Risacher F. Factors affecting the electrode-gel-skin interface impedance in electrical impedance tomography. Med Biol Eng Comput 1996;34(6):397–408.

6. Singh S, Singh J. Transdermal drug delivery by passive diffusion and iontophoresis: A review. *Med Res Rev* 1993;13(5):569–621.
7. Bard AJ, Faulkner LR. *Electrochemical Methods*. New York: John Wiley & Sons; 1980.
8. Almasi JJ, Hart MW, Schmitt OH, Watanabe Y. Bioelectrode voltage offset time profiles and their impact on ECG measurement standards. *Can Med Biol Eng Conf* 4th, Winnipeg, Manitoba, Canada, 1972.
9. McAdams ET. Effect of surface topography on the electrode-electrolyte interface impedance, Part 1: The high frequency, small signal interface impedance. *Surface Topogr* 1989;2: 107–122.
10. Fricke H. The theory of electrolytic polarization. *Philos Mag* 1932;7:310–318.
11. Cole KS, Curtis HJ. Transverse electric impedance of squid giant axon. *J Gen Physiol* 1938;22:3764.
12. Sluyters-Rechbach M, Sluyters JH. Sine wave methods in the study of electrode processes. In: Bard AJ, editor. *Electroanalytical Chemistry*, vol. 4. New York: Marcel Dekker; 1970. pp 1–128.
13. De Levie R. The influence of surface roughness of solid electrodes on electrochemical measurements. *Electrochim Acta* 1965;10:113–130.
14. de Levie R. On the impedance of electrodes with rough interfaces. *J Electroanal Chem* 1989;261:1–9.
15. Maritan A, Toigo F. On skewed arc plots of impedance of electrodes with an irreversible electrode process. *Electrochim Acta* 1990;35:141–145.
16. McAdams ET. Effect of surface topography on the electrode-electrolyte interface impedance, Part 2: The low frequency ( $F < 1$  Hz), small signal interface impedance. *Surface Topogr* 1989;2:223–232.
17. Bergveld P. *Med Biol Eng Comput* 1976;14:479–482.
18. Brummer SB, Robblee LS, Hambrecht FT. Criteria for selecting electrodes for electrical stimulation: Theoretical and practical considerations. *Ann NY Acad Sci USA* 1983;405: 159–171.
19. Brummer SB, Turner MJ. Electrical stimulation of the nervous system: The principle of safe charge injection with noble metal electrodes. *Bioelectrochem Bioenerget* 1975; 2:13–25.
20. Dymond AM. *IEEE Trans BME* 1976;23:274–280.
21. Lilly JC, Hughes JR, Alvord EC, Galkin TW. Brief, noninjurious electric waveform for stimulation of the brain. *Science* 1955;121:468–469.
22. Weinman J. Biphasic stimulation and electrical properties of metal electrodes. *J Appl Physiol* 1965;20:787–790.
23. Fischler H, Schwan HP. Polarisation impedance of pacemaker electrodes: *In vitro* simulating practical operation. *Med Biol Eng Comput* 1981;19:579–588.
24. Schwan HP. Electrode polarization impedance and measurements in biological materials. *Ann NY Acad Sci USA* 1968;148:191–209.
25. Schwan HP. Alternating current electrode polarisation. *Bio-physik* 1966;3:181–201.
26. Simpson RW, Berberian JG, Schwan HP. Nonlinear AC and DC polarization of platinum electrodes. *IEEE Trans Biomed Eng* 1980;27:166–171.
27. Jaron D, Briller SA, Schwan HP, Geselowitz DB. Nonlinearity of cardiac pacemaker electrodes. *IEEE Trans Biomed Eng* 1969;16:132–138.
28. Onaral B, Schwan HP. Linear and non-linear properties of platinum electrode polarization: Part 1. Frequency dependence at very low frequencies. *Med Biol Eng Comput* 1982;20:299–306.
29. McAdams ET, Henry P, Anderson JMcC, Jossinet J. Optimal electrolytic chloriding of silver ink electrodes for use in electrical impedance tomography. *Clin Phys Physiol Meas* 1992;13(Suppl 1):19–23.
30. McAdams ET, Jossinet J. The importance of electrode-skin impedance in high resolution electrocardiography. *Automedica* 1991;13:187–208.
31. McAdams ET, Jossinet J. A Physical Interpretation of Schwan's limit voltage of linearity. *Med Biol Eng Comput* 1994; March: 126–130.
32. McAdams ET, Jossinet J. DC nonlinearity of the solid electrode-electrolyte interface impedance. *Inn Tech Biol Med* 1991;12:329–343.
33. McAdams ET, Jossinet J. A physical interpretation of Schwan's limit current of linearity. *Ann Biomed Eng* 1992; 20:307–319.
34. K Stokes. Cardiac pacing electrodes. *Proc IEEE* 1996;84(3): 457–467.
35. Stokes K. Implantable pacing lead technology. *IEEE Eng Med Biol* 1990;9(2):43–49.
36. Williams DF. *The Williams Dictionary of Biomaterials*. Liverpool University Press; 1999.
37. Geddes LA. *Electrodes and the Measurement of Bioelectric Events*. New York: John Wiley & Sons; 1972.
38. Crenner F, Angel F, Ringwald C. Ag/AgCl electrode assembly for thin smooth muscle electromyography. *Med Biol Eng Comput* 1989;27:346–356.
39. Kingma YJ, Lenhart J, Bowes KL, Chambers MM, Durdle NG. Improved Ag/AgCl pressure electrodes. *Med Biol Eng Comput* 1983;21:351–357.
40. Geddes LA, Baker LE, Moore AG. Optimum electrolytic chloriding of silver electrodes. *Med Biol Eng* 1969;7:49–56.
41. Heath R. Tin-stannous chloride electrode element. U.S. Patent 4,852,585, 1989.
42. Mannheimer JS. *Lampe GN. Clinical Transcutaneous Electrical Nerve Stimulation*. Philadelphia, F.A. Davis, PA; 1987.
43. Prausnitz MR, Bose VG, Langer R, Weaver JC. Electroporation of mammalian skin: A mechanism to enhance transdermal drug delivery. *Proc Natl Acad Sci USA* 1993;90:10504–20508.
44. Brown L, Langer R. Transdermal delivery of drugs. *Ann Rev Med* 1988;39:221–229.
45. Rosendal T. Further studies on the conducting properties of human skin to direct and alternating current. *Acta Physiol Scand* 1945;8:183–202.
46. Rosendal T. Concluding studies on the conducting properties of human skin to alternating current. *Acta Physiol Scan* 1945;9:39–49.
47. Salter DC. A study of some electrical properties of normal and pathological skin in vivo. Ph.D. dissertation, University of Oxford. Oxford (UK): 1980.
48. Klingman AM. Skin permeability: Dermatologic aspects of transdermal drug delivery. *Am Heart J* 1984;108(1):200–207.
49. Reilly JP. *Electrical Stimulation and Electropathology*. Cambridge, UK: Cambridge University Press; 1992.
50. Chien YW. Transdermal controlled-release drug administration. In: Swarbrick J, editor. *Novel Drug Delivery Systems*. New York: Marcel Dekker Inc.; 1982. p 149.
51. Edelberg R. Electrical properties of the skin. In: Elden HR, editor. *A Treatise of the Skin*. New York: John Wiley & Sons; 1971.
52. Yamamoto Y, Yamamoto T. Dispersion and correlation of the parameters for skin impedance. *Med Biol Eng Comput* 1978;16:592–594.

53. Chien YW. Development of transdermal drug delivery systems. *Drug Develop Industr Pharm* 1987;13(4&5):589–651.
54. Rothman S. Electrical behavior. In: *Physiology and Biochemistry of the Skin*. Chicago (IL): The University of Chicago Press; 1956. p 9–25.
55. Lawler JC, Davis MJ, Griffith EC. Electrical characteristics of the skin. *J Invest Dermatol* 1960; 301–308.
56. Rosell J, Colominas J, Riu P, Pallas-Areny R, Webster JG. Skin impedance from 1 Hz to 1 MHz. *IEEE Trans Biomed Eng* 1980;35:649–651.
57. Almasi JJ, Schmitt OH. Systemic and random variations of ECG electrode system impedance. *Ann N Y Acad Sci* 1970;170:509–519.
58. Grimnes S. Dielectric breakdown of human skin in vivo. *Med Biol Eng Comput* 1983;21:379–381.
59. Schmitt OH, Almasi JJ. Electrode impedance and voltage offset as they affect efficacy and accuracy of VCG and ECG measurements. Proc. XIth International Vectorcardiography Symposium, New York, 1970; 245–253.
60. Yamamoto T, Yamamoto Y. Analysis for the change of skin impedance. *Med Biol Eng Comput* 1977;15:219–227.
61. Searle A, Kirkup L. A direct comparison of wet, dry and insulating bioelectric recording electrodes. *Physiol Meas* 2000;21:271–283.
62. McAdams ET, Lacknermeier A, Woolfson ET, Moss GP, McCafferty DF. In vivo ac impedance monitoring of percutaneous drug delivery. Proc. 9th Int. Conf. on BioImpedance, Heidelberg, Germany, 1995: 344–347.
63. De Talhouet H, Webster JG. The origin of skin-stretch-caused motion artefacts under electrodes. *Physiol Meas* 17:81–93.
64. Tam HW, Webster JG. Minimizing motion artifact by skin abrasion. *IEEE Trans Biomed Eng* 1977; BME 24:134–140.
65. Zinc R. Distortion and interference in the measurement of electrical signals from the skin (ECG, EMG, EEG). *Innovation and Technology in Biology and Medicine*, 12, special issue. 1991; 1: 46–59.
66. McLaughlin J, McAdams ET, Anderson JMcC. Novel dry electrode ECG sensor system. 16th Annual Int Conf IEEE Eng Med Biol Soc Baltimore (MD), Nov. 1994:804.
67. Jossinet J, McAdams ET. Skin Impedance. *Innovation and technology in biology and medicine*, 12, special issue. 1991;1:21–31.
68. Carim HM. Bioelectrodes. In: Webster JG. editor *Encyclopaedia of Medical Devices and Instrumentation*. New York: Wiley & Sons; 1988. p 195–226.
69. Oh SY, Leung L, Bommannan D, Guy RH, Potts RO. Effect of current, ionic strength and temperature on the electrical properties of skin. *J Controlled Release* 1993;27:115–125.
70. Olson WH, Schmincke DR, Henley BL. Time and frequency dependence of disposable ECG electrode-skin impedance. *Med Instrum* 1979;13:269–272.
71. McAdams ET. Surface biomedical electrode technology. *Int Med Device Diagnost Ind* 1990; 44–48.
72. McAdams ET, McLaughlin JA, Anderson J McC. Multi-electrode systems for electrical impedance tomography. *Physiol Meas* 1994;15:A101–A106.
73. McAdams ET, McLaughlin J, Brown BN, McArdle F. In: London HD, editor. *The NIBEC EIT harness, Clinical and Physiological Applications of Electrical Impedance Tomography*. Chapt 8, UCL Press; 1993. p 85–92.
74. McAdams ET, Jossinet J. Hydrogel electrodes in bio-signal recording. Proceedings of the 12th Annual International Conference of the IEEE, Philadelphia, PA: Engineering in Medicine and Biology Society; 1990: 1490–1491.
75. McAdams ET, Lacknermeier A, Jossinet J. AC impedance of the hydrogel-skin interface. 16th Annual Int. Conf IEEE Eng in Med and Biol Soc Baltimore (MD), 1994: 870–871.
76. Carim HM, Hawkinson RW. EKG electrode electrolyte-skin AC impedance studies. Proc. 4th Ann Conf IEEE Eng Med Biol Soc 1982:503–504.
77. Yamamoto T, Yamamoto Y. Electrical properties of the epidermal stratum corneum. *Med Biol Eng* 1976;14:151–158.
78. Geddes LA. A. Historical perspectives 2: The electrocardiograph. In: Bronzino JD, editor. *The Biomedical Engineering Handbook*. Boca Raton FL: CRC Press; 1995; p 788–798.
79. Waller AD. A demonstration on man of electromotive changes accompanying the heart's beat. *J Physiol* 1887; 8:229–234.
80. Waller AD. On the electromotive changes connected with the beat of the mammalian heart, and of the human heart in particular. *Phil Trans R Soc London Ser B* 1989;180:169–194.
81. Waller AD. Introductory address on the electromotive properties of the human heart. *Brit Med J* 1888;2:751–754.
82. Barker LF. Electrocardiography and phonocardiography: A collective review. *Bull Johns Hopkins Hosp* 1910;21:358–359.
83. Rowbottom ME, Susskind C. In: *Electricity and Medicine: History of their Interaction*. San Francisco (CA): San Francisco Press; 1984.
84. Barron SL. The development of the electrocardiograph in Great Britain. *Br Med J* 1950;1:720–725.
85. Lewes D. Multipoint electrocardiography without skin preparation. *Lancet* 1965;2:17–18.
86. Wolferth CC, Wood FC. The electrocardiographic diagnosis of coronary occlusion by the use of chest leads. *Am J Med Sci* 1932;183:30–35.
87. Barnes AR, et al. Standardization of precordial leads. *Am Heart J* 1938;15:235–239.
88. Burch GE, DePasquale NP: A History of Electrocardiography with a New Introduction by Joel D Howell, 2nd ed. San Francisco, CA: Jeremy Norman; 1990.
89. Ungerleider HE. A new precordial electrode. *Am Heart J* 1939;18:94.
90. Welch W. Self-retaining electrocardiographic electrode. *JAMA* 1951;147:1042.
91. Jasper HH, Carmichael L. Electrical potentials from the intact human. *Science* 1935;81:51–53.
92. Khan A, Greatbatch W. Physiologic electrodes. In: Ray CD. editor. *Medical Engineering*. Chicago, IL: Year Book Medical Publishers; 1974.
93. Manley AG, Medical electrode. US patent 3,977,392, 1976.
94. K Krug, Marecki NM. Porous and other medical and pressure sensitive adhesives. *Adhes Age* 1983;26(12):19–23.
95. Hymes AC. Monitoring and stimulating electrode. U.S. Patent 4,274,420, June 23, 1981.
96. Dempsey GJ, McAdams ET, McLaughlin J, Anderson JMcC. NIBEC cardiac mapping harness. 14th Annual Int. Conf. IEEE Eng. In Med and Biol Soc Paris, France, Nov 1992: 2702–2703.
97. Lymberis A. Research and Development of Smart Wearable Health Applications: The Challenge Ahead, Wearable eHealth Systems for Personalised Health Management, Studies in Health Technology and Informatics 108. Lymberis A, de Rossi D, editors, IOS Press; 2004.
98. Axisa F, Schmitt PM, Gehin C, Delhomme G, McAdams E, Dittmar A. Flexible technologies and smart clothing for citizen medicine, home healthcare and disease prevention. *IEEE Trans Inform Technol Biomed* 2005;9(3): 325–336.
99. Adams G. An Essay on Electricity. London; 1785.

100. Aldini G. Account of Late Improvements in Galvanism. London; 1803.
101. Duchenne GBA. In: De l'Électrisation Localisée et de son Application à la Physiologie, à la Pathologie et à la Thérapeutique. 1855.
102. Duchenne GBA. In: Baillière JB et al., editors. Mécanisme de la Physiologie Humaine. 1876.
103. Schechter DC. In: Exploring the Origins of Electrical Cardiac Stimulation. Medtronic; 1983.
104. Robinson AJ, Snyder-Mackler L. Clinical Electrophysiology: Electrotherapy, Electrophysiologic Testing. Baltimore (MD): Williams and Wilkins; 1995.
105. Low J, Reed A. Electrotherapy Explained: Principles and Practice. Oxford: Butterworth-Heinemann Ltd; 1994.
106. Stankevich BA. 4% of professional liability claims involve electromedicine equipment. *Mod Health Care* 1980;10(12): 74–76.
107. Pearce JA. The thermal performance of electrosurgical dispersive electrodes. Ph.D. dissertation. Purdue University, West Lafayette (IN); 1980.
108. Wiley JD, Webster JG. Analysis and control of the current distribution under circular dispersive electrodes. *IEEE Trans Biomed Eng* 1982;29:381–385.
109. Caruso PM, Pearce JA, DeWitt DP. Temperature and current density distributions at electrosurgical dispersive electrode sites. Proc 7th N Engl Bioeng Conf., Troy, New York, March 22–23, 1979: 373–376.
110. V Krasteva, Papazov S. Estimation of current density distribution under electrodes for external defibrillation. *Bio-Medical Engineering Online*, 2002; 1:7. Available <http://www.biomedical-engineering-online.com/content/1/1/7>.
111. Y Kim, Schimpf PH. Electrical behavior of defibrillation and pacing electrodes. Proc IEEE 1996;84(3):446–456.
112. Kim Y, Fahy JB, Tupper B. Optimal electrode designs for electrosurgery, defibrillation, and external cardiac pacing *IEEE Trans Biomed Eng* 1986;33:845–853.
113. Netherly SG, Carim HM. Biomedical electrode with lossy dielectric properties. US pat 5,836,942, 1998.
114. Ferrari RK. X-ray transmissive transcutaneous stimulating electrode. US pat 5,571,165, 1996.
115. McAdams ET, Andrews P. Biomedical electrodes and biomedical electrodes for electrostimulation. US pat 2003, 134,545, 2003.
116. Szeto AYJ. Pain relief from transcutaneous electrical nerve stimulation (TENS). In: Webster JG. ed. Encyclopedia of Medical Devices and Instrumentation. New York: John Wiley & Sons; 1988. p 2203–2220.
117. AXELGAARD J. Reverse current controlling electrode. US pat 2004,158,305, 2004.
118. Sarlandière. "Mémoires sur l'électropuncture considérée comme moyen nouveau de traiter efficacement la goutte, les rhumatismes et les affections nerveuses. Paris, 1825.
119. Hyman AS. Resuscitation of the stopped heart by intracardiac therapy. *Arch Intern Med* 1932;50:283.
120. Mittal T. Pacemakers – A journey through the years. *Ind J Thorac Cardiovasc Surg* 2005;21:236–249.
121. Myers GH, Parsonnet V. Pacemaker electrodes In: Myers GH, Engineering in the Heart and Blood. New York: Wiley-Interscience; 1969.
122. Greatbatch W, Holmes CF. History of implantable devices. *IEEE Eng Med Biol* 1991; Sept: 36–49.
123. Chardack WM, Gage AA, Greatbatch W. Correction of complete heart block by a self-contained and subcutaneously implanted pacemaker. *J Thorac Cardiovasc Surg* 1961;42: 418.
124. Lagergren H, Johansson L. Intracardiac stimulation for complete heart block. *Acta Chir Scand* 1963;125:562–566.
125. Parsonnet V, Zucker IR, Asa MM. Preliminary investigation of the development of a permanent implantable pacemaker utilizing an intracardiac dipolar electrode. *Clin Res* 1962; 10:391.
126. Timmis G. The electrobiology and engineering of pacemaker leads. In: Saksena S, Goldschlager N. eds. Electrical Therapy for Cardiac Arrhythmias. New York: Saunders W.B. Co.; 1990.
127. Admundson DC, McArthur W, Mosharrafa M. The porous endocardial electrode. *PACE* 1979;2:40–50.
128. Lagergren H, Edhag O, Wahlberg I. A low threshold non-dislocating endocardial electrode. *J Thorac Cardiovasc Surg* 1976;72:259.
129. Lewin G, Myers GH, Parsonnet V, Zucker IR. A non-polarizing electrode for physiological stimulation. *Trans Am Soc Artif Intern Organs* 1967;13:345.
130. Ellenbogen KA, Wood MA. Cardiac Pacing and ICDs. New York: Blackwell Science Inc; 2002.
131. Mond H, Stokes KB. The electrode-tissue interface: The revolutionary role of steroid elution. *PACE* 1991;15:95–107.
132. Mond HG, Stokes KB. The steroid-eluting electrode: A 10-year experience. *Pacing Clin Electrophysiol* 1996 Jul; 19(7):1016–1020.
133. Lenarz T, Battmer R-D, Goldring JE, Neuburger J, Kuzma J, Reuter G. New electrode concepts (Modiolus–Hugging Electrodes). *Adv Otorhinolaryngol Basel Karger* 2000;57:347–353.
134. Maynard EM. Visual prostheses. *Annu Rev Biomed Eng* 2001;3:145–168.
135. Peckham PH, Knutson JS. Functional electrical stimulation for neuromuscular applications. *Annu Rev Biomed Eng* 2005;7:327–360.
136. Rutten WLC. Selective electrical interfaces with the nervous system. *Annu Rev Biomed Eng* 2002;4:407–452.
137. Weiland JD, Liu W, Humayun MS. Retinal prosthesis. *Annu Rev Biomed Eng* 2005;7:361–401.
138. Drake KL, Wise KD, Farraje J, Anderson DJ, BeMent SL. Performance of planar multisite microprobes in recording extracellular single-unit intracortical activity. *IEEE Trans Biomed Eng* 1988;35:719–732.
139. Schwartz AB. Cortical neural prosthetics. *Annu Rev Neurosci* 2004;27:487–507.
140. Aguiló J. Microprobe multisensor for graft viability monitoring during organ preservation and transplantation. 2nd Annual International IEEE-EMB Special Topic Conference on Microtechnologies in Medicine & Biology, Madison, WI, February 2002; 15–20.
141. Mastrototaro JJ, Massoud HZ, Pilkington TC, Ideker RE. Rigid and flexible thin-film multielectrode assays for transmural cardiac recording. *IEEE Trans Biomed Eng* 1992; 39:271–279.
142. Linquette-Mailley SC, Hyland M, Mailley P, McLaughlin J, McAdams ET. Electrochemical and structural characterisation of electrodeposited iridium oxide thin film electrodes applied to neurostimulating electrical signal. *Mater Sci Eng* 2002;21:167–175.
143. Mortimer JT, Bhadra N. Peripheral nerve and muscle stimulation. In: Horch KW, Dhillon GS, editors. Neuroprosthetics: Theory and Practice (Series on Bioengineering & Biomedical Engineering), vol. 2. New York: World Scientific; 2004. p 638–744.
144. Hyland M, McLaughlin J, Zhou DM, McAdams E. Surface modification of thin film gold electrodes for improved in vivo performance. *Analyst* 1996;121:705–709.
145. Rieger R, Taylor J, Comi E, Donaldson N, Russold M, Mahony CMO, McLaughlin JA, McAdams E, Demosthenous A, Jarvis JC. Experimental determination of compound A-P

- direction and propagation velocity from multi-electrode nerve cuffs. *Med Biol Eng Comput Phys* 2004;26:531–534.
146. Prohaska OJ, Olcaytug P, Pfundner P, Dragaun H. Thin film multiple electrode probes: Possibilities and limitations. *IEEE Trans Biomed Eng* 1986;33:223–229.
  147. Schoenberg AG, Klingler DR, Baker CD, Worth NP, Booth HE, Lyon PC. Final report: Development of test methods for disposable ECG Electrodes. UBTL Technical Report No. 1605–005, Salt Lake City (UT); 1979.
  148. Hollander JI, ECG-Electrodes. Report No. 83.336, MFI-TNO, Utrecht, The Netherlands, 1983.
  149. Nessler N, Reischer W, Salchner M. Electronic skin replaces volunteer experiments. *Measure Sci Rev* 2003;3(2):71–74.

### Reading List

- Bell GH, Knox AC, Small AJ. Electrocardiography electrolytes. *Br Heart J* 1939;1:229–236.
- Geddes LA, Baker LE. Principles of Applied Biomedical Instrumentation, 3rd edition. New York: John Wiley & Sons; 1989.
- Licht S. History of electrotherapy. In: Licht S. ed. Therapeutic Electricity and Ultraviolet Radiation. New Haven, CT: Elizabeth Licht Pub; 1959. p 1–69.

See also DEFIBRILLATORS; ELECTROCARDIOGRAPHY, COMPUTERS IN; ELECTROENCEPHALOGRAPHY; ELECTROSURGICAL UNIT (ESU); FUNCTIONAL ELECTRICAL STIMULATION; TRANSCUTANEOUS ELECTRICAL NERVE STIMULATION (TENS).